A reaction diffusion model for competing pioneer and climax species
by Sharon Lynn Brown

A thesis submitted in partial fulfillment of the requirements for the degree of Doctor of Philosophy in Mathematics
Montana State University

Abstract:
Presented is a reaction-diffusion model for the interaction of a pioneer and climax species. The linear stability analysis of the kinetic equilibria are examined and the existence of a Hopf bifurcation is shown. A specific model is used to demonstrate the dynamics of the system. Diffusion is introduced into the kinetic system to model the spatial dispersion of the species. An analysis for the existence of a Turing bifurcation is performed. Again a specific model is examined for the possibility of Turing bifurcations and bifurcation diagrams are produced. Finally traveling wave solutions for the full reaction-diffusion system are examined. It is found using geometric singular perturbation theory that there exists a traveling wave solution to the system with wave speed of $0(\varepsilon)$.

A REACTION DIFFUSION MODEL FOR COMPETING PIONEER AND CLIMAX SPECIES

by

Sharon Lynn Brown

A thesis submitted in partial fulfillment
of the requirements for the degree

of

Doctor of Philosophy

in

Mathematics

MONTANA STATE UNIVERSITY
Bozeman, Montana

November 1998

APPROVAL

of a thesis submitted by

Sharon Lynn Brown

This thesis has been read by each member of the thesis committee and has been found to be satisfactory regarding content, English usage, format, citations, bibliographic style, and consistency, and is ready for submission to the College of Graduate Studies.

11/20/98
Date

Jack D. Dockery
Chairperson, Graduate Committee

Approved for the Major Department

11/20/98
Date

John Lund
Head, Mathematical Sciences

Approved for the College of Graduate Studies

11/23/98
Date

Joseph J. Fedock
Graduate Dean

STATEMENT OF PERMISSION TO USE

In presenting this thesis in partial fulfillment for a doctoral degree at Montana State University, I agree that the Library shall make it available to borrowers under rules of the Library. I further agree that copying of this thesis is allowable only for scholarly purposes, consistent with "fair use" as prescribed in the U. S. Copyright Law. Requests for extensive copying or reproduction of this thesis should be referred to University Microfilms International, 300 North Zeeb Road, Ann Arbor, Michigan 48106, to whom I have granted "the exclusive right to reproduce and distribute copies of the dissertation for sale in and from microform or electronic format, along with the right to reproduce and distribute my abstract in any format in whole or in part."

Signature Sharon L. Brown

Date 11-16-98

ACKNOWLEDGEMENTS

I would like to thank both Jack Dockery and Mark Pernarowski for their patience and guidance throughout my time in Montana. I truly appreciate all their help and suggestions along the way. I would also like to thank Joe Raquepas and Kyle Riley for their friendship during these last few years of writing. Finally I would like to thank my family for believing in me and standing behind me throughout this whole process. Thank you Mom, Cathy, Patty, Larry, Jim and Michael. I couldn't have done this without you. I dedicate this thesis to my father, Robert Bruce Brown, I wish you could have been here to celebrate with me.

TABLE OF CONTENTS

LIST OF TABLES

LIST OF FIGURES

ABSTRACT

Presented is a reaction-diffusion model for the interaction of a pioneer and climax species. The linear stability analysis of the kinetic equilibria are examined and the existence of a Hopf bifurcation is shown. A specific model is used to demonstrate the dynamics of the system. Diffusion is introduced into the kinetic system to model the spatial dispersion of the species. An analysis for the existence of a Turing bifurcation is performed. Again a specific model is examined for the possibility of Turing bifurcations and bifurcation diagrams are produced. Finally traveling wave solutions for the full reaction-diffusion system are examined. It is found using geometric singular perturbation theory that there exists a traveling wave solution to the system with wave speed of $O(\epsilon)$.

CHAPTER 1

Introduction

In an ecosystem, the competition among plant or animal species for natural resources is important in determining the evolution of the system. For example each tree in a forest competes with its neighbors for light, space, carbon dioxide, and soil nutrients. Although the intensity of the competition may or may not be affected by the species type of the neighboring trees, it is affected by neighboring population density. Similarly an animal may not be affected by what type of competitor is consuming its food, but the amount of food available will be affected by the density of the competitor population. We try to model the effects of population density on the survival and growth of an individual species by assuming that the species' per capita growth rate (i.e., fitness) is a function of a weighted total density variable. This total density variable is a linear combination of the densities of the interacting species with coefficients weighting the intensity of the effect of each species, both the intra-specific and inter-specific species competition. The intra-specific competition describes the extent by which each individual within a population affects and is affected by the other individuals within that particular population. Inter-specific competition describes the effects on individuals due to a species of a differing population. In both cases these effects may be either positive or negative. See [15] for examples of both intra and inter-specific competition. An example of such a model is the Lotka-Volterra system where the per capita growth rate is just a linear combination of the densities of the interacting populations [18].

Typically a fitness function will possess certain monotonicity properties as a function of it's density. We would expect that for large enough values of the density

variable, corresponding to crowding, the fitness of a species should decrease. For example, certain varieties of pine and poplar have higher fitnesses at low density but have fitnesses which decrease with an increase in the density of the surrounding forest. In a forest ecosystem, a tree population whose fitness monotonically decreases with density is called a pioneer species. We adopt that terminology here. An example of such functions can be seen in the Lotka-Volterra system where the fitness, f_i, of a pioneer species is linear:

$$f_i(y_i) = r_i - y_i, \tag{1.1}$$

with $y_i = \sum_{j=1}^{n} c_{ij}x_j$ representing the weighted total density variable for the i^{th} population and x_j represents the population density of the j^{th} population. It has been suggested by Ricker, [21], that certain fish populations have exponential pioneer fitnesses of the form (see Figure 1)

$$f(y) = e^{r(1-y)} - a. \tag{1.2}$$

Hassell and Comins [10] studied a two-species competition model with a pioneer fitness of the form

$$f(y) = \frac{r}{(1+by)^p} - a. \tag{1.3}$$

Certainly not all species fall into the category of a pioneer. For many species their survival and reproduction rates will benefit from an increase in density, at least for a period of time. Things such as group defense for prey, increased gene pool, and enhanced soil nutrients can represent the benefits of a higher density. An example of such species are oak or maple trees. At intermediate densities these species benefit from the presence of additional trees which provide protection and improved soil conditions; but ultimately individual reproduction and survival decrease at increasingly higher densities. We refer to such a species as a climax species. Its fitness will mono-

tonically increase to a maximum value and then monotonically decrease as a function of the weighted total density. Cushing [2] in his analysis of age-structured populations and Selgrade and Namkoong [23, 24, 22] for a forest model suggest climax fitnesses in the form (see Figure 2)

$$f(y) = ye^{r(1-y)} - a. \tag{1.4}$$

In this thesis we will analyze a two dimensional system of differential equations which model the interaction between a pioneer species and a climax species. In Chapter 2 we analyze the kinetic interaction model. The chapter is a review of results presented in [23, 24, 22] along with analyses of a specific example, referred to as the Selgrade model. We present local stability results for the equilibria of the general model using linear stability analysis. Results for the Selgrade model showing the existence and stability of bifurcating periodic solutions originating from a Hopf bifurcation of an interior equilibrium point are presented. For this specific model we show that the periodic solutions are stable.

In Chapter 3, we consider a model for interacting pioneer and climax species with the addition of a spatial variable in a diffusion term, modeling the spatial movement of the species. Only one spatial dimension is introduced. We again analyze the stability of the spatially homogeneous equilibria found in Chapter 2. The analysis of the bifurcation of these steady states is performed with local analysis of the shape of the bifurcation diagram. Again the specific example introduced in Chapter 2, Selgrade's model, is examined in detail. Numerical results suggest that the initial mode to bifurcate need not be a mode one solution of the form $a\cos(\pi x)$, and because of this the stability of the bifurcating solutions are not determined. We present numerical results showing that the bifurcation diagram near the critical point could open to the right or the left depending on the parameters space. We also give numerical evidence that for some range of the parameter space the higher order modes bifurcate

prior to the first mode as a certain bifurcating parameter is increased.

In Chapter 4, traveling wave solutions to the model are examined. First traveling waves in the absence of one species are determined. We show the existence of traveling waves for each species in the absence of the other. Next we analyze the existence of a traveling wave with $O(\epsilon)$ wave speed. This is an invasive wave connecting the equilibria along the opposing axes. An approximate solution is found using methods of matched asymptotic expansions. Next we show using geometric singular perturbation theory the existence of the traveling wave for small wave speed that is near the approximate solution.

CHAPTER 2

Kinetic Model Equations

In this chapter we will analyze a two dimensional system of differential equations which models the interaction between a pioneer species and a climax species. We let u denote the density of the pioneer species with its fitness function, f, being a monotonically decreasing function having only one positive zero. The climax species density we represent as v. Its fitness function, g, will increase to a maximum and then decrease, having exactly two positive zeros. See Figures 1 and 2 for examples of pioneer and climax species fitness functions respectively.

Both fitnesses will be taken to depend on total density variables, y_i, defined as a linear combination of the population densities. We define them as

$$y_1 = c_{11}u + c_{12}v, \tag{2.1}$$

$$y_2 = c_{21}u + c_{22}v, \tag{2.2}$$

where $c_{ij} \geq 0$ is an interaction coefficient which weights the effect of the j^{th} population on the i^{th} population. The coefficients c_{11} and c_{22} pertain to intra-species interaction, and c_{12} and c_{21} refer to inter-species interaction.

The model equations for this system of interacting pioneer and climax species are given by,

$$\begin{aligned} \frac{du}{dt} &= uf(y_1), \\ \frac{dv}{dt} &= vg(y_2). \end{aligned} \tag{2.3}$$

In vector form, (2.3) may be written as

$$\frac{d\vec{u}}{dt} = \mathbf{F}(\vec{u}). \tag{2.4}$$

This vector field is defined on the positive cone in $\mathbb{R}^2$. By restricting $c_{12} \neq 0$ and $c_{21} \neq 0$ and rescaling y_1 and y_2 we may assume that c_{12} and c_{21} are equal to one. Thus, without loss of generality we let $c_{12} = c_{21} = 1$ throughout. Then interaction matrix C becomes;

$$C = \begin{pmatrix} c_{11} & 1 \\ 1 & c_{22} \end{pmatrix}. \tag{2.5}$$

In the first section the equilibria of system (2.3) along with their stability are discussed. In the following section we show the existence of a Hopf bifurcation. Finally in the third section a specific example of system (2.3), which will be used throughout the thesis is examined.

Equilibria and Stability

Equilibria of system (2.3) occur where the nullclines of the pioneer species intersect the nullclines of the climax species. Let $z_1 > 0$ be the zero of f. Then the u-nullclines for system (1) are given by

$$u = 0 \text{ and } z_1 = c_{11}u + v. \tag{2.6}$$

We assume that z_1 is a non-degenerate zero of f, and indeed we assume $f'(z_1) < 0$.

Let w_1 and w_2 denote the zeros of g, with $0 < w_1 < w_2$, $g'(w_1) > 0$, and $g'(w_2) < 0$. The v-nullclines are

$$v = 0, \;\; w_1 = u + c_{22}v, \text{ and } w_2 = u + c_{22}v. \tag{2.7}$$

Notice that all the nullclines are straight lines and that two of the v-nullclines associated with the zeros of g are parallel. In Figure (3) we indicate a typical plot of these nullclines noting that slopes and equilibria location depend on c_{11}, c_{22} and the specific model.

There are six equilibrium points for this system, four of which always occur on the axes. The equilibria along the axes are

$$p_0 = (0,0),\ \ p_1 = (0, \frac{w_1}{c_{22}}),\ \ p_2 = (0, \frac{w_2}{c_{22}}),\ \ p_3 = (\frac{z_1}{c_{11}}, 0). \tag{2.8}$$

These points correspond to one of the species being extinct or, in the case of p_0, both being extinct. The other equilibria are

$$q_i = (\frac{c_{22}z_1 - w_i}{det(C)}, \frac{c_{11}w_i - z_1}{det(C)}) = (u_i^*, v_i^*), \quad i = 1, 2, \tag{2.9}$$

where $det(C)$ is the determinant of the interaction coefficient matrix (2.5). Lastly we note that to be of biological significance, it is necessary for both components of the equilibria to be nonnegative.

To determine the stability of the equilibria, we first find the eigenvalues of the Jacobian of the vector field at each of these points. The Jacobian can be expressed in the following form:

$$D\mathbf{F}(\vec{u}) = \begin{pmatrix} f(y_1) & 0 \\ 0 & g(y_2) \end{pmatrix} + \begin{pmatrix} uf'(y_1) & 0 \\ 0 & vg'(y_2) \end{pmatrix} \begin{pmatrix} c_{11} & 1 \\ 1 & c_{22} \end{pmatrix}.$$

For the equilibrium point p_0 given in (2.8),

$$D\mathbf{F}(p_0) = \begin{pmatrix} f(0) & 0 \\ 0 & g(0) \end{pmatrix}. \tag{2.10}$$

The eigenvalues are given by $\lambda_1 = f(0)$ and $\lambda_2 = g(0)$. Since we assume the fitness functions satisfy $f(0) > 0$ and $g(0) < 0$ if follows that p_0 is a saddle.

The next two equilibria from equation (2.8), $p_{1,2}$, can be examined simultaneously. The Jacobian for these points is given by

$$D\mathbf{F}(p_{1,2}) = \begin{pmatrix} f(\frac{w_{1,2}}{c_{22}}) & 0 \\ \frac{w_{1,2}}{c_{22}}g'(w_{1,2}) & w_{1,2}g'(w_{1,2}) \end{pmatrix}. \tag{2.11}$$

The eigenvalues of $D\mathbf{F}(p_{1,2})$ are $\lambda_1 = f(\frac{w_{1,2}}{c_{22}})$ and $\lambda_2 = w_{1,2}g'(w_{1,2})$. Recall that $g'(w_1) > 0$ and $g'(w_2) < 0$, therefore λ_2 is positive for p_1 and is negative for p_2. The

sign of λ_1 is determined by $f(\frac{w_{1,2}}{c_{22}})$, which can either be positive or negative. If λ_1 is negative then p_1 is a saddle and p_2 is a sink. However, if λ_1 is positive then p_1 is a source and p_2 is a saddle.

Evaluating the Jacobian at the equilibrium p_3 stated in equation (2.8) gives,

$$D\mathbf{F}(p_3) = \begin{pmatrix} z_1 f'(z_1) & \frac{z_1}{c_{11}} f'(z_1) \\ 0 & g(\frac{z_1}{c_{11}}) \end{pmatrix}. \tag{2.12}$$

Here the eigenvalues are $\lambda_1 = z_1 f'(z_1)$ and $\lambda_2 = g(\frac{z_1}{c_{11}})$. Since $f'(z_1) < 0$ it follows that $\lambda_1 < 0$. On the other hand λ_2 can change sign depending on the value of $g(\frac{z_1}{c_{11}})$. For p_3 between the two u-intercepts of the v-nullclines corresponding to $g = 0$ (see Figure 3), $\lambda_2 = g(\frac{z_1}{c_{11}}) > 0$, so p_3 is a saddle, otherwise p_3 is stable.

Lastly we consider the equilibria off the axes, q_1 and q_2. From (2.9) we find

$$D\mathbf{F}(q_i) = \begin{pmatrix} c_{11} u_i^* f'(z_1) & u_i^* f'(z_1) \\ v_i^* g'(w_i) & c_{22} v_i^* g'(w_i) \end{pmatrix}. \tag{2.13}$$

The characteristic equation is given by

$$\lambda^2 - tr(D\mathbf{F}(q_i))\lambda + det(D\mathbf{F}(q_i)) = 0$$

where

$$tr(D\mathbf{F}(q_i)) = c_{11} u_i^* f'(z_1) + c_{22} v_i^* g'(w_i), \tag{2.14}$$

$$det(D\mathbf{F}(q_i)) = u_i^* v_i^* f'(z_1) g'(w_i) det(C). \tag{2.15}$$

The eigenvalues are given by

$$\lambda_\pm = \frac{tr(D\mathbf{F}(q_i)) \pm \sqrt{(tr(D\mathbf{F}(q_i)))^2 - 4det(D\mathbf{F}(q_i))}}{2}. \tag{2.16}$$

We look first at the equilibrium q_2. Since $f'(z_1) < 0$ and $g'(w_2) < 0$ it follows from (2.14) that $tr(D\mathbf{F}(q_2)) < 0$. The sign of $det(D\mathbf{F}(q_2))$ depends on $det(C)$. If $det(C) < 0$ then $det(D\mathbf{F}(q_2)) < 0$ and the eigenvalues are real and of opposite sign,

thus q_2 is a saddle point. If $det(C) > 0$ then $det(D\mathbf{F}(q_2)) > 0$ but, $\mathbf{Re}(\lambda_\pm)$ will remain less than zero so in this case q_2 is a stable equilibrium.

Finally consider the equilibrium q_1. Here $tr(D\mathbf{F}(q_1))$ may be positive, negative or zero. However, if $det(C) > 0$ then, since $f'(z_1) < 0$ and $g'(w_1) > 0$ it follows by (2.15) that $det(D\mathbf{F}(q_1)) < 0$. Thus both eigenvalues are real, and of opposite sign, making q_1 a saddle. On the other hand if $det(C) < 0$ then the eigenvalues of $D\mathbf{F}(q_1)$ have real parts with the same sign. In this case if $tr(D\mathbf{F}(q_1)) < 0$ the q_1 is locally asymptotically stable, and if $tr(D\mathbf{F}(q_1)) > 0$ then q_1 is unstable. In the next section we show that by varying either c_{11} or c_{22}, q_1 may undergo a Hopf bifurcation yielding a periodic orbit.

We summarize the stability of the equilibria for system (2.3) in Table 1 below.

Table 1: Equilibria of the Kinetic System

point	condition	stability
$p_0 = (0,0)$	none	saddle
$p_1 = (0, \frac{w_1}{c_{22}})$	$f(\frac{w_2}{c_{22}}) < 0$	saddle
	$f(\frac{w_2}{c_{22}}) > 0$	unstable
$p_2 = (0, \frac{w_2}{c_{22}})$	$f(\frac{w_2}{c_{22}}) < 0$	stable
	$f(\frac{w_2}{c_{22}}) > 0$	saddle
$p_3 = (\frac{z_1}{c_{11}}, 0)$	$g(\frac{z_1}{c_{11}}) < 0$	stable
	$g(\frac{z_1}{c_{11}}) > 0$	saddle
$q_1 = (\frac{c_{22}z_1 - w_1}{detC}, \frac{c_{11}w_1 - z_1}{detC})$	$detC > 0$	saddle
	$detC < 0$ and $tr(D\mathbf{F}(q_1)) < 0$	stable
	$detC < 0$ and $tr(D\mathbf{F}(q_1)) > 0$	unstable
$q_2 = (\frac{c_{22}z_1 - w_2}{detC}, \frac{c_{11}w_2 - z_1}{detC})$	$detC > 0$	stable
	$detC < 0$	saddle

Hopf Bifurcation

In this section we show that the equilibrium q_1 may undergo a Hopf bifurcation as we

vary c_{11} or c_{22}. In general, for a Hopf bifurcation to occur as a parameter changes, complex eigenvalues of the Jacobian at the equilibrium point must cross the imaginary axis. This crossing results in a change of the stability of the equilibrium point and often gives rise to periodic solutions. From equation (2.16) we see that for $D\mathbf{F}(q_1)$ to have complex eigenvalues we need

$$(tr(D\mathbf{F}(q_1))^2 < 4det(D\mathbf{F}(q_1)).$$

The inequality implies that $det(D\mathbf{F}(q_1))$ must be greater than zero, and so by (2.15) with $g'(w_1) > 0$, $f'(z_1) < 0$ we have that $det(C)$ must be less than zero. By choosing parameter values such that $tr(D\mathbf{F}(q_1)) = 0$ we get purely imaginary eigenvalues for the Jacobian at q_1. In equation (2.14) we see that by varying c_{11} or c_{22} we can make $tr(D\mathbf{F}(q_1)) = 0$. Thus, we can choose either c_{11} or c_{22} as the bifurcation parameter. Biologically, adjusting these parameters would be equivalent to the stocking or harvesting of one particular species or, amplifying or diminishing the intra-species competition.

Setting $tr(D\mathbf{F}(q_1)) = 0$ and solving for c_{11} gives

$$c_{11} = \frac{c_{22}z_1g'(w_1)}{(c_{22}z_1 - w_1)f'(z_1) + c_{22}w_1g'(w_1)} \tag{2.17}$$

or c_{22},

$$c_{22} = \frac{c_{11}w_1f'(z_1)}{(c_{11}w_1 - z_1)g'(w_1) + c_{11}z_1f'(z_1)}. \tag{2.18}$$

Let c_{11}^* and c_{22}^* denote these respective values. To ensure that u_1^* and v_1^* are positive, making q_1 biologically significant, we need

$$c_{22}z_1 - w_1 < 0 \text{ and } c_{11}w_1 - z_1 < 0. \tag{2.19}$$

These inequalities also imply both c_{11}^* and c_{22}^* are positive.

Having purely imaginary eigenvalues is not enough to produce a Hopf bifurcation. We also need the eigenvalues to cross the imaginary axis transversality as

the bifurcation parameter is varied. This amounts to the real part of the eigenvalues having a nonzero derivative with respect to the parameter at the critical value of the bifurcation parameter (i.e. at c_{11}^* or c_{22}^*). If we have complex eigenvalues, we see from equation (2.16) that the real part of the eigenvalues are

$$\begin{aligned}\alpha(c_{ii}) &= \frac{1}{2}tr(D\mathbf{F}(q_1(c_{ii}), c_{ii})), \\ &= \frac{1}{2}\frac{[(c_{22}z_1 - w_1)c_{11}f'(z_1) + (c_{11}w_1 - z_1)c_{22}g'(w_1)]}{det(C)}.\end{aligned}$$

Choosing c_{11} as the bifurcation parameter and fixing c_{22} gives

$$\alpha'(c_{11}^*) = \frac{1}{2}\frac{(c_{22}z_1 - w_1)f'(z_1) + c_{22}w_1g'(w_1)}{det(C)}.$$

Therefore with the first inequality of (2.19) we see that $\alpha'(c_{11}^*) < 0$. Thus, as c_{11} decreases through c_{11}^* the fixed point q_1 destabilizes and a periodic solution bifurcates.

Letting c_{22} be the bifurcating parameter and fixing c_{11} gives

$$\alpha'(c_{22}^*) = \frac{1}{2}\frac{(c_{11}w_1 - z_1)g'(w_1) + c_{11}z_1f'(z_1)}{det(C)},$$

and using (2.19) again, this implies $\alpha'(c_{22}^*) > 0$. Therefore, q_1 stabilizes with periodic solutions bifurcating as c_{22} increases past c_{22}^*.

We can summarize the above by stating that a Hopf bifurcation occurs at q_1 with respect to the parameter c_{11} as c_{11} decreases through c_{11}^*. Likewise a Hopf bifurcation occurs with respect to c_{22} as c_{22} increases through c_{22}^*.

The following theorem [9] can be used to determine the stability of the bifurcating periodic solution arising from the Hopf bifurcation of q_1 at c_{11}^* or c_{22}^*.

Theorem 2.1 *Suppose that the system* $\frac{d\vec{x}}{dt} = \vec{h}_\mu(\vec{x}) = \begin{bmatrix} h_\mu(\vec{x}) \\ k_\mu(\vec{x}) \end{bmatrix}$, $\vec{x} \in \mathbb{R}^2$, $\mu \in \mathbb{R}$ *has an equilibrium* $(\vec{x}_0, \mu_0)$ *at which a Hopf bifurcation occurs. Let*

$$\frac{d}{d\mu}(\mathbf{Re}(\lambda(\mu))|_{\mu=\mu_0} = d \neq 0,$$

where $\lambda(\mu)$ and $\bar{\lambda}(\mu)$ are the eigenvalues of the linearized system. Then there is a three-dimensional center manifold passing through $(\vec{x}_0, \mu_0)$ in $\mathbb{R}^2 \times \mathbb{R}$ and a smooth system of coordinates for which the Taylor expansion of degree 3 on the center manifold is given by the following;

$$\begin{aligned} \dot{x} &= (d\mu + a(x^2+y^2))x - (\omega + c\mu + b(x^2+y^2))y \\ \dot{y} &= (\omega + c\mu + b(x^2+y^2))x + (d\mu + a(x^2+y^2))y, \end{aligned} \tag{2.20}$$

with a given by

$$\begin{aligned} a &= \frac{1}{16}[h_{xxx} + h_{xyy} + k_{xxy} + k_{yyy}] + \frac{1}{\mathbf{Im}(\lambda(\mu_0))}[h_{xy}(h_{xx} + h_{yy}) \\ &\quad -k_{xy}(k_{xx} + k_{yy}) - h_{xx}k_{xx} + h_{yy}k_{yy}]. \end{aligned} \tag{2.21}$$

If $a \neq 0$, there is a surface of periodic solutions in the center manifold which has a quadratic tangency at μ_0 agreeing to second order with the paraboloid $\mu = -(\frac{a}{d})(x^2 + y^2)$. If $a < 0$, then these periodic solutions are stable limit cycles, while if $a > 0$, the periodic solutions are repelling.

For system (2.3) the stability coefficient a given in (2.21) at q_1 is given by

$$\begin{aligned} 16a &= \frac{c_{11}^2 w_1 f''(z_1)}{c_{22} v_1^*} + \frac{c_{22} z_1 g''(w_1)}{u_1^*} + c_{11} u_1^* f'(z_1) detC[\frac{g''}{g'}]'(w_1) \\ &\quad + c_{11} v_1^* g'(w_1) detC[\frac{f''}{f'}]'(z_1). \end{aligned} \tag{2.22}$$

In the next section we use (2.22) and Theorem 2.1 to determine the stability of the bifurcated periodic solutions in a specific pioneer-climax model.

Selgrade Model

In this section, we will analyze the pioneer-climax model introduced in Selgrade [22] and Selgrade and Namkoong [23, 24]. In this model both the pioneer and climax

fitness functions are exponential functions of the total population density. The fitness function for the pioneer species is given by

$$f(y_1) = -1 + exp(1 - 2y_1), \tag{2.23}$$

with a zero at $z_1 = \frac{1}{2}$ (see Figure 1).

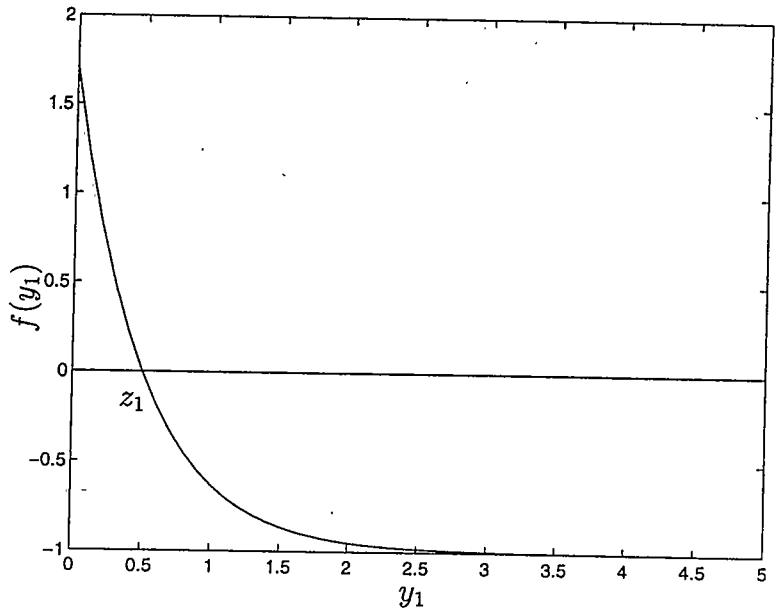

Figure 1: Pioneer Species Fitness Function, f

The climax species' fitness function is given by

$$g(y_2) = -1 + y_2 exp[\frac{1}{2}(1 - y_2)], \tag{2.24}$$

and has zeros at $w_1 = 1$ and $w_2 \approx 3.513$ (see Figure 2).

For this example we choose $c_{11} > 0$ as the bifurcation parameter and fix the value of c_{22} at one. With this in mind, it follows from (2.5) that $det(C) = c_{11} - 1$. As we saw in the first two sections, a Hopf bifurcation for this system will only occur when $det(C) < 0$, therefore we restrict our attention to $c_{11} \in (0, 1)$.

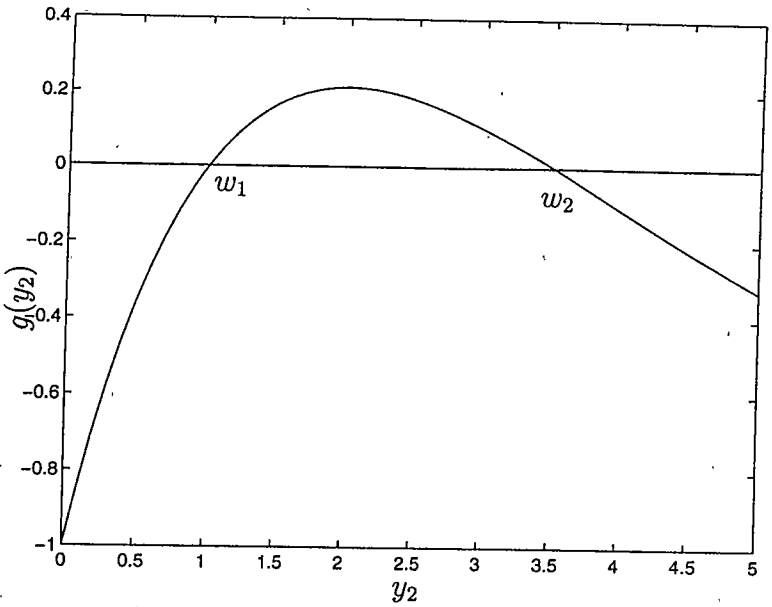

Figure 2: Climax Species Fitness Function, g

In the case of $c_{22} = 1$, the u-nullclines for (2.3) are given by

$$\begin{aligned} u &= 0, \\ v &= \frac{1}{2} - c_{11}u, \end{aligned}$$

and the v-nullclines are

$$\begin{aligned} v &= 0, \\ v &= 1 - u, \\ v &\approx 3.513 - u. \end{aligned}$$

In Figure 3 we show the nullclines and the equilibria of the system for a typical value of c_{11}. The equilibria along the axes are given by

$$p_0 = (0,0),\ p_1 = (0,1),\ p_2 \approx (0, 3.513) \text{ and } p_3 = (\frac{1}{c_{11}}, 0). \qquad (2.25)$$

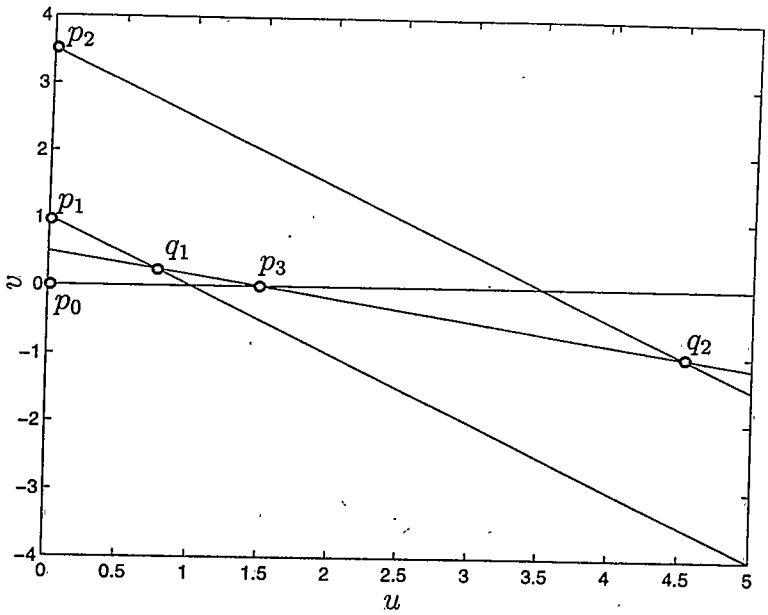

Figure 3: Pioneer and Climax Nullclines

The equilibria interior to the positive cone are

$$q_1 = (\frac{1}{2(1-c_{11})}, \frac{1-2c_{11}}{2(1-c_{11})}) \text{ and } q_2 \approx (\frac{6.02}{2(1-c_{11})}, \frac{1-7.02c_{11}}{2(1-c_{11})}). \tag{2.26}$$

From the general stability results presented in Section 1 we can easily determine the stability of the fixed points for this model. We see from Table 1 that the stability for a number of the fixed points is not dependent on c_{11}. Notice that both p_0 and p_1 are always unstable and since $f(w_2) < 0$ it follows that p_2 is stable. The last equilibrium whose stability does not depend directly on c_{11} is q_2. It is unstable when $det(C) < 0$. From Table 1 we see that the stability of p_3 and q_1 depend on c_{11}.

The stability of p_3 varies with the sign of $g(\frac{1}{c_{11}})$. If $g(\frac{1}{c_{11}}) < 0$ then p_3 is a sink and if $g(\frac{1}{c_{11}}) > 0$ then p_3 is a saddle. In terms of c_{11}, $g(\frac{1}{c_{11}})$ is positive for $c_{11} > \frac{1}{2}$ or $c_{11} < \frac{1}{2w_2}$ and $g(\frac{1}{c_{11}})$ is negative for $\frac{1}{2w_2} < c_{11} < \frac{1}{2}$. Thus, p_3 is a sink if $c_{11} > \frac{1}{2}$ or $c_{11} < \frac{1}{2w_2}$ and a saddle if $\frac{1}{2w_2} < c_{11} < \frac{1}{2}$.

Next we note that the point q_1 undergoes a Hopf bifurcation at $c_{11} = c_{11}^* = \frac{1}{6}$.

In particular for $c_{11} > \frac{1}{6}$, q_1 is stable and for $0 < c_{11} < \frac{1}{6}$, q_1 is unstable with a branch of periodic orbits that bifurcate at $c_{11} = \frac{1}{6}$. The stability of these periodic orbits is determined by the value of a given in (2.22). Evaluating (2.22) at $c_{11}^* = \frac{1}{6}$ for the particular fitness functions under consideration gives $a < 0$ and therefore the bifurcating periodic orbits are locally asymptotically stable. Thus, the system has a supercritical Hopf bifurcation at $c_{11} = \frac{1}{6}$. The local form of the bifurcation diagram are determined by the sign of $\lambda'(c_{11}^*)$ and a. With both $\mathbf{Re}(\lambda'(c_{11}^*)) < 0$, and $a < 0$, locally at q_1 the bifurcation diagram is a parabola that opens to the left, from which it follows that the periodic solutions are locally asymptotically stable. Figure 4 shows the bifurcation diagram for the pioneer species, u. It was created using xppaut [5] with $c_{11} = 0.3333$ and initial condition $u = 0.75$, $v = 0.25$.

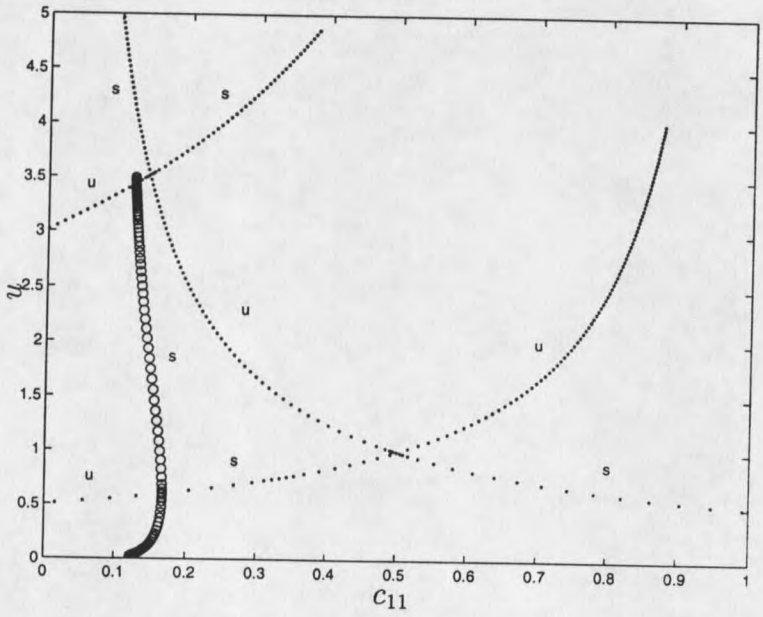

Figure 4: Hopf Bifurcation Diagram for the Pioneer Species, u.

In general, the analysis done here for c_{11} as the bifurcation parameter may be duplicated for the case of c_{22} as the parameter with c_{11} fixed. The stability diagram

in Figure 5 is for a Hopf bifurcation of q_1 with general c_{11} and c_{22} values. In this figure the $a = 0$ curve was calculated using AUTO [19]. For a Hopf bifurcation to occur at q_1 we need the $tr(D\mathbf{F}(q_1)) = 0$ and $det(C) < 0$. The stability of the bifurcating periodic orbits depends on the sign of a at the bifurcating point. In Figure 5 $det(C) = 0$, $trD\mathbf{F}(q_1) = 0$ and $a = 0$ are graphed in the (c_{11}, c_{22})-plane. Periodic orbits emerge from q_1 for (c_{22}, c_{11}) in the lower region of the graph with $0 < c_{22} < 2$ on the curve $trD\mathbf{F}(q_1) = 0$ and below the graph of $det(C) = 0$. From this we see that the Hopf bifurcation curve, $trD\mathbf{F}(q_1) = 0$, always lies below the $a = 0$ curve in the region where $a < 0$. Thus the bifurcated periodic orbits must be locally asymptotically stable by Theorem 2.1.

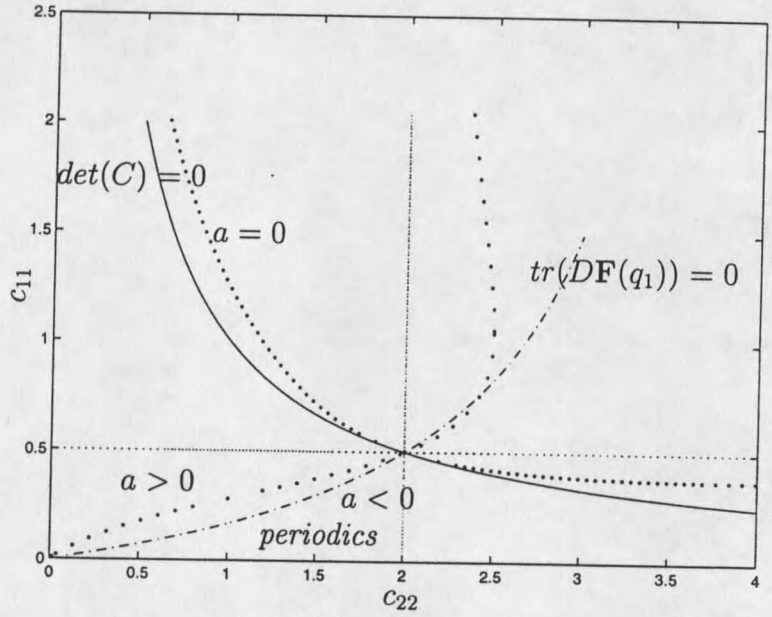

Figure 5: Stability Region for Periodic Solutions Resulting from Hopf Bifurcation. The dotted line is the $a = 0$ curve, the solid line is the $det(C) = 0$ curve and the dot-dash-dot line is the $tr(D\mathbf{F}(q_1)) = 0$ curve.

For simple models, like the one presented in this chapter, it would seem reasonable that the climax species, being more robust at higher population densities,

would have a greater chance of survival and would eventually exclude the pioneer species as the total density increased. The ultimate dynamical result of an undisturbed pioneer-climax system has been assumed to be the exclusion of the pioneer. However contrary to this belief, our model shows that the densities of both species may fluctuate in a stable periodic fashion for all time. Selgrade and Namkoong [23] argue that the inevitability of a pioneer giving way to a climax species is sometimes an invalid assumption. They give examples of two species usually classified as intolerant pioneers, the Populous termuloides (quaking aspen) in Utah and the Liriodendron tulipifera (yellow-popular) in Georgia, that may be evidence of persistence of pioneer species in "climax" communities.

CHAPTER 3

Introduction of Diffusion

In this chapter we will introduce a spatial variable into the dynamics of the interacting species model of Chapter 2. In an ecosystem we see that spatial considerations, such as the size of the domain of the species, the conditions along the domain boundary, the concentration of the species throughout and the make-up of the terrain within the domain will affect the existence and survival of a species. We can see that the differences in individual species are partly due to the non-constant environment in which they live, and that the effects of the spatial distribution of the individual species will influence the way they interact. We will see that spatial heterogeneity can have an important effect on the balance that exists between the interaction of differing species. With these spatial effects in mind we will introduce a spatial variable into our pioneer-climax model.

One of the most important sources of collective motion on the molecular level is diffusion, which is a consequence of the perpetual motion of individual molecules. Okubo [17] describes diffusion as the phenomenon by which an organism as a whole spreads due to the irregular motion of each individual. Among the first to draw an analogy between the random motion of molecules and that of organisms was Skellam [27]. He suggested that for a population that is reproducing continuously with rate α and spreading over space in a random way, a suitable continuous description could be

$$\frac{\partial P}{\partial t} = D\nabla^2 P + \alpha P, \tag{3.1}$$

where D is called the dispersion rate or the diffusion coefficient and $P(x,t)$ is the population density. Applying this assumption, Skellam modeled the spread of a muskrat

population over central Europe. Comparing his results with that of actual data he was able to demonstrate that the spread of certain populations can be explained using a diffusion approximation. Since then diffusion models have been used to model the population of a number of species (see [16], [3],[17] and the references therein).

Typically diffusion is thought of as a stabilizing process, something that will have a smoothing or homogenizing influence on the system eventually leading to a uniform spatial distribution. However, in the 1950's Turing suggested that under certain conditions diffusion can act as a destabilizing influence on the system producing steady state solutions that are spatially heterogeneous: *"A reaction diffusion system exhibits diffusion-driven instability or Turing instability if the homogeneous steady state is stable to small perturbations in the absence of diffusion but unstable to small spatial perturbations when diffusion is present"* [16].

We will consider the following system of equations, where $A(x,t)$ and $B(x,t)$ represent two species,

$$\begin{aligned} \frac{\partial A}{\partial t} &= F(A,B) + D_A \frac{\partial^2 A}{\partial x^2} \\ \frac{\partial B}{\partial t} &= G(A,B) + D_B \frac{\partial^2 B}{\partial x^2}. \end{aligned} \tag{3.2}$$

Turing's idea is that if in the absence of diffusion (i.e. $D_A = D_B = 0$), A and B tend to a linearly stable uniform steady state, then under certain conditions, spatially inhomogeneous patterns can evolve by diffusion driven instability if $D_A \neq D_B$. The reaction rates at any given point may not be able to adjust quickly enough to reach equilibrium. If the conditions are right, a small spatial disturbance can become unstable and a pattern begins to grow. Such an instability is said to be diffusion driven and the change in stability due to diffusion is often called a Turing bifurcation.

We will continue to model the interaction of a pioneer species with a climax species but will now introduce diffusion. For simplicity we consider only one spatial

variable and scalar diffusion coefficients. The system of equations are given by,

$$\begin{aligned} u_t &= D_1 u_{xx} + u f(y_1) \\ v_t &= D_2 v_{xx} + v g(y_2), \end{aligned} \tag{3.3}$$

with Neumann boundary conditions are given by

$$\begin{aligned} u_x(0,t) &= v_x(0,t) = 0, \\ u_x(L,t) &= v_x(L,t) = 0. \end{aligned} \tag{3.4}$$

Neumann boundary conditions impose the condition that the species will not grow or decline due to fluctuations across the boundary of their domain. This may be due to an unfavorable environment outside of their domain such as a change in terrain conditions, lack of water or low food supply. Possibly the boundary conditions are due to either man made or geographical boundaries such as fences, cliffs or water edges. In all cases the assumption is that for some reason the species can not wander across the boundary of their domain.

The functions y_1, y_2 were given in equations (2.1) and (2.2) with interaction coefficients c_{ij} as in (2.5). Once again the fitness functions are as in the kinetic system (2.3), with f representing a pioneer species fitness function and g a climax species fitness function. The parameters D_1 and D_2 are the diffusion coefficients of the pioneer and climax species respectively.

In the first section the stability of the steady states of the kinetic system, which correspond to uniform steady states of (3.3), are examined. The next two sections deal with the analysis of a Turing bifurcation and the shape of the bifurcation diagram. In the last section we consider the Selgrade kinetic model introduced in Chapter 1 but with diffusion included.

Stability of Uniform Steady States

In this section we will examine the stability of the uniform steady states of (3.3). Note that the steady state solutions of (2.3) correspond to uniform steady state solutions for (3.3)-(3.4). It is to our advantage to first nondimensionalize (3.3). In this regard let $\hat{x} = \frac{x}{L}$ and $\hat{t} = \frac{D_2}{L^2}t$, in (3.3):

$$\begin{aligned} \frac{du}{d\hat{t}} &= du_{\hat{x}\hat{x}} + \gamma u f(y_1), \\ \frac{dv}{d\hat{t}} &= v_{\hat{x}\hat{x}} + \gamma v g(y_2), \end{aligned} \tag{3.5}$$

where $d = \frac{D_1}{D_2}$ and $\gamma = \frac{L^2}{D_2}$, with boundary conditions given by

$$\begin{aligned} u_{\hat{x}}(0,\hat{t}) &= v_{\hat{x}}(0,\hat{t}) = 0, \\ u_{\hat{x}}(1,\hat{t}) &= v_{\hat{x}}(1,\hat{t}) = 0. \end{aligned} \tag{3.6}$$

For convenience the hat superscripts will be dropped.

Suppose (u^*, v^*) is an equilibrium point for the kinetic system (2.3). Then in view of the boundary conditions (3.6) we see that $u = u^*$ and $v = v^*$ is a trivial steady state solution to (3.5)-(3.6). To investigate the stability of this solution we linearize (3.5) about (u^*, v^*). The linearized system is:

$$\begin{aligned} u_t &= du_{xx} + \gamma[u^* f'(y_1^*)c_{11} + f(y_1^*)](u - u^*) + \gamma[u^* f'(y_1^*)](v - v^*), \\ v_t &= v_{xx} + \gamma[v^* g'(y_2^*)](u - u^*) + \gamma[v^* g'(y_2^*)c_{22} + g(y_2^*)](v - v^*). \end{aligned} \tag{3.7}$$

Let $\tilde{u} = u - u^*$ and $\tilde{v} = v - v^*$ then (3.7) becomes,

$$\begin{aligned} \tilde{u}_t &= d\tilde{u}_{xx} + \gamma[u^* f'(y_1^*)c_{11} + f(y_1^*)]\tilde{u} + \gamma[u^* f'(y_1^*)]\tilde{v}, \\ \tilde{v}_t &= \tilde{v}_{xx} + \gamma[v^* g'(y_2^*)]\tilde{u} + \gamma[v^* g'(y_2^*)c_{22} + g(y_2^*)]\tilde{v}. \end{aligned}$$

This system can be written in the following form:

$$\begin{bmatrix} \tilde{u}_t \\ \tilde{v}_t \end{bmatrix} = \begin{bmatrix} d\frac{d^2}{dx^2} & 0 \\ 0 & \frac{d^2}{dx^2} \end{bmatrix} \begin{bmatrix} \tilde{u} \\ \tilde{v} \end{bmatrix} + \gamma D\mathbf{F}(u^*, v^*) \begin{bmatrix} \tilde{u} \\ \tilde{v} \end{bmatrix}, \tag{3.8}$$

where $D\mathbf{F}(u^*, v^*)$ is the Jacobian of the vector field given in (2.3) evaluated at the point (u^*, v^*). Since the problem (3.8) is linear we look for solutions in the form

$$\vec{\tilde{u}}(x,t) = \sum_{m=0}^{\infty} \vec{U}_m e^{\lambda_m t} \cos(m\pi x). \tag{3.9}$$

Substituting this form into (3.8) using the orthogonality of $\{\cos(m\pi x)\}$ and canceling $e^{\lambda_m t}$, we obtain, for each m

$$\lambda_m \vec{U}_m = [-(m\pi)^2 \mathbf{D} + \gamma D\mathbf{F}(u^*, v^*)]\vec{U}_m \tag{3.10}$$

where $\mathbf{D}$ is the diagonal matrix of diffusion coefficients. In order for this system to have a nontrivial solution it is necessary that

$$det[\lambda_m \mathbf{I} + (m\pi)^2 \mathbf{D} - \gamma D\mathbf{F}(u^*, v^*)] = 0. \tag{3.11}$$

If solutions to (3.11) give $\mathbf{Re}(\lambda_m) > 0$ for any m, then (u^*, v^*) is an unstable homogeneous steady state of the linearized diffusive system and therefore unstable in the nonlinear diffusive system [1], i.e. unstable to m^{th}-mode perturbations of the form $\vec{v}\cos(m\pi x)$. However if in (3.11), $\mathbf{Re}(\lambda) < 0$ for all m, then the equilibrium point is stable in both the linear and nonlinear diffusive system [28]. Notice that equation (3.11) becomes the eigenvalue equation for the kinetic system (2.3) when $m = 0$. If an equilibrium point was unstable in (2.3) then at $m = 0$ the real part of an eigenvalue for (3.8) will be greater than zero, and thus the equilibrium point will also be unstable in the diffusive system (3.5). Since we are concerned with instability only due to the introduction of diffusion we are interested in linear instability of the equilibria that is solely spatially dependent. So, in the absence of diffusion we are concerned only with the stable equilibria of the kinetic system (2.3).

Table 1 gives the stability of the fixed points in the kinetic system. Recall that z_1 is a zero of f and that w_1 and w_2 are zeros of g. Since p_0 and p_1 are unstable in all cases, the first point to consider in the diffusive system is p_2 with $f(\frac{w_2}{c_{22}}) < 0$. $D\mathbf{F}(p_2)$ is given in equation (2.11). Equation (3.11) evaluated at this equilibrium point is

$$\begin{vmatrix} \lambda_m + d(m\pi)^2 - \gamma f(\frac{w_2}{c_{22}}) & 0 \\ -\gamma \frac{w_2}{c_{22}} g'(w_2) & \lambda_m + (m\pi)^2 - \gamma w_2 g'(w_2) \end{vmatrix} = 0.$$

Since $f(\frac{w_2}{c_{22}}) < 0$ and $g'(w_2) < 0$, the eigenvalues are negative. Thus p_2 remains stable in the diffusive system.

Next point to consider the equilibrium p_3 with $g(\frac{z_1}{c_{11}}) < 0$. Equation (2.12) gives $D\mathbf{F}(p_3)$. Equation (3.11) at this equilibrium point is

$$\begin{vmatrix} \lambda_m + d(m\pi)^2 - \gamma z_1 f'(z_1) & -\gamma \frac{z_1}{c_{11}} f'(z_1) \\ 0 & \lambda_m + (m\pi)^2 - \gamma g(\frac{z_1}{c_{11}}) \end{vmatrix} = 0.$$

Since $f'(z_1) < 0$ and $g(\frac{z_1}{c_{11}}) < 0$ the eigenvalues, λ_m, remain negative for all m, and therefore p_3 is stable.

We consider the interior equilibrium points next. Refer to equation (2.13) for the Jacobian of the kinetic system at these equilibria. The eigenvalue equation is

$$\begin{vmatrix} \lambda_m + d(m\pi)^2 - \gamma c_{11} u_i^* f'(z_1) & -\gamma u_i^* f'(z_1) \\ -\gamma v_i^* g'(w_i) & \lambda_m + (m\pi)^2 - \gamma c_{22} v_i^* g'(w_i) \end{vmatrix} = 0$$

with eigenvalues

$$\begin{aligned} \lambda_{m\pm} &= -\frac{1}{2}[(d+1)(m\pi)^2 - \gamma tr(D\mathbf{F}(q_i))] \\ &\quad \pm \frac{1}{2}\sqrt{[(d+1)(m\pi)^2 - \gamma tr(D\mathbf{F}(q_i))]^2 - 4h_m(d)} \end{aligned} \tag{3.12}$$

where

$$h_m(d) = d(m\pi)^4 - \gamma(dc_{22}v_i^* g'(w_i) + c_{11}u_i^* f'(z_1))(m\pi)^2 + \gamma^2 det(D\mathbf{F}(q_i)). \tag{3.13}$$

From Table 1 we see that q_2 is stable when $det(C) > 0$. Since $f'(z_1) < 0$ and $g'(w_2) < 0$, equations (2.14) - (2.15) give us that $tr(D\mathbf{F}(q_2)) < 0$ and $det(D\mathbf{F}(q_2)) > 0$.

This implies that

$$-\frac{1}{2}[(d+1)(m\pi)^2 - \gamma tr(D\mathbf{F}(q_2))] < 0$$

and from (3.13) that $h_m(d) > 0$, independent of m or d. Therefore $\mathbf{Re}(\lambda_{m_\pm})$ are negative and q_2 with $det(C) > 0$ is stable in the diffusive system.

The last point to consider is q_1 with $det(C) < 0$ and $tr(D\mathbf{F}(q_1)) < 0$. In this case $det(D\mathbf{F}(q_1)) > 0$, since $g'(w_1) > 0$. The above conditions give us that

$$-\frac{1}{2}[(d+1)(m\pi)^2 - \gamma tr(D\mathbf{F}(q_1))] < 0 \tag{3.14}$$

but we see that $h_m(d)$ may change sign. If $h_m(d) < 0$ for some m we see from (3.11) that $\mathbf{Re}(\lambda_{m_+})$ would be positive. This would cause a change in the stability of q_1 due to the introduction of diffusion. We will examine this case further in the next section.

Analytical Bifurcation Analysis

In this section we consider the steady state solution $(u^*, v^*) \equiv q_1$. Since we are interested with a diffusion driven instability we require that q_1 is linearly stable in the absence on any spatial variation. We see from Table 1 that q_1 is linearly stable in the kinetic system provided

$$det(C) < 0 \text{ and } tr(D\mathbf{F}(q_1)) < 0. \tag{3.15}$$

These conditions imply $det(D\mathbf{F}(q_1)) > 0$ (see 2.15).

In the previous section we considered the full reaction diffusion system linearized about the steady states. Equation (3.12) gives the eigenvalues of the linearized system about q_1. For the equilibrium to become unstable to spatial disturbances, with d as the bifurcation parameter, we require $\mathbf{Re}(\lambda_m(d)) > 0$, for some d and for some $m \neq 0$. With (3.15) satisfied we have from (3.14) that

$$-\frac{1}{2}[(d+1)(m\pi)^2 - \gamma tr(D\mathbf{F}(q_1))] < 0.$$

However $h_m(d)$ given in (3.13) may change sign. If $h_m(d) < 0$, then $\mathbf{Re}(\lambda_m(d)) > 0$ and q_1 will have a diffusion driven instability.

First we consider the conditions under which $h_m(d)$ will change sign as a function of d. If we rewrite (3.13) as follows:

$$\begin{aligned} h_m(d) &= d[(m\pi)^4 - \gamma(m\pi)^2 c_{22} v_1^* g'(w_1)] \\ &\quad +(\gamma^2 det(D\mathbf{F}(q_1)) - \gamma(m\pi)^2 c_{11} u_1^* f'(z_1)), \end{aligned} \tag{3.16}$$

then we see that the second term in the sum is positive. Solving $h_m(d) = 0$ for d gives us

$$d = d_m^* \equiv \frac{\gamma[(m\pi)^2 c_{11} u_1^* f'(z_1) - \gamma det(D\mathbf{F}(q_1))]}{(m\pi)^2[(m\pi)^2 - \gamma c_{22} v_1^* g'(w_1)]}. \tag{3.17}$$

For (3.17) to be positive we need

$$(m\pi)^2 - \gamma c_{22} v_1^* g'(w_1) < 0. \tag{3.18}$$

Then for $0 < d < d_m^*$, $h_m(d) > 0$ and for $d > d_m^* > 0$, $h_m(d) < 0$ and at $d = d_m^*$, $h_m(d_m^*) = 0$.

From equation (3.12) we see that $\lambda_{m_+}(d_m^*) = 0$, for $d < d_m^*$, $\mathbf{Re}(\lambda_{m_+}(d)) < 0$ and for $d > d_m^*$, $\lambda_{m_+}(d)$ is real and positive. Thus the m^{th} modal solution of q_1 becomes unstable as d increases through d_m^*. Therefore we say that q_1 becomes unstable due to the introduction of diffusion, or a Turing instability of q_1 occurs at $d = d_m^*$. In the next section we will examine the bifurcating solutions and the bifurcation diagram for the first modal solution, i.e. $m = 1$. Also, from the sign of $\lambda'_{1_+}(d_1^*)$ and the shape of the bifurcation diagram we can determine the local stability of these bifurcating solutions [16].

Local Bifurcation Analysis of Bifurcating Solutions near q_1

In this section we do a local bifurcation analysis about the uniform steady state solution q_1 to determine the shape and direction of the bifurcation diagram with d as

the bifurcation parameter. We use standard perturbation methods, see e.g. Britton [1].

We look for inhomogeneous perturbations of the steady state solutions of (3.5), i.e. solutions to

$$\mathbf{D}\vec{u}_{xx} + \gamma\vec{f} = 0, \tag{3.19}$$

with

$$\vec{u}_x(0) = \vec{u}_x(1) = 0, \tag{3.20}$$

where $\vec{u} = \begin{bmatrix} u \\ v \end{bmatrix}$, $\mathbf{D} = \begin{bmatrix} d & 0 \\ 0 & 1 \end{bmatrix}$ and $\vec{f}(u,v) = \begin{bmatrix} \tilde{f}(u,v) \\ \tilde{g}(u,v) \end{bmatrix} = \begin{bmatrix} uf(y_1) \\ vg(y_2) \end{bmatrix}$. To look for the steady state solution of (3.19) we will expand $\vec{u}$ and d in terms of a small parameter ϵ,

$$\vec{u} = \vec{u}(x) = \sum_{n=0}^{\infty} \vec{u}_n(x)\epsilon^n, \quad d = \sum_{n=0}^{\infty} d_n\epsilon^n, \tag{3.21}$$

where $\vec{u}_0(x) = q_1 = \begin{bmatrix} u_1^* \\ v_1^* \end{bmatrix}$, $d_0 = d_1^*$, and ϵ is a measure of the amplitude of the bifurcating solution. We are free to define ϵ as we choose, and will do so after we develop a few more concepts. Substituting (3.21) into (3.19) and Taylor expanding the system in powers of ϵ, we get a series of equations to solve.

The $O(1)$ equation is

$$\begin{aligned} d_0 u_{0_{xx}} + \gamma\tilde{f}_u(u_0, v_0) &= 0, \\ v_{0_{xx}} + \gamma\tilde{g}_v(u_0, v_0) &= 0, \end{aligned} \tag{3.22}$$

with $\tilde{f}_u(u_0, v_0) = c_{11}u_0 f'(z_1)$ and $\tilde{g}_v(u_0, v_0) = c_{22}v_0 g'(w_1)$. This system is trivially satisfied since $(u_0, v_0) = (u_1^*, v_1^*)$ is a uniform steady state solution to the system.

The $O(\epsilon)$ equations are

$$\begin{aligned} d_0 u_{1_{xx}} + \gamma(\tilde{f}_u(u_0, v_0)u_1 + \tilde{f}_v(u_0, v_0)v_1) &= 0, \\ v_{1_{xx}} + \gamma(\tilde{g}_u(u_0, v_0)u_1 + \tilde{g}_v(u_0, v_0)v_1) &= 0. \end{aligned} \tag{3.23}$$

Let

$$\mathbf{L} = \begin{bmatrix} d_0\frac{d^2}{dx^2} + \gamma\tilde{f}_u(u_0, v_0) & \gamma\tilde{f}_v(u_0, v_0) \\ \gamma\tilde{g}_u(u_0, v_0) & \frac{d^2}{dx^2} + \gamma\tilde{g}_v(u_0, v_0) \end{bmatrix}, \tag{3.24}$$

then the $O(\epsilon)$ equations can be written as $\mathbf{L}\vec{u}_1 = 0$.

To solve this system as well as the higher order equations we need to know more about the kernel of the linear operator $\mathbf{L}$. In this section we choose to look only at the first modal nullvector. Thus we will need to consider vectors for $\mathbf{L}$ in the form

$$\vec{\phi}(d_0) = \begin{bmatrix} a \\ b \end{bmatrix} \cos(m\pi x), \tag{3.25}$$

with $m = 1$. For $\mathbf{L}\vec{\phi}(d_0) = 0$ the parameters a and b must satisfy

$$\begin{aligned} (d_0\pi^2 - \gamma\tilde{f}_u(u_0, v_0))a - \gamma\tilde{f}_v(u_0, v_0)b &= 0, \\ -\gamma\tilde{g}_u(u_0, v_0)a + (\pi^2 - \gamma\tilde{g}_v(u_0, v_0))b &= 0, \end{aligned} \tag{3.26}$$

By the definition of d_0 these two equations are linearly dependent and either could be used to give the ratio of a to b. Next we consider the adjoint operator.

Definition 3.1 *[1] The formal adjoint operator* $\mathbf{L}^*$ *of* $\mathbf{L}$ *is defined to be that operator which satisfies*

$$\langle \mathbf{L}\vec{u}, \vec{v} \rangle = \langle \vec{u}, \mathbf{L}^*\vec{v} \rangle$$

for all $\vec{u}$ *in the domain of* $\mathbf{L}$ *and* $\vec{v}$ *in the domain of* $\mathbf{L}^*$.

The inner product is defined as the $L^2(0, 1)$ inner product, $\langle \vec{u}, \vec{v} \rangle = \int_0^1 \vec{u}^T\vec{v}dx$.

For this system, the adjoint operator is given by

$$\mathbf{L}^* = \begin{bmatrix} d_0\frac{d^2}{dx^2} + \gamma\tilde{f}_u(u_0, v_0) & \gamma\tilde{g}_u(u_0, v_0) \\ \gamma\tilde{f}_v(u_0, v_0) & \frac{d^2}{dx^2} + \gamma\tilde{g}_v(u_0, v_0) \end{bmatrix}.$$

A nullvector for $\mathbf{L}^*$ corresponding to $m = 1$ at the bifurcation point is of the form

$$\vec{\phi}^*(d_0) = \begin{bmatrix} a^* \\ b^* \end{bmatrix} \cos(\pi x),$$

where a^* and b^* must satisfy the linearly dependent equations

$$\begin{aligned}(d_0\pi^2 - \gamma\tilde{f}_u(u_0,v_0))a^* - \gamma\tilde{g}_u(u_0,v_0)b^* &= 0,\\ -\gamma\tilde{f}_v(u_0,v_0)a^* + (\pi^2 - \gamma\tilde{g}_v(u_0,v_0))b^* &= 0.\end{aligned} \tag{3.27}$$

Again either equation can be used to find the ratio of a^* to b^*. The coefficients a, b, a^* and b^* are chosen so that the normalization condition $< \vec{\phi}, \vec{\phi}^* >= 1$ is satisfied. This implies that

$$\frac{1}{2}(aa^* + bb^*) = 1.$$

Since we are doing a bifurcation analysis about a nonzero solution we let ϵ be a measure of the amplitude of the perturbation from this steady state. It is convenient to define ϵ in the following manner:

$$\epsilon =< \vec{u} - \vec{u}_0, \vec{\phi}^*(d_0) > . \tag{3.28}$$

Again we consider the $O(\epsilon)$ equation $\mathbf{L}\vec{u}_1 = 0$. We know from (3.26) that

$$\mathbf{L}\vec{\phi}(d_0) = 0.$$

If we assume that the null space of $\mathbf{L}$ is one-dimensional, then $\vec{u}_1$ must be a scalar multiple of $\vec{\phi}(d_0)$. Let

$$\vec{u}_1 = \alpha\vec{\phi}(d_0)$$

α a constant. Using (3.28) it follows that

$$< \vec{u}_1, \vec{\phi}^*(d_0) >= 1.$$

Substituting $\vec{u}_1 = \alpha\vec{\phi}(d_0)$ into the above inner product gives $\alpha = 1$ and $\vec{u}_1 = \vec{\phi}(d_0)$.

The $O(\epsilon^2)$ equations are,

$$\mathbf{L}\vec{u}_2 + \frac{1}{2}\gamma[\vec{f}_{uu}u_1^2 + 2\vec{f}_{uv}u_1v_1 + \vec{f}_{vv}v_1^2] + \mathbf{D}_1\vec{u}_{1_{xx}} = 0, \tag{3.29}$$

where $\mathbf{D}_n = \begin{bmatrix} d_n & 0 \\ 0 & 0 \end{bmatrix}$ and for the rest of this section all derivatives of $\vec{f}$ are evaluated at (u_0, v_0). Let

$$\vec{F} = -\frac{1}{2}\gamma[\vec{f}_{uu}u_1^2 + 2\vec{f}_{uv}u_1v_1 + \vec{f}_{vv}v_1^2] - \mathbf{D}_1\vec{u}_{1_{xx}},$$

then we can rewrite this system as $\mathbf{L}\vec{u}_2 = \vec{F}$. Using the following theorem [14] we can solve this system.

Theorem 3.2 *(Fredholm Alternative)* $\mathbf{L}\vec{u} = \vec{h}$ *has a solution if and only if* $\left\langle \vec{h}, \vec{\phi}^* \right\rangle = 0$ *for every vector* $\vec{\phi}^*$ *satisfying* $\mathbf{L}^*\vec{\phi}^* = 0$. *Furthermore,* $dimN(\mathbf{L}) = dimN(\mathbf{L}^*)$.

Thus, under the assumption that the dimension of the null space of $\mathbf{L}$ is one-dimensional, $\mathbf{L}\vec{u}_2 = \vec{F}$ has a solution if and only if

$$< \vec{F}, \vec{\phi}^*(d_0) >= 0. \tag{3.30}$$

This inner product corresponds to

$$< -\mathbf{D}_1\vec{u}_{1_{xx}}, \vec{\phi}^*(d_0) > -\frac{1}{2} < \vec{f}_{uu}u_1^2 + 2\vec{f}_{uv}u_1v_1 + \vec{f}_{vv}v_1^2, \vec{\phi}^*(d_0) >= 0. \tag{3.31}$$

First consider the second inner product in (3.31). Each term in this inner product will be a constant multiplying the integral, $\int_0^1 \cos^3(\pi x)dx = 0$. Therefore, (3.31) becomes

$$< -\mathbf{D}_1\vec{u}_{1_{xx}}, \vec{\phi}^*(d_0) >= 0.$$

It follows that $d_1 = 0$.

The $O(\epsilon^3)$ equations are

$$\begin{aligned} \mathbf{L}\vec{u}_3 \;=\; & -\gamma[\vec{f}_{uu}u_1u_2 + \vec{f}_{uv}(u_1v_2 + u_2v_1) + \vec{f}_{vv}v_1v_2] \\ & -\gamma[\frac{1}{6}\vec{f}_{uuu}u_1^3 + \frac{1}{2}\vec{f}_{uuv}u_1^2v_1 + \frac{1}{2}\vec{f}_{uvv}u_1v_1^2 + \frac{1}{6}\vec{f}_{vvv}v_1^3] \\ & -\mathbf{D}_1\vec{u}_{2_{xx}} + \mathbf{D}_2\vec{u}_{1_{xx}}. \end{aligned} \tag{3.32}$$

Letting $d_1 = 0$ and $\vec{G}$ be the right hand side of the above equation gives,

$$\mathbf{L}\vec{u}_3 = \vec{G}.$$

This again has a solution if and only if $\vec{G}$ is orthogonal to the null space of the adjoint, i.e.

$$< \vec{G}, \vec{\phi}^*(d_0) >= 0.$$

Solving for d_2 gives the expression

$$\begin{aligned} d_2 &= \frac{2}{\pi^2 ab}[\gamma < \frac{1}{6}\vec{f}_{uuu}u_1^3 + \frac{1}{2}\vec{f}_{uuv}u_1^2 v_1 + \frac{1}{2}\vec{f}_{uvv}u_1 v_1^2 + \frac{1}{6}\vec{f}_{vvv}v_1^3, \vec{\phi}^*(d_0) > \\ &\quad +\gamma < \vec{f}_{uu}u_1 u_2 + \vec{f}_{uv}(u_1 v_2 + u_2 v_1) + \vec{f}_{vv}v_1 v_2, \vec{\phi}^*(d_0) >]. \end{aligned} \tag{3.33}$$

Since $d_1 = 0$, the sign of d_2 will determine the direction of the bifurcation diagram. It may be positive or negative depending on the other parameters of the system.

Selgrade Model with Diffusion

In this section we consider the Selgrade model introduced in Chapter 2 with diffusion introduced. We examine the populations of pioneer and climax species but now a spatial dimension is included. We will consider the effects of diffusion on the stability of the interior equilibrium point q_1 and examine possible bifurcations at this point. We also discuss the stability of the bifurcating spatially heterogeneous steady state solutions and give numerically generated results for the bifurcation diagrams.

The specific model equations are of the form (3.3)-(3.4) with fitness functions are as in the kinetic model equations (2.23) and (2.24). Again we consider this model with weighted density parameters $c_{22} = 1$ and $c_{11} \in (0, 1)$. As stated before, there is nothing special about this arrangement, the analysis for varying c_{22} and fixing c_{11} can be done in a similar manner.

As noted in the previous sections the introduction of diffusion into this system does not change the stability of any of the equilibria of the kinetic system except for q_1. At this equilibrium point the introduction of diffusion may cause the once stable point to become unstable. The parameter range to consider q_1 over would be $\frac{1}{6} < c_{11} < \frac{1}{2}$, since for these values of c_{11}, q_1 is both biologically feasible and stable.

We see that a Turing bifurcation occurs at q_1 for $d > 0$, when (3.18) is satisfied. For this specific system at q_1 with $m = 1$, (3.18) becomes

$$\pi^4 - \gamma\pi^2\left[\frac{1-2c_{11}}{4(1-c_{11})}\right] < 0.$$

This inequality along with the bounds on c_{11} puts a lower bound on γ, i.e. $\gamma > 5\pi^2$. d_1^* is given as

$$d_1^* = \frac{4c_{11}\pi^2\gamma + \gamma^2(1-2c_{11})}{\gamma\pi^2(1-2c_{11}) - 4\pi^4(1-c_{11})}.$$

The stability analysis starts with looking at the eigenvalues and functions of the linear system. The eigenfunction are of the same form along with the equations for a, b, a^*, and b^* as developed in the previous section. In particular we want to look for solutions of the $O(\epsilon^n)$ equations with the specific fitness functions of this example. Again we find from the $O(\epsilon)$ equation that $\vec{u}_1 = \begin{bmatrix} a \\ b \end{bmatrix} cos(\pi x)$ and from the $O(\epsilon^2)$ equation that $d_1 = 0$. It is in the $O(\epsilon^3)$ equation that having specific fitness functions allows us to go farther in the analysis of the stability of the bifurcating solutions and the shape of the bifurcation curve.

Consider the first inner product of the right hand side of equation (3.33). This inner product evaluated for the specific fitness functions at q_1 is given by

$$\frac{3}{8}\gamma \begin{pmatrix} a^*[\frac{1}{6}(\frac{4c_{11}^2(4c_{11}-3)}{c_{11}-1})a^3 + \frac{1}{2}(\frac{4c_{11}(3c_{11}-2)}{c_{11}-1})a^2b \\ +\frac{1}{2}(\frac{4(2c_{11}-1)}{c_{11}-1})ab^2 + \frac{1}{6}(\frac{4}{c_{11}-1})b^3] \\ +b^*[\frac{1}{6}(\frac{5(2c_{11}-1)}{16(c_{11}-1)})a^3 + \frac{1}{2}(\frac{2c_{11}-7)}{-16(c_{11}-1}))a^2b \\ +\frac{1}{2}(\frac{14c_{11}-19)}{-16(c_{11}-1)})ab^2 + \frac{1}{6}(\frac{26c_{11}-31}{-16(c_{11}-1)})b^3] \end{pmatrix}. \tag{3.34}$$

The next inner product requires that we first solve for u_2 and v_2. Using equation (3.29) with $d_1 = 0$ we get that

$$\mathbf{L}\vec{u}_2 = -\frac{1}{2}\gamma[\vec{f}_{uu}u_1^2 + 2\vec{f}_{uv}u_1v_1 + \vec{f}_{vv}v_1^2], \tag{3.35}$$

where $u_1 = a\cos(\pi x)$ and $v_1 = b\cos(\pi x)$. From the form of the right hand side of (3.35) we can assume u_2 and v_2 are of the form

$$\begin{aligned} u_2 &= \alpha_0 + \alpha_1\cos(\pi x) + \alpha_2\cos(2\pi x) \\ v_2 &= \beta_0 + \beta_1\cos(\pi x) + \beta_2\cos(2\pi x) \end{aligned} \tag{3.36}$$

We solve for α_n and β_n by substituting (3.36) into (3.35) and equating coefficients of the $\cos(n\pi x)$ terms. We see that α_1 and β_1 are zero and that α_0, β_0, α_2 and β_2 are nonzero. Now with $\alpha_1 = \beta_1 = 0$ substituted into (3.36) we can evaluate the next inner product of (3.33). This inner product is

$$\gamma\begin{pmatrix} \left[\frac{a\alpha_0}{2} + \frac{a\alpha_2}{4}\right]\left[a^*\left(\frac{2c_{11}(3c_{11}-2)}{1-c_{11}}\right) + b^*\left(\frac{-3(1-2c_{11})}{8(1-c_{11})}\right)\right] \\ + \left[\frac{1}{2}(a\beta_0 + b\alpha_0) + \frac{1}{4}(a\beta_2 + b\alpha_2)\right]\left[a^*\left(\frac{2(2c_{11}-1)}{1-c_{11}}\right) + b^*\left(\frac{1+2c_{11}}{8(1-c_{11})}\right)\right] \\ + \left[\frac{b\beta_0}{2} + \frac{b\beta_2}{4}\right]\left[a^*\left(\frac{2}{1-c_{11}}\right) + b^*\left(\frac{5-2c_{11}}{8(1-c_{11})}\right)\right] \end{pmatrix}. \tag{3.37}$$

In each of these inner products we can rewrite the parameters a, a^*, b^*, α_0, α_2, β_0 and β_2 in terms of γ, c_{11} and b (b is an arbitrary choice since any of the parameters, a, a^* or b^* could be used in place of b by using equations (3.26) and (3.27)). Therefore from (3.33), we see that d_2 is also a function of γ, c_{11} and b. Recall that $\gamma = \frac{L^2}{D_2}$ represents a measure of the domain size for fixed values of D_2 and that c_{11} represents the intra-species competition of the pioneer species. By choosing $b = 1$ and using AUTO [19] we can find a curve such that $d_2 = 0$ in the γ-c_{11} plane given in Figure 6.

Also in this figure is a graph of the curve where d_2 is undefined along which d_1^* for the first mode is equal to d_2^* of the second mode. On this curve the null space

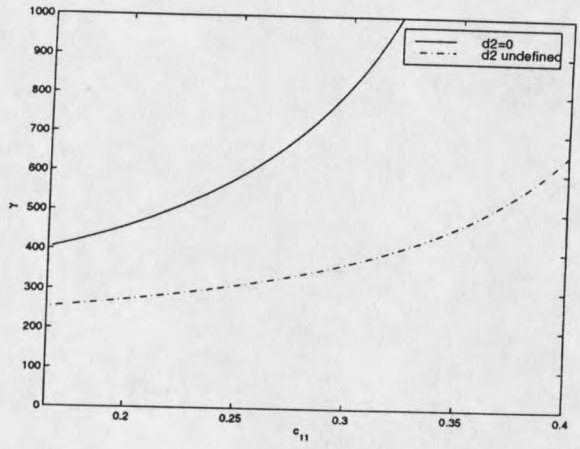

Figure 6: Graph of $d_2 = 0$ and d_2 undefined.

of $\mathbf{L}$ is at least two-dimensional, instead of the assumed one dimensional null space consisting of the first mode.

Looking at Figure 7 we see the for γ below the d_2 undefined curve in Figure 6 that $d_2 < 0$. For γ between the d_2 undefined and $d_2 = 0$ curves we have $d_2 > 0$ and for γ above $d_2 = 0$ curve, $d_2 < 0$.

The following two Figures 8 and 9 show the bifurcation diagram for the pioneer species in the Selgrade model using d as the bifurcation parameter with $c_{11} = 0.25$ and two different γ values. In Figure 8 $\gamma = 320$, for which $d_2 > 0$ value and the bifurcating branch opens to the right.

For the same model, in Figure 9 we have $\gamma = 240$ which gives us $d_2 < 0$ so that the bifurcating branch of solutions opens to the left. Both bifurcation diagrams where computed using AUTO [19].

The stability of these bifurcating solutions not only depend on the sign of d_2 but also on the stability of the equilibrium point before and after the bifurcation. For some parameter values the mode one solution is not the first modal solution to bifurcate. In Figure 10 we have graphed the bifurcating eigenvalue for the system with

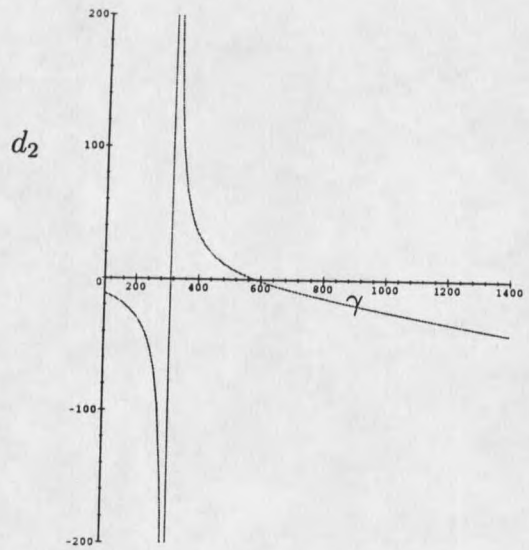

Figure 7: Graph of d_2 verses γ for $c_{11} = 0.25$.

$c_{11} = 0.25$, $\gamma = 240$ and $d = d_1^*$, the bifurcating parameter value for $m = 1$. These values have been substituted into equation (3.12) and $\lambda_+(m)$ is plotted. In Figure 10 a positive change in d would result in a bifurcation of the mode one solution occurring before any other modes.

Figure 11 is again a graph of $\lambda_+(m)$ with the same c_{11} and d values but for $\gamma = 320$. From this figure we see for $m = 2$ that $\lambda_+(2) > 0$ and $\lambda_+(1) = 0$. Thus the mode two solution is the first mode to bifurcate with the mode one solution bifurcating for a larger value of d.

Figure 12 shows the bifurcation diagram for the Selgrade model with the same parameter values as those in Figure 11. In this figure the dashed line corresponds to the mode two solutions and shows these solutions will bifurcate off the q_1 solution for

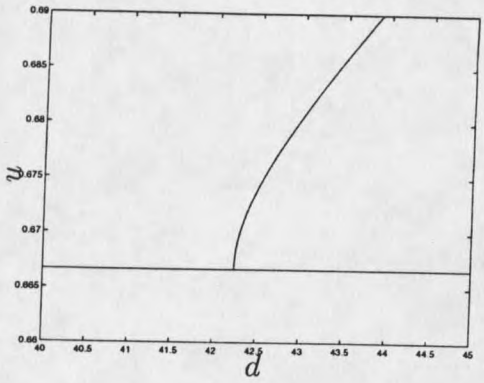

Figure 8: Bifurcation diagram for $c_{11} = 0.25$, $\gamma = 320$.

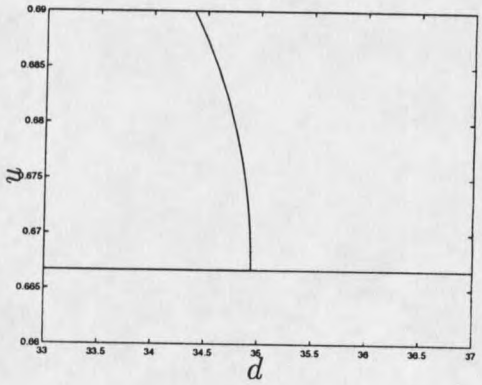

Figure 9: Bifurcation diagram for $c_{11} = 0.25$, $\gamma = 240$.

smaller values of d than the mode one solutions designated by the solid line.

In this chapter we have considered a system of reaction-diffusion equations to model the interaction of a pioneer and climax species. We have found that the q_1 equilibrium point is the only uniform steady state that could bifurcate from a stable equilibrium to an unstable equilibrium via a Turing bifurcation. Using $d = \frac{D_1}{D_2}$, the ratio of the diffusion coefficients, as the bifurcation parameter we demonstrated that the m^{th} modal solution of q_1 will go unstable for $d > d_m^*$. The stability of the inhomogeneous solutions is determined by the stability of q_1 near the bifurcation point and the sign of the $O(\epsilon^3)$ term in the ϵ expansion of the bifurcation parameter, d.

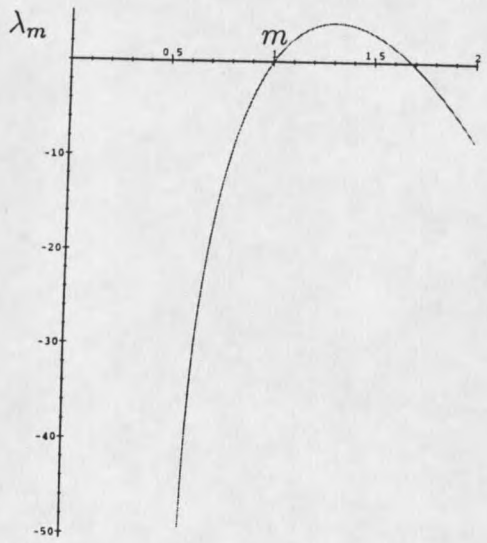

Figure 10: Graph of λ_m verses m for $c_{11} = .25$, $\gamma = 240$ and $d = d_1^*$.

We found that this term, d_2, is dependent on c_{11} and γ, and in the Selgrade model it can take on both positive and negative values. We have also shown numerically that the mode one solution for the Selgrade model is not always the first inhomogeneous solution to bifurcate for increasing values of d. In Figures 11 and 12 we see with the given c_{11} and γ values the mode two solution bifurcated at smaller d values than that of the mode one solution. Numerical investigations for the Selgrade model as of yet have not shown any formation of stable spatially heterogeneous equilibria, however an exhaustive search in the parameter space has not been done.

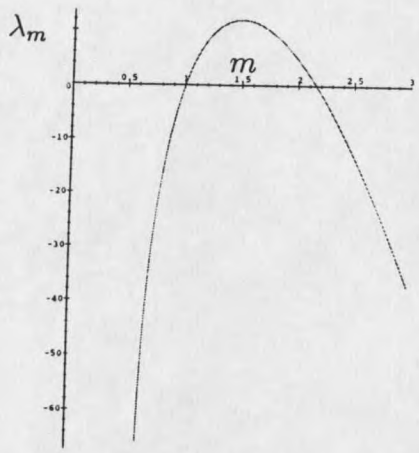

Figure 11: Graph of λ_m verses m for $c_{11} = .25$, $\gamma = 320$ and $d = d_1^*$.

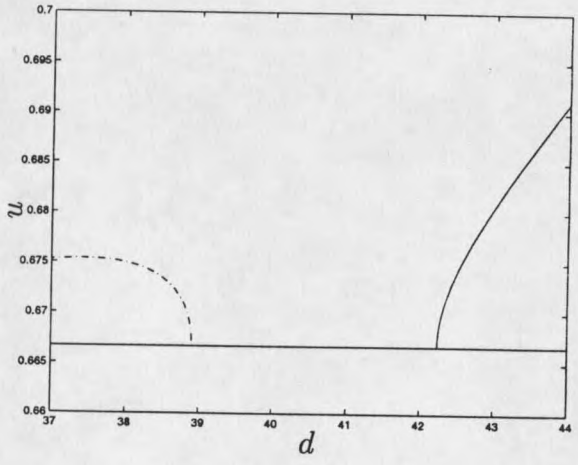

Figure 12: Bifurcation Diagram for $c_{11} = .25$ and $\gamma = 320$, mode two solutions are shown with dashed line, mode one solutions with solid line.

CHAPTER 4

Traveling Waves

Traveling waves make up an important class of solutions of reaction-diffusion equations. They are solutions that move over space while maintaining a characteristic "shape" or profile. Many phenomena arising in various physical, biological and ecological contexts can be modeled by traveling waves. For example, shock waves, nerve impulses, various oscillatory chemical reactions, insect dispersal, and interacting populations where spatial effects are important.

A mathematical feature associated with a traveling wave solution is that the partial differential equation problem reduces to a set of ordinary differential equations. If we let $u(x,t)$ represent a traveling wave, then the shape of this solution will remain the same for all time and will move at a constant speed c. For an observer moving at the same speed and direction, the wave will appear to be stationary. The connection between the stationary and the moving observer is

$$u(x,t) = U(z), \quad \text{where } z = x - ct. \tag{4.1}$$

In this case, with $c > 0$, the wave is moving to the right and z is the moving observers coordinate. See Figure 13 for an example of the stationary and moving observers perspective [3].

Note that $U(z)$ is now a function of the single variable z and it follows that $u_x = U'$ and $u_t = -cU'$, where prime represents the derivative with respect to z. For our model to be physically realistic, $U(z)$ has to be bounded for all z and nonnegative because it still represents the population density. The wave solutions

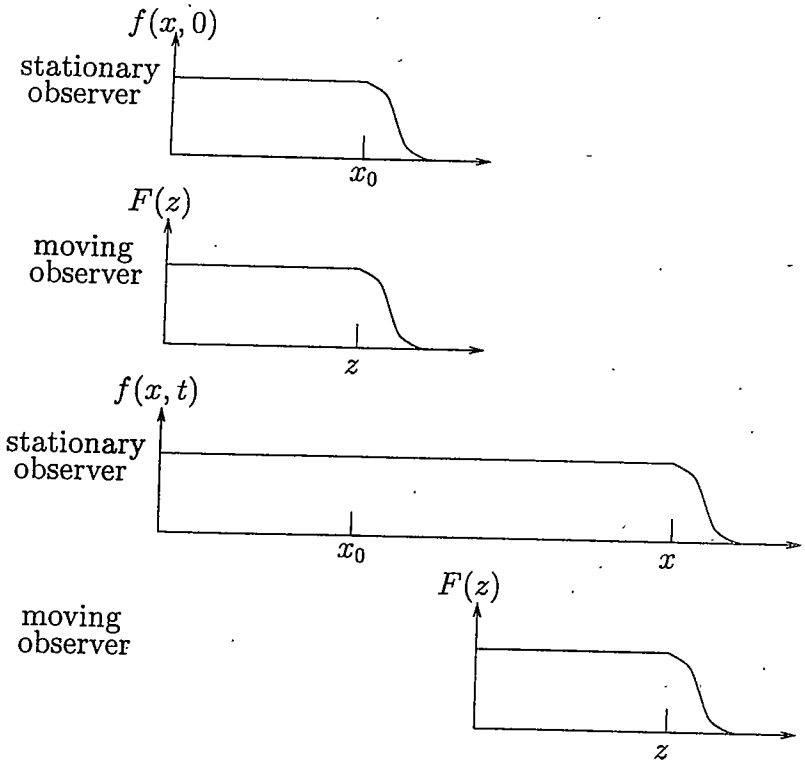

Figure 13: Traveling Waves in stationary and moving descriptions.

we will be concerned with will represent a smooth transition between two different steady states, i.e. a heteroclinic connection between the steady states.

Substituting $u(x,t) = U(z)$ and $v(x,t) = V(z)$ into (3.3) we get the following system of second-order ordinary differential equations

$$\begin{aligned} -cU' &= D_1U'' + Uf(Y_1), \\ -cV' &= D_2V'' + Vg(Y_2) \end{aligned} \tag{4.2}$$

or

$$\begin{aligned} D_1U'' + cU' + Uf(Y_1) &= 0, \\ D_2V'' + cV' + Vg(Y_2) &= 0, \end{aligned} \tag{4.3}$$

where Y_1 and Y_2 are y_1 and y_2 evaluated at $U(z)$ and $V(z)$.

In the following sections we will look for traveling wave solutions of (4.3). In the first section we will examine traveling waves that occur along an axis, i.e. traveling waves under the assumption that one of the species is not present. In the second section we will look at the existence of a slow moving traveling wave in the positive quadrant connecting two steady states of the system. First we use the method of matched asymptotic expansion which suggests the existence of such a traveling wave then we use geometric singular perturbation theory to prove the existence of such a wave.

Traveling Waves Along an Axis

A traveling wave along the axes would biologically represent the natural movement of a population in the absence of the competing species. We will be looking for connections between the steady states.

Traveling Waves Along the U Axis

In this section we will look for traveling waves along the pioneer or u-axis. For this we will assume $v = 0$ in (3.3). We are thus considering a single species model given by

$$u_t = D_1 u_{xx} + u f(y_1), \quad y_1 = c_{11} u. \tag{4.4}$$

The zero of f is given by $y_1 = c_{11}u = z_1$ or $u = \frac{z_1}{c_{11}}$. Notice that f is now dependent only on u. For notational purposes we let $\tilde{f}(u) = u f(y_1)$.

If a traveling wave solution to (4.4) exists it can be written in the form

$$u(x,t) = U(z), \quad z = x - ct, \tag{4.5}$$

where c is the wave speed. We will determine the sign of c at a later point. Substituting (4.5) into (4.4) we obtain,

$$D_1 U'' + cU' + \tilde{f}(U) = 0, \tag{4.6}$$

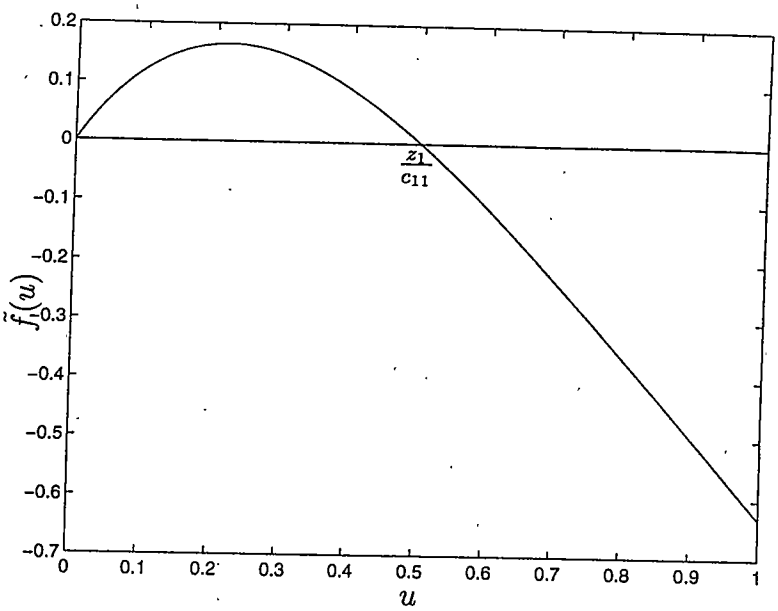

Figure 14: $\tilde{f}(u)$

where again the prime represents the derivative with respect to z. We are interested in traveling wave solutions of (4.4) corresponding to connecting orbits of (4.6). Thus we have a nonlinear eigenvalue problem to determine values of c such that a non-negative solution $U(z)$ of (4.6) exists which satisfies

$$\lim_{z\to\infty} U(z) = 0, \quad \lim_{z\to-\infty} U(z) = \frac{z_1}{c_{11}}. \tag{4.7}$$

We will analyze (4.6) via phase-plane methods. To that end let

$$W = \frac{dU}{dz}.$$

then (4.6) becomes

$$\begin{aligned} \frac{dU}{dz} &= W, \\ \frac{dW}{dz} &= -\frac{c}{D_1}W - \frac{1}{D_1}\tilde{f}(U). \end{aligned} \tag{4.8}$$

The equilibria of (4.8) are $(U_1, W_1) = (0, 0)$ and $(U_2, W_2) = (\frac{z_1}{c_{11}}, 0)$.

Next we consider the stability of these equilibria. The Jacobian of (4.8) is given by

$$J_i = \begin{bmatrix} 0 & 1 \\ -\frac{1}{D_1}\tilde{f}_U(U_i) & -\frac{c}{D_1} \end{bmatrix}, \qquad i = 1, 2, \tag{4.9}$$

with eigenvalues

$$\lambda_{i\pm} = \frac{1}{2}\left(-\frac{c}{D_1} \pm \sqrt{\left(\frac{c}{D_1}\right)^2 - \frac{4}{D_1}\tilde{f}_U(U_i)}\right). \tag{4.10}$$

The real part of these eigenvalues depend on the sign of c and the sign of $\tilde{f}_U(U_i)$. Recalling that f, the pioneer fitness function, is always a decreasing function of its argument we see that $\tilde{f}_U(0) > 0$ and that $\tilde{f}_U(\frac{z_1}{c_{11}}) < 0$. See Figure 14 for an example of a graph of $\tilde{f}$.

Next we determine the sign of c. First multiply (4.6) by U' and then integrate from $-\infty$ to ∞ to obtain

$$\int_{-\infty}^{\infty} \left[D_1 U' U'' + c(U')^2 + U'\tilde{f}(U)\right] dz = 0.$$

Using the limits in (4.7) and the fact that we are connecting steady states so that $U'(\pm\infty) = 0$, the above integrates to give us

$$\begin{aligned} c\int_{-\infty}^{\infty} (U')^2 dz &= -\int_{-\infty}^{\infty} \tilde{f}(U)U' dz \\ &= -\int_{\frac{z_1}{c_{11}}}^{0} \tilde{f}(U) dU \\ &= \int_{0}^{\frac{z_1}{c_{11}}} \tilde{f}(U) dU. \end{aligned}$$

Thus the sign of c is the same as the sign of $\int_0^{\frac{z_1}{c_{11}}} \tilde{f}(U)dU$, which by Figure (14) we see is positive. Therefore $c > 0$. It is important to mention that if we chose to look for a connection from 0 to $\frac{z_1}{c_{11}}$ such that $\lim_{z\to-\infty} U(z) = 0$ and $\lim_{z\to\infty} U(z) = \frac{z_1}{c_{11}}$, c would be of the opposite sign.

Now using $c > 0$ and our previous work we see from equation (4.10) that $(\frac{z_1}{c_{11}}, 0)$ is a saddle for all c and that $(0, 0)$ is a stable spiral for $c^2 < 4D_1\tilde{f}_U(0)$ and a

stable node for $c^2 \geq 4D_1\tilde{f}_U(0)$. It is not biologically feasible for $(0,0)$ to be a spiral because we would then get negative values for $U(z)$. Hence we need only consider the case where $c^2 \geq 4D_1\tilde{f}_U(0)$. Since $(\frac{z_1}{c_{11}}, 0)$ is a saddle point, there are exactly two trajectories which tend to this point as $z \to -\infty$ in the direction of the eigenvector corresponding to the positive (unstable) eigenvalue, λ_+, one with $W > 0$ and one with $W < 0$. This eigenvector is given by $(U_+, W_+)^T = \alpha(1, \lambda_+)^T$ for any constant α. Choosing $\alpha < 0$ will give us the trajectory in the fourth quadrant of the UW-phase plane.

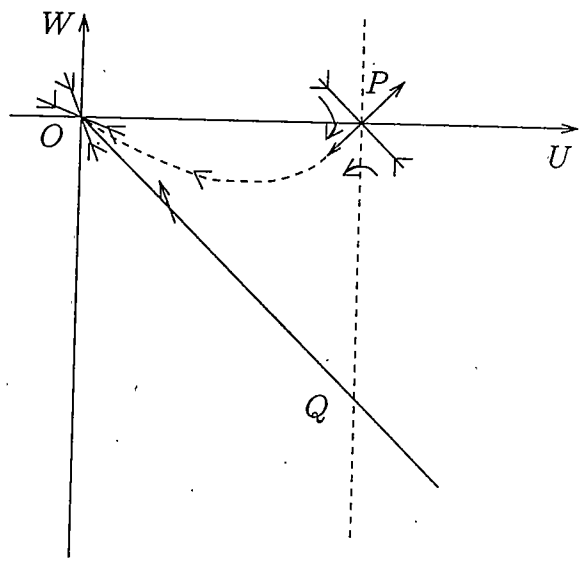

Figure 15: The phase plane for traveling wave solutions with triangle OPQ.

If we consider the triangle in Figure 15 we will show that for given values of c, $c^2 \geq 4D_1\tilde{f}_U(0)$, no trajectory may exit this triangle. It would then follow that the marked trajectory must tend to 0 as $z \to \infty$ and there must be traveling wave solutions for these values of c. On triangle OPQ, O and P are the equilibria points $(0,0)$ and $(\frac{z_1}{c_{11}}, 0)$ respectively. The point Q corresponds to the point where the line $W = -mU$ intersects the line $U = \frac{z_1}{c_{11}}$, thus Q has the coordinates $(\frac{z_1}{c_{11}}, -m\frac{z_1}{c_{11}})$.

The slope, $-m$, of the line $W = -mU$ will be determined later. Along the line OP, $W \equiv 0$ and along the line PQ, $U \equiv \frac{z_1}{c_{11}}$. On PQ, $U' < 0$ since $U' = W$ and $W < 0$ on PQ. Looking at OP we see that $W' < 0$ since $W' = -\frac{1}{D_1}\tilde{f}(U)$ and $\tilde{f}(U) > 0$ for $0 < U < \frac{z_1}{c_{11}}$ along OP. So it remains only to prove that no trajectories cross OQ going out of the triangle OPQ for some value of m. This will be true if $W' + mU' > 0$ on OQ. On OQ

$$\begin{aligned} W' + mU' &= -\frac{c}{D_1}W - \frac{1}{D_1}\tilde{f}(U) + mW \\ &= -\frac{c}{D_1}(-mU) - \frac{1}{D_1}\tilde{f}(U) + m(-mU) \\ &\geq -\frac{c}{D_1}(-mU) - \frac{1}{D_1}kU + m(-mU) \\ &= -(m^2 - \frac{c}{D_1}m + \frac{k}{D_1})U, \end{aligned}$$

where

$$k = \sup_{U \in (0, \frac{z_1}{c_{11}})} \frac{\tilde{f}(U)}{U} \geq \tilde{f}'(0) \tag{4.11}$$

Thus $W' + mU' > 0$ on OQ if

$$m^2 - \frac{c}{D_1}m + \frac{k}{D_1} < 0. \tag{4.12}$$

Therefore if this quadratic has two real zeros and m lies between them the inequality on $W' + mU'$ will be satisfied. If we consider the zeros of (4.12), we see that the quadratic will have two real zeros if $c^2 > \frac{4}{D_1}k$. Note that for c values that satisfy this inequality we still get that $c^2 > \frac{4}{D_1}\tilde{f}'(0)$ $(k \geq \tilde{f}'(0))$ so $(0,0)$ is still a stable node. For such c values there exist m values such that the unstable manifold coming from the saddle point $(\frac{z_1}{c_{11}}, 0)$ can not leave the triangle OPQ. We want to show that for these c and m values the solution that lies on the unstable manifold of the saddle point $(\frac{z_1}{c_{11}}, 0)$ in the fourth quadrant must then limit on $(0,0)$ as $z \to \infty$. To this end we state the following definition and theorems.

Definition 4.1 *[31] A point $x_0 \in \mathbb{R}^n$ is called an ω limit point of $x \in \mathbb{R}^n$, denoted $\omega(x)$, if there exists a sequence $\{z_i\}$, $z_i \to \infty$ such that the flow,*

$$\phi(z_i, x) \to x_0.$$

α limit points are defined similarly by taking a sequence $\{z_i\}$, $z_i \to -\infty$. The set of all ω limit points of a flow is called the ω limit set. The α limit set is similarly defined.

The first theorem we need is the Pioncaré-Bendixson Theorem.

Theorem 4.2 *(Pioncaré-Bendixson)[9] A nonempty compact ω or α limit set of a planar flow, which contains no equilibrium points, is a closed orbit.*

For the next theorem we let

$$\begin{aligned} \dot{x} &= h(x, y), \\ \dot{y} &= k(x, y) \end{aligned} \tag{4.13}$$

where h and k are sufficiently smooth.

Theorem 4.3 *(Bendixson Criterion)[9] If on a simply connected region $D \subseteq \mathbb{R}^2$ the expression $\frac{\partial h}{\partial x} + \frac{\partial k}{\partial y}$ is not identically zero and does not change sign then (4.13) has no closed orbits lying entirely in D.*

To prove our solution tends to $(0, 0)$ as $z \to \infty$ we assume the contrary. Let $p \in \mathbb{R}^2$ be a point on the unstable manifold of $(\frac{z_1}{c_{11}}, 0)$ in the triangle OPQ. Choose c and m such that p remains in OPQ as $z \to \infty$ but does not limit on $(0, 0)$. Then the ω limit set of p does not contain the equilibrium $(0, 0)$, so by Theorem 4.2 the ω limit set of p must be a closed orbit. However, if we consider system (4.8) we see that

$$\frac{\partial h}{\partial U} + \frac{\partial k}{\partial W} = -\frac{c}{D_1} \neq 0,$$

and does not change sign in OPQ, a simply connected region in $\mathbb{R}^2$. So by Theorem 4.3 there are no closed orbits in OPQ. This is a contradiction, thus it must be that the ω limit set of p is an equilibrium point. By the direction fields and the continuity of the flow we see that the only such equilibrium point it could be is $(0,0)$. Hence we have the connection between $(\frac{z_1}{c_{11}}, 0)$ and $(0,0)$ and therefore the existence of a traveling wave form $\frac{z_1}{c_{11}}$ to 0.

Figure 16, developed using pplane [20] in Matlab, illustrates the phase plane trajectories for this case. As we see from this figure there is a trajectory from $(\frac{z_1}{c_{11}}, 0)$ to $(0,0)$ lying entirely in the quadrant $U \geq 0$, $U' \leq 0$ with $0 \leq U \leq \frac{z_1}{c_{11}}$ for all wave speeds such that $c^2 \geq 4D_1\tilde{f}_U(0)$. Thus for these c values we get a biologically feasible traveling wave solution to (4.6) with (4.10) satisfied.

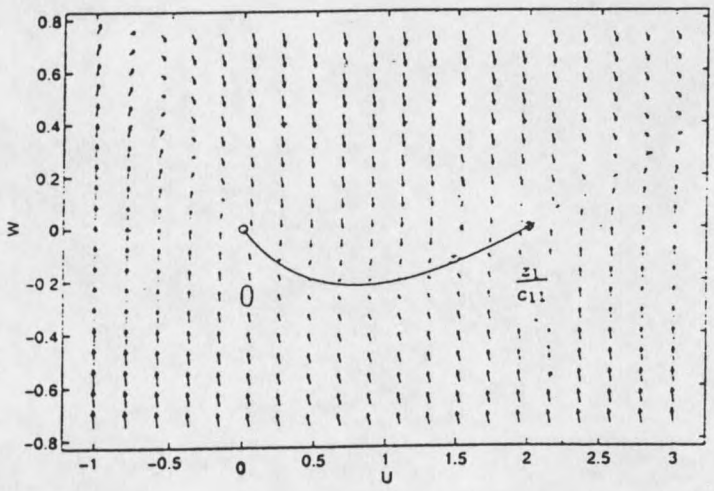

Figure 16: Phase plane portrait of connecting trajectory from $\frac{z_1}{c_{11}}$ to 0 with wave speed $c \geq \sqrt{4D_1\tilde{f}'(0)}$. Calculated for the Selgrade model with $c_{11} = 0.25$, $c = 3$, $D_1 = 1$

Figure 17 gives an example of a traveling wave front solution to (4.6) with $c^2 \geq 4D_1\tilde{f}_U(0)$, $c > 0$. This figure was developed using xtc [4] and the Selgrade

model with no flux boundary conditions, initial condition $u = 2.5 * H(6 - x)$ and using method of lines with a Gear integrator. A large but finite domain was used to compute an approximation of the traveling wave. The arrow represents the direction of the wave to a stationary observer. As the wave sweeps through the domain from left to right the population density approaches the value $\frac{z_1}{c_{11}}$ at any particular location.

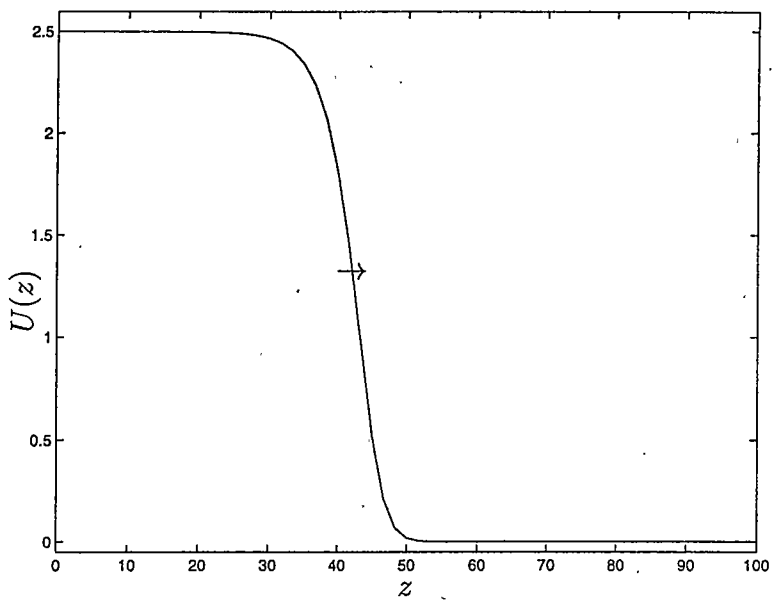

Figure 17: Example of Traveling wave front for the Pioneer species connecting $\frac{z_1}{c_{11}}$ to 0. The wave is moving to the right over time. Selgrade model with $c_{11} = 0.2$, $D_1 = 1$

Traveling Waves Along the V Axis

In this section we will consider possible traveling wave solutions along the climax or v-axis. Again these waves represent possible movement of the climax species in the absence of the pioneer species. Letting $u = 0$ in (3.3) we have

$$v_t = D_2 v_{xx} + vg(y_2), \quad y_2 = c_{22}v. \tag{4.14}$$

The zeros of $vg(y_2)$ are $v = 0$, $v = \frac{w_1}{c_{22}}$ and $v = \frac{w_2}{c_{22}}$. Again we now have a single species model with g dependent on v only. We will let $\tilde{g}(v) = vg(y_2)$.

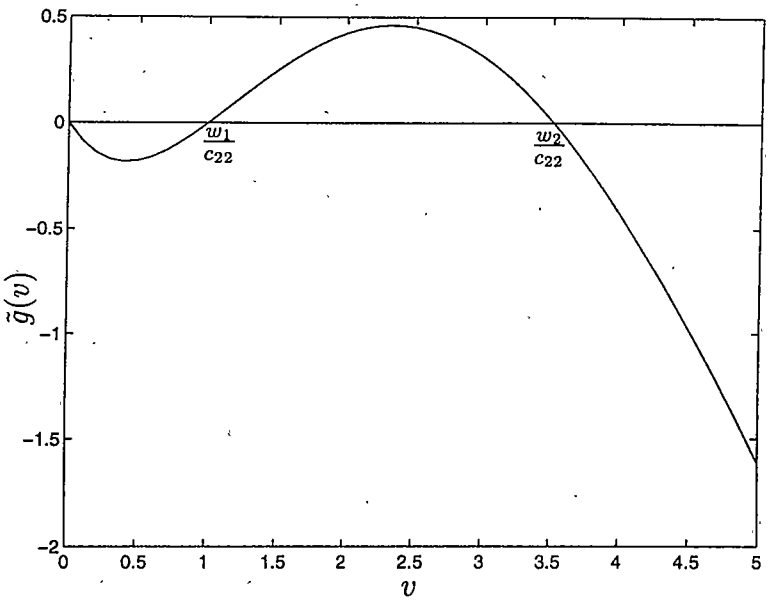

Figure 18: $\tilde{g}(v)$

To look for traveling wave solutions of (4.14) we set

$$v(x,t) = V(z), \quad z = x - ct, \tag{4.15}$$

obtaining

$$D_2 V'' + cV' + \tilde{g}(V) = 0. \tag{4.16}$$

Prime is as before, the derivative with respect to z. The corresponding autonomous system is given by

$$\begin{aligned} V' &= P \\ P' &= -\frac{c}{D_2}P - \frac{1}{D_2}\tilde{g}(V). \end{aligned} \tag{4.17}$$

This system has three equilibria, $(V_0, P_0) = (0,0)$, $(V_1, P_1) = (\frac{w_1}{c_{22}}, 0)$ and $(V_2, P_2) = (\frac{w_2}{c_{22}}, 0)$. To determine the stability of these equilibria we consider the Jacobian of the system (4.17), given by:

$$J_i = \begin{pmatrix} 0 & 1 \\ -\frac{1}{D_2}\tilde{g}_V(V_i) & -\frac{c}{D_2} \end{pmatrix}, \tag{4.18}$$

whose eigenvalues are given by

$$\lambda_{i\pm} = \frac{1}{2}\left[-\frac{c}{D_2} \pm \sqrt{\left(\frac{c}{D_2}\right)^2 - \frac{4}{D_2}\tilde{g}_V(V_i)}\right]. \tag{4.19}$$

In Figure 18 we see a graph of $\tilde{g}$. Now $\tilde{g}$ is such that $\tilde{g}_V(0) < 0$, $\tilde{g}_V(\frac{w_1}{c_{22}}) > 0$ and $\tilde{g}_V(\frac{w_2}{c_{22}}) < 0$ with $\tilde{g}(V) < 0$ for $V \in (0, \frac{w_1}{c_{22}})$ and $\tilde{g}(V) > 0$ for $V \in (\frac{w_1}{c_{22}}, \frac{w_2}{c_{22}})$. The linear analysis gives us that $(0,0)$ and $(\frac{w_2}{c_{22}}, 0)$ are saddle points for all values of c and that $(\frac{w_1}{c_{22}}, 0)$ is a spiral for $c^2 < 4D_2\tilde{g}_V(\frac{w_1}{c_{22}})$ and a node when $c^2 \geq 4D_2\tilde{g}_V(\frac{w_1}{c_{22}})$.

We look for a traveling wave connecting the equilibria $(0,0)$ to $(\frac{w_2}{c_{22}}, 0)$. This will correspond to a solution, $V(z)$, for the system (4.17) which satisfies

$$\lim_{z\to-\infty} V(z) = 0, \quad \lim_{z\to\infty} V(z) = \frac{w_2}{c_{22}}. \tag{4.20}$$

A similar calculation as that used in the previous subsection can be used here to determine the sign of c the wave speed. When we solve for c in this case we obtain

$$c = \frac{-\int_0^{\frac{w_2}{c_{22}}} \tilde{g}(V)dV}{\int_{-\infty}^{\infty}(V')^2 dz}.$$

Thus c is the opposite sign as $\int_0^{\frac{w_2}{c_{22}}} \tilde{g}(V)dV$. Again if we had chosen the opposite direction for a connection between 0 and $\frac{w_2}{c_{22}}$ we would find that c would be the same sign as $\int_0^{\frac{w_2}{c_{22}}} \tilde{g}(V)dV$. We will assume that $\int_0^{\frac{w_2}{c_{22}}} \tilde{g}(V)dV > 0$ giving $c < 0$ with the limits in (4.20) satisfied.

Looking at the phase plane diagram of (4.17), (Figure 19, developed using pplane [20] in Matlab) we see that to get a trajectory to connect $(0,0)$ to $(\frac{w_2}{c_{22}}, 0)$ it would have to come from the unstable manifold of $(0,0)$ and connect to the stable manifold of $(\frac{w_2}{c_{22}}, 0)$. Call this trajectory, $T(c)$. We will prove that such a connection exist for a unique value of c. To do this we need to first develop a lemma stated in [1]and [7].

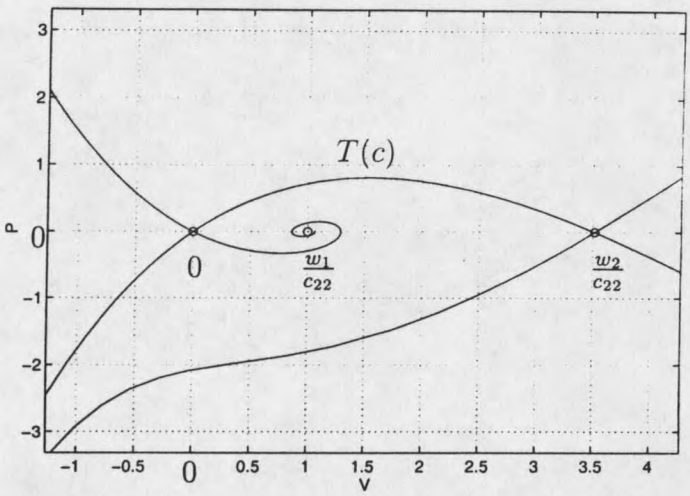

Figure 19: Phase plane portrait for climax species $T(c)$ depicts the connecting trajectory corresponding to the traveling wave solution from 0 to $\frac{w_2}{c_{22}}$ for the PDE system. Calculated for Selgrade model with $c_{22} = 1$, $D_2 = 1$, $c = 0.33228$.

Let us consider trajectory $T(c)$ in Figure 19 for $V \in (0, \frac{w_2}{c_{22}})$. This trajectory is monotone since it lies in the region where $V' = P > 0$. Thus there is a well defined function $Q(V)$ such that $Q(V) = \frac{dV}{dz}$ or $Q(V(z)) = P(z)$. Then

$$Q' = \frac{dQ}{dV} = \frac{P'}{V'} = \frac{-\frac{c}{D_2}Q - \frac{1}{D_2}\tilde{g}}{Q}$$

so that

$$-Q' - \frac{1}{D_2}\frac{\tilde{g}}{Q} = \frac{c}{D_2} \tag{4.21}$$

with $Q(\frac{w_2}{c_{22}}) = 0$. Notice Q' is bounded for Q bounded away form zero, thus the trajectory, $T(c)$, will be bounded. We can now state and prove the following lemma.

Lemma 4.4 *[1] Let $\tilde{g}(V) \geq 0$ for $(\frac{w_2}{c_{22}} - V)$ small and positive. Let $Q_i(V)$, $i = 1, 2$, be solutions of*

$$-Q' - \frac{1}{D_2}\frac{\tilde{g}}{Q} = \frac{c}{D_2} \quad \textit{for } V \in (0, \tfrac{w_2}{c_{22}})$$

with $Q_i(\frac{w_2}{c_{22}}) = 0$. *If* $c_1 = c_2$, *then* $Q_1(V) = Q_2(V)$ *whenever* $Q_1(V) > 0$, $0 < V < \frac{w_2}{c_{22}}$. *If* $c_1 < c_2$, *then* $Q_1(V) > Q_2(V)$ *whenever* $Q_1(V) > 0$, $0 < V < \frac{w_2}{c_{22}}$.

Proof: From equation (4.21) we see that

$$\begin{aligned}\frac{1}{D_2}(c_1 - c_2) &= -Q_1' - \frac{1}{D_2}\frac{\tilde{g}}{Q_1} + Q_2' + \frac{1}{D_2}\frac{\tilde{g}}{Q_2} \\ &= Q_2' - Q_1' - \frac{1}{D_2}(\frac{\tilde{g}}{Q_1} - \frac{\tilde{g}}{Q_2}) \\ &= Q_2' - Q_1' - \frac{1}{D_2}(Q_2 - Q_1)\frac{\tilde{g}}{Q_1 Q_2}. \end{aligned} \tag{4.22}$$

Define $G(V)$ as

$$G(V) = (Q_2 - Q_1) exp\left\{\int_a^V -\frac{\tilde{g}(t)}{D_2 Q_1(t) Q_2(t)} dt\right\},$$

where $0 < a < \frac{w_2}{c_{22}}$. Then we have

$$\frac{dG}{dV} = \frac{1}{D_2}(c_1 - c_2) exp\left\{\int_a^V -\frac{\tilde{g}(t)}{D_2 Q_1(t) Q_2(t)} dt\right\}.$$

If $c_1 = c_2$, then $G'(V) = 0$ and $\lim_{V \to \frac{w_2}{c_{22}}} G(V) = 0$. Because $\tilde{g}(V) > 0$ for V near $V = \frac{w_2}{c_{22}}$ the exponential stays bounded as $V \to \frac{w_2}{c_{22}}$; thus $G(V) \equiv 0$ and $Q_1 \equiv Q_2$. If $c_1 < c_2$, then $G'(V) < 0$ and $\lim_{V \to \frac{w_2}{c_{22}}} G(V) = 0$ so that $G(V) > 0$ for $a < V < \frac{w_2}{c_{22}}$ and $Q_1 > Q_2$. Finally if $c_1 > c_2$ we get $Q_1 < Q_2$.

Using this lemma we will be able to prove the existence of a unique wave speed $c < 0$ for which there is a corresponding traveling wave front from $(0, 0)$ to $(\frac{w_2}{c_{22}}, 0)$. To show that there is at most one c we assume the contrary. Let $T(c_1)$ and $T(c_2)$ be two trajectories from $(0, 0)$ to $(\frac{w_2}{c_{22}}, 0)$ with speeds c_1 and c_2 respectively. Then by Lemma 4.4 one of these trajectories is strictly below the other for $V \in (0, \frac{w_2}{c_{22}})$. However, if we consider the unstable eigenvector at $(0, 0)$ corresponding to the positive eigenvalue we see that it is a decreasing function of c. Letting $\lambda_+(0)$ be the positive eigenvalue of $(0, 0)$ as a function of c, we get

$$\lambda_+(0) = \frac{1}{2}\left[-\frac{c}{D_2} + \sqrt{(\frac{c}{D_2})^2 - \frac{4}{D_2}\tilde{g}_V(0)}\right] \tag{4.23}$$

Thus

$$\begin{aligned} \frac{d\lambda_+(0)}{dc} &= -\frac{1}{2D_2}\left[1 - \frac{c}{D_2}\frac{1}{\sqrt{(\frac{c}{D_2})^2 - \frac{4}{D_2}\tilde{g}_V(0)}}\right] \\ &< 0 \end{aligned} \tag{4.24}$$

Thus the unstable eigenvector near $(0,0)$ for $V \in (0, \frac{w_2}{c_{22}})$ has a slope that is a decreasing function of c. Therefor if $c_1 < c_2$ then $T(c_1) > T(c_2)$ near $(0,0)$ (see Figure 20).

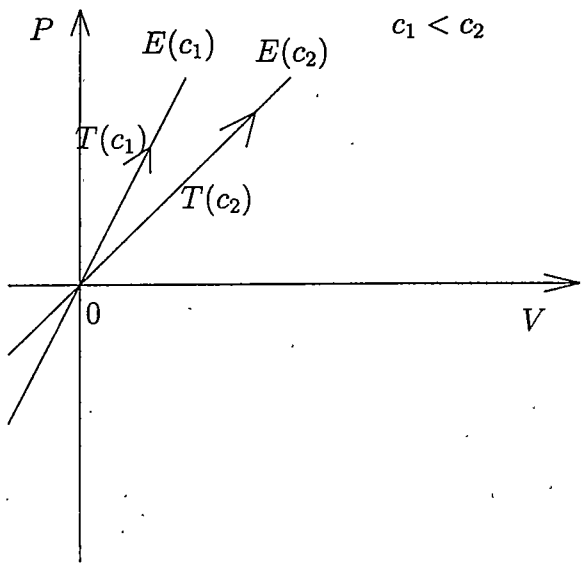

Figure 20: Eigenvectors at $(0,0)$. For $c_1 < c_2$, $T(c_1) > T(c_2)$.

Similarly if we consider the negative eigenvalue of $(\frac{w_2}{c_{22}}, 0)$ we see that the stable eigenvector for $V \in (0, \frac{w_2}{c_{22}})$ is also a decreasing function of c. Letting $\lambda_-(\frac{w_2}{c_{22}})$ denote the negative eigenvalue of $(\frac{w_2}{c_{22}}, 0)$;

$$\lambda_-(\frac{w_2}{c_{22}}) = \frac{1}{2}\left[-\frac{c}{D_2} - \sqrt{(\frac{c}{D_2})^2 - \frac{4}{D_2}\tilde{g}_V(\frac{w_2}{c_{22}})}\right] \tag{4.25}$$

so that

$$\begin{aligned} \frac{d\lambda_-(\frac{w_2}{c_{22}})}{dc} &= -\frac{1}{2D_2}\left[1 + \frac{c}{D_2}\frac{1}{\sqrt{(\frac{c}{D_2})^2 - \frac{4}{D_2}\tilde{g}_V(\frac{w_2}{c_{22}})}}\right] \\ &< 0 \end{aligned} \tag{4.26}$$

Thus $\lambda_-(\frac{w_2}{c_{22}})$ is a decreasing function of c, i.e. if $c_1 < c_2$, $\lambda_-(c_1) > \lambda_-(c_2)$ and the slopes of the eigenvectors increase as c decreases. But because the trajectory that we are concerned with have negative slopes near $(\frac{w_2}{c_{22}}, 0)$ we can conclude that if $c_1 < c_2$ then $T(c_1) < T(c_2)$ for $V \in (0, \frac{w_2}{c_{22}})$ (see Figure 21). This implies that near $(0,0)$ if $T(c_1)$ is below $T(c_2)$ then at $(\frac{w_2}{c_{22}}, 0)$ it must be above $T(c_2)$. This contradicts our result form Lemma 4.4 and thus there must be at most one value of c.

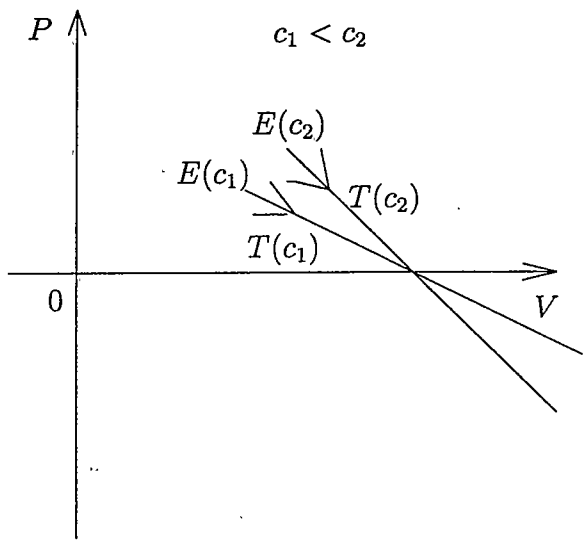

Figure 21: Eigenvectors at $(\frac{w_2}{c_{22}}, 0)$. For $c_1 < c_2$, $T(c_1) < T(c_2)$, when $0 < V < \frac{w_2}{c_{22}}$.

Now it is left to show the existence of such a wave speed c. For this we will use a continuity argument. To show a connection from $(0,0)$ to $(\frac{w_2}{c_{22}}, 0)$ we will show that for $|c|$ sufficiently large the trajectory from $(0,0)$ leaves the half strip $H = \{0 < V < \frac{w_2}{c_{22}}, P > 0\}$ through $\{V = \frac{w_2}{c_{22}}, P > 0\}$, and for $|c|$ sufficiently small, the trajectory leaves H through $\{0 < V < \frac{w_2}{c_{22}}, P = 0\}$. Using the continuous dependency of the solutions on c, Theorem 4.2, and Theorem 4.3 we will show that there is some intermediate value of c such that the trajectory tends to $(\frac{w_2}{c_{22}}, 0)$ as $z \to \infty$.

Consider $c < 0$, $|c|$ large. We wish to compare the solution of (4.17) which leaves the origin in the positive quadrant, with a solution of

$$\begin{aligned} V' &= P \\ P' &= aP - bV \end{aligned} \tag{4.27}$$

where a and b will be determined.

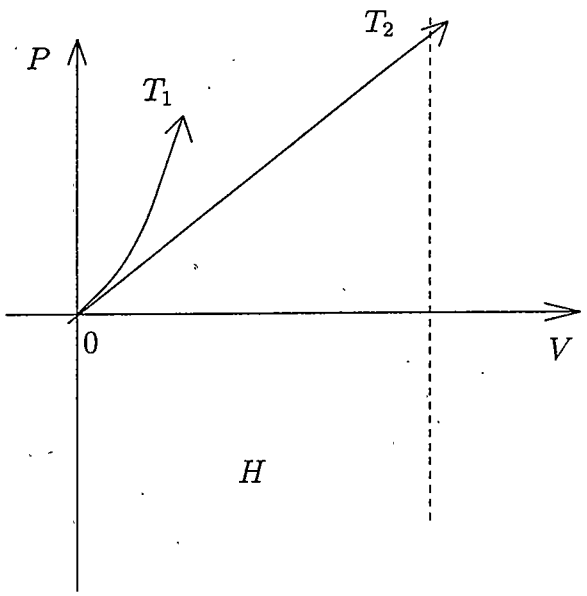

Figure 22: Trajectories for the system, where T_1 is the unstable manifold for the ODE system and T_2 is the unstable manifold for the linear ODE system.

The relevant trajectories T_1 and T_2 are shown in Figure 22. Where T_1 is a piece of the unstable manifold of $(0,0)$ for (4.17) and T_2 is a piece of the unstable manifold of $(0,0)$ for (4.27). We wish to choose a and b for (4.27) in such a way that T_2 is a straight line with positive slope and that if $|c|$ is sufficiently large, then T_1 leaves the origin above T_2 and can not subsequently cross below it. Because the trajectory, T_1 is bounded away from the origin (see equation (4.21)), it must then leave the half strip H through $\{V = \frac{w_2}{c_{22}}, P > 0\}$. If we consider the system (4.27) the eigenvalues of the

system are $\lambda = \frac{a \pm \sqrt{a^2-4b}}{2}$. The positive eigenvalue $\lambda_+ = \frac{a+\sqrt{a^2-4b}}{2}$ corresponds to the trajectory T_2. If $a^2 > 4b$ then T_2 is a straight line with positive slope. T_1 leaves the origin above T_2 if the positive eigenvalue of the system (4.17) is greater than that of T_2. This implies that

$$\frac{1}{2}\left[-\frac{c}{D_2} + \sqrt{(\frac{c}{D_2})^2 - \frac{4}{D_2}\tilde{g}(0)}\right] > \frac{a+\sqrt{a^2-4b}}{2}. \tag{4.28}$$

T_1 can not subsequently cross below T_2 if the slope of the flow of T_1 at all points is greater than that of T_2, that is, if

$$\frac{-\frac{c}{D_2}P - \frac{1}{D_2}\tilde{g}(V)}{P} > \frac{aP - bV}{P}. \tag{4.29}$$

Sufficient requirements for this inequality to hold would be for $c < -D_2 a$ and $b > \frac{1}{D_2}\frac{\tilde{g}(V)}{V}$. If we define k by

$$k = \sup_{V \in (0, \frac{w_2}{c_{22}})} \frac{\tilde{g}(V)}{V}, \tag{4.30}$$

then (4.29) is satisfied by choosing $b = \frac{1}{D_2}k$ and $c < -aD_2$. The inequality $a^2 > 4b$ is satisfied if $a^2 > 4k$ and (4.28) is then satisfied for $|c|$ sufficiently large. So for sufficiently large $|c|$ values T_1 must leave the half strip H along the boundary $\{V = \frac{w_2}{c_{22}}, P > 0\}$. Next we show that for small values of $|c|$ it must exit H through $\{0 < V < \frac{w_2}{c_{22}}, P = 0\}$.

Consider the system (4.17) with $c = 0$. It becomes

$$V' = P \tag{4.31}$$

$$P' = \frac{-1}{D_2}\tilde{g}(V). \tag{4.32}$$

This is a Hamiltonian system with the Hamiltonian given by:

$$H(V,P) = \frac{P^2}{2} + \int_0^V \frac{1}{D_2}\tilde{g}(s)ds. \tag{4.33}$$

Solutions to (4.31) correspond to level sets of the Hamiltonian equation. Figure 23, calculated using pplane [20] in Matlab, shows the level sets of (4.33). The

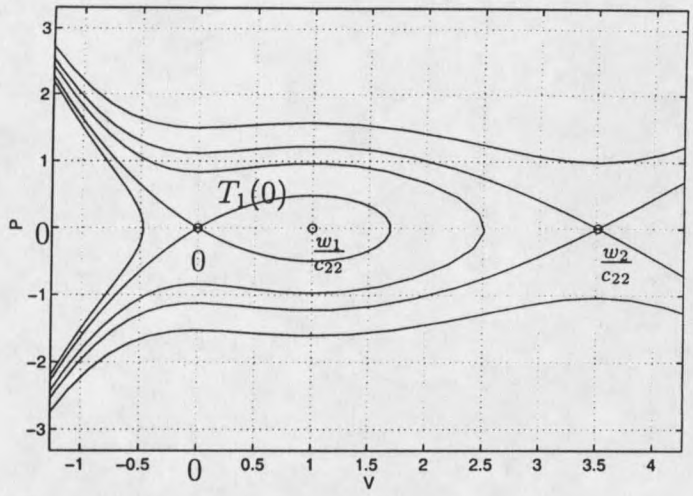

Figure 23: Level sets of the Hamiltonian for the ODE system. Calculated for the Selgrade model with $c_{22} = 1$, $D_2 = 1$.

trajectory corresponding to T_1 originating from the origin is associated with the level set given by

$$H(V,P) = \frac{P^2}{2} + \int_0^V \frac{1}{D_2}\tilde{g}(s)ds = 0. \tag{4.34}$$

This would imply that $\int_0^V \frac{1}{D_2}\tilde{g}(s)ds < 0$ along this trajectory. However for this problem we have assumed $\int_0^{\frac{w_2}{c_{22}}} \frac{1}{D_2}\tilde{g}(s)ds > 0$, hence the trajectory leaves the half-strip H on $\{0 < V < \frac{w_2}{c_{22}}, P = 0\}$. Since solutions to (4.17) depend continuously on c it follows that there must be a c such that the trajectory leaving the saddle point $(0,0)$ tends to $(\frac{w_2}{c_{22}}, 0)$ as $z \to \infty$. If the trajectory does not tend to the equilibrium then by Theorem 4.2 it must approach a closed orbit. But looking at the system (4.16) we have

$$\frac{\partial h}{\partial V} + \frac{\partial k}{\partial P} = -\frac{c}{D_2} \neq 0$$

and does not change sign throughout $\mathbb{R}^2$. Thus by Theorem 4.3 there are no closed orbits. Therefore the trajectory must approach $(\frac{w_2}{c_{22}}, 0)$ as $z \to \infty$ and there is a

traveling wave front from $V = 0$ to $V = \frac{w_2}{c_{22}}$ for a unique c value with $c < 0$.

Figure 24 shows an example of a typical traveling wave solution to (4.16). The arrow represents the direction of movement of the wave to a stationary observer. As the wave moves through the domain from right to left the population density of the climax species approaches the value $\frac{w_2}{c_{22}}$ throughout the domain. This wave was developed using xtc with initial condition given by $v = 3.513 * H(x - 90)$, no flux boundary conditions, and using method of lines with a Gear integrator.

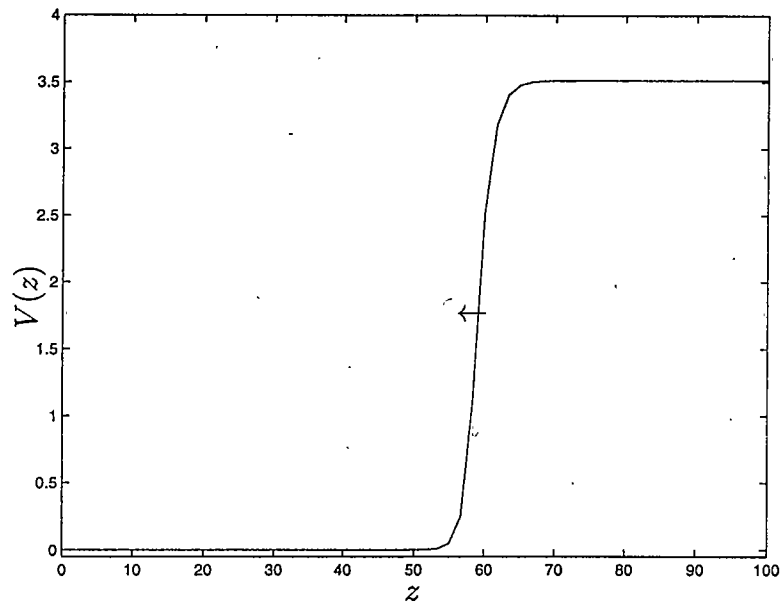

Figure 24: Traveling wave example for traveling wave along v-axis. The wave moves to the left in time. Calculated for the Selgrade model with $c_{22} = 1$, $D_2 = 1$

Traveling Wave Between the Axis

In this section we consider traveling waves for the full system. The particular wave we look for connects the two equilibria $(\frac{z_1}{c_{11}}, 0)$ to $(0, \frac{w_2}{c_{22}})$. This wave was first observed while looking at numerical solutions of the Selgrade model where the diffusion coefficients differed greatly in magnitude, $D_2 << D_1$, and c_{11} was such that the

nullcline of the pioneer species crossed the pioneer axis between the nullclines of the climax species (see Figure 3). The observed wave appeared to travel at an extremely slow speed, with the phase plane diagram as in Figure 25 (see also Figure 26 for the graphs of the traveling wave solution for the climax, V, and pioneer species, U). This solution was found using a shooting method in AUTO [19] by shooting from the equilibrium $(0, \frac{w_2}{c_{22}})$ in the unstable eigenvalue direction for small periods of time. We looked for solutions to the steady state system of ordinary differential equations (4.3) that satisfied a set of boundary conditions requiring the solution starting from $(0, \frac{w_2}{c_{22}})$ to approach the equilibrium $(\frac{z_1}{c_{11}}, 0)$ having small wave speed. We then graphed these solutions to determine with of these appeared to be following the upper nullcline of the climax species. We ran AUTO again starting with these solutions. This process was continued until a solutions was found that has small wave speed and was within 0.00001 of the equilibrium $(\frac{z_1}{c_{11}}, 0)$. Thus we found a solution that appears to be on the the nullcline of the climax species that runs along the u-axis with a quick transition or jump to the upper nullcline of the climax species where the fitness function for the climax species is zero (see Figure 3). Our concern is whether such a wave can exist in the general model.

With these observations in mind we will consider the system (3.3) with $D_2 = \epsilon^2$ and $D_1 = 1$:

$$\begin{aligned} u_t &= u_{xx} + \tilde{f}(y_1) \\ v_t &= \epsilon^2 v_{xx} + \tilde{g}(y_2), \end{aligned} \tag{4.35}$$

where

$$\tilde{f}(y_1) = u f(y_1), \tag{4.36}$$

$$\tilde{g}(y_2) = v g(y_2), \tag{4.37}$$

with f and g the fitness functions of the pioneer and climax species respectively. We

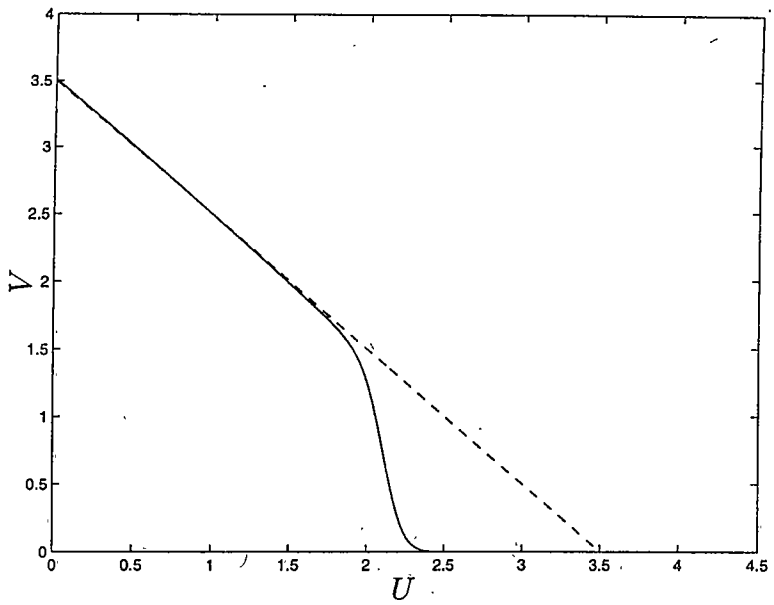

Figure 25: U-V Phase plane diagram of Traveling wave solutions to the full system. Calculated for Selgrade model with $c_{11} = 0.109$, $c_{22} = 1$.

look for a traveling wave solution to the above system (4.35) with a wave speed of order ϵ. Thus for the traveling wave coordinates we let $U(z) = u(x,t)$ and $V(z) = v(x,t)$ as before but with $z = x - \epsilon ct$. Here we assume c is $O(1)$. Therefore the above system becomes

$$\begin{aligned} U'' + \epsilon c U' + \tilde{f}(Y_1) &= 0, \\ \epsilon^2 V'' + \epsilon c V' + \tilde{g}(Y_2) &= 0. \end{aligned} \tag{4.38}$$

Again $'$ represents the derivative with respect to z.

We will examine the existence of solutions to (4.38) in two ways. In the first section we will look an $O(1)$ approximation to the system using standard methods of matched asymptotic expansions (see e.g. Grindrod [8] and Kevorkian and Cole [12]). This system exhibits singular behavior in the dynamics of the climax species. In the second section we will prove the existence of a solution to (4.38) using methods of

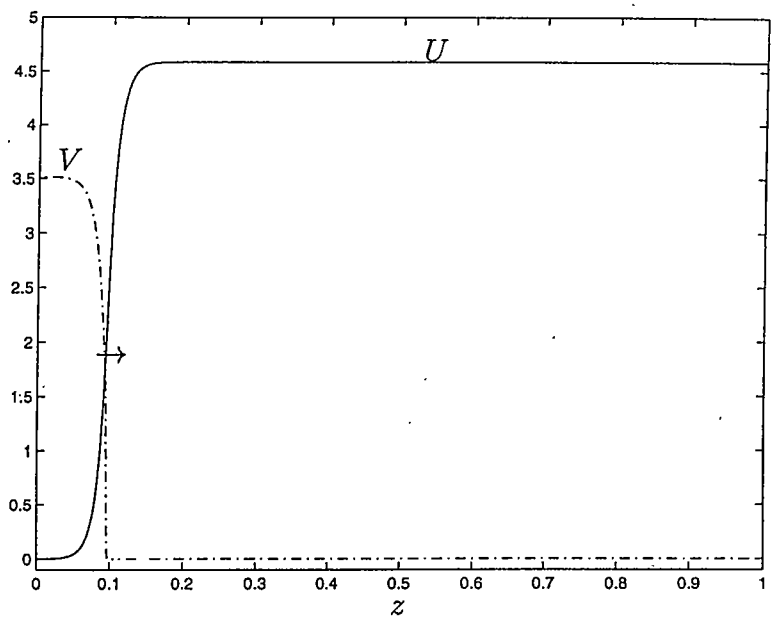

Figure 26: Wave solutions of Pioneer and Climax species from $(\frac{r_1}{c_{11}}, 0)$ to $(0, \frac{w_2}{l} c_{22})$. Calculated for Selgrade model with $c_{11} = 0.109$, $c_{22} = 1$.

geometric singular perturbation based on results developed in [13] and [30].

Matched asymptotic expansion

When a problem contains a small parameter, ϵ, we may try to analyze the behavior of the solution in the limit $\epsilon \to 0$. In doing this our aim is to obtain an approximation to the true solution, valid for small ϵ. Often the solution may be expressed as an ϵ expansion of the form

$$U = U_0(z) + \epsilon^{\alpha} U_1(z) + \epsilon^{2\alpha} U_2(z) + \cdots \tag{4.39}$$

where $\alpha > 0$ is some constant.

By substituting (4.39) (and similar expansions for V) into the original problem and equating order of ϵ terms we seek to solve for $U_k(z)$. However such a series solution may exhibit what is called singular behavior. Singular behavior refers to the situation

where the quotients

$$\frac{U_{i+1}(z)}{U_i(z)}$$

are not bounded at some value of z. When this is the case the $\epsilon^{(i+1)\alpha}U_{i+1}(z)$ term is no longer negligible compared to $\epsilon^{i\alpha}U_i(z)$. The process of equating terms of similar order, by which we solved for the U_i, is no longer justified at these values of z. The regular expansion cannot approximate the solution close to these points.

In general when a regular series becomes singular at a point we can try to obtain a new expansion which is valid in a local neighborhood of that point. To do so we first rescale the independent variables. The idea is to stretch out the neighborhood of the singular point by introducing a new independent variable. If the singular point is given by $z = z^*$ then the new independent variable would be of the form

$$\xi = \frac{z - z^*}{\epsilon^a} \tag{4.40}$$

for some $a > 0$. The old expansion, valid away from $z = z^*$, is called the outer expansion, while the new expansion, in the stretched variable ξ, is called the inner expansion.

Once the inner and outer solutions have been found they need to be matched in the region close to z^*. These solutions are formally valid in separate regions, however we need to assert that there is some region of overlap where this matching must occur. For our problem the singularity occurs when the solution jumps from one nullcline of the climax species to another. Thus the outer solution will have two parts one on each nullcline with the inner solution occurring at the jump.

First we will consider the outer solutions to the system (4.38). We assume an expansion of the U and V variables, similar to that of (4.39), of the following form;

$$\begin{aligned} U(z,\epsilon) &= U_0(z) + \epsilon U_1(z) + \ldots \\ V(z,\epsilon) &= V_0(z) + \epsilon V_1(z) + \ldots \end{aligned} \tag{4.41}$$

By substituting (4.41) into (4.38) and equating terms of $O(1)$ we obtain

$$\begin{aligned} U_0'' + \tilde{f}(Y_{1_0}) &= 0 \\ g(Y_{2_0}) &= 0, \end{aligned} \tag{4.42}$$

where $Y_{1_0} = c_{11}U_0 + V_0$ and $Y_{2_0} = U_0 + c_{22}V_0$. The two solutions of $\tilde{g}(Y_{2_0}) = 0$ that we want to connect are the nullclines $V_0 = 0$ and $V_0 = \frac{w_2}{c_{22}} - \frac{1}{c_{22}}U_0$ where w_2 is a zero of $g(y_2)$. Let

$$V_0^{\pm} = h_{\pm}(U_0), \tag{4.43}$$

where

$$h_-(U_0) = \frac{w_2}{c_{22}} - \frac{1}{c_{22}}U_0, \tag{4.44}$$

$$h_+(U_0) = 0. \tag{4.45}$$

By substituting (4.43) into (4.42) we see that a solution to the system must solve the following equation,

$$U_0'' + \tilde{f}(Y_{1_0}^{\pm}) = 0 \tag{4.46}$$

where

$$Y_{1_0}^{\pm} = c_{11}U_0 + h_{\pm}(U_0) \tag{4.47}$$

with the following limit conditions holding;

$$\lim_{z\to-\infty} U_0(z) = 0 \quad \text{and} \quad \lim_{z\to\infty} U_0(z) = \frac{z_1}{c_{11}}. \tag{4.48}$$

By use of phase plane arguments we will construct a solution to (4.46) that is C^1 in U_0.

First we consider the outer solution on the nullcline $V_0 = h_+(U_0)$. Then, (4.46) becomes

$$U_0'' + \tilde{f}(Y_{1_0}^{+}) = 0 \tag{4.49}$$

where

$$Y_{1_0}^{+} = c_{11}U_0 + h + (U_0) = c_{11}U_0 \tag{4.50}$$

with the second limit of (4.48) satisfied. Rewriting the (4.49) as a first order system of equations we get,

$$\begin{aligned} U_0' &= W_0 \\ W_0' &= -\tilde{f}(Y_{1_0}^{+}). \end{aligned} \tag{4.51}$$

This system has two equilibria

$$(U_0, W_0) = (0,0) \text{ and } (\frac{z_1}{c_{11}}, 0).$$

The Jacobian of the system is given by

$$J = \begin{bmatrix} 0 & 1 \\ -\tilde{f}_{U_0} & 0 \end{bmatrix}. \tag{4.52}$$

with eigenvalues

$$\lambda_{\pm} = \pm\sqrt{-\tilde{f}_{U_0}}. \tag{4.53}$$

Now from (4.36) and (4.47) we see that

$$\tilde{f}_{U_0} = U_0 \frac{df}{dY_{1_0}^{\pm}} \frac{dY_{1_0}^{\pm}}{dU_0} + f(Y_{1_0}^{\pm}). \tag{4.54}$$

Evaluating (4.54) for (4.45) at $(0,0)$ we get

$$\tilde{f}_{U_0} = f(0) > 0. \tag{4.55}$$

Note that $Y_{1_0}^{+} = 0$ at $(0,0)$. Thus the equilibrium $(0,0)$ is a center. For the equilibrium $(\frac{z_1}{c_{11}}, 0)$ we get that $Y_{1_0}^{+} = z_1$, $\frac{dY_{1_0}^{+}}{dU_0} = c_{11}$ so that

$$\tilde{f}_{U_0} = z_1 \frac{df}{dY_{1_0}^{+}} < 0. \tag{4.56}$$

The inequality in (4.56) is due to the fact that f is a decreasing function of Y_{1_0}. Therefore we find that $(\frac{z_1}{c_{11}}, 0)$ is a saddle. The phase plane diagram, calculated

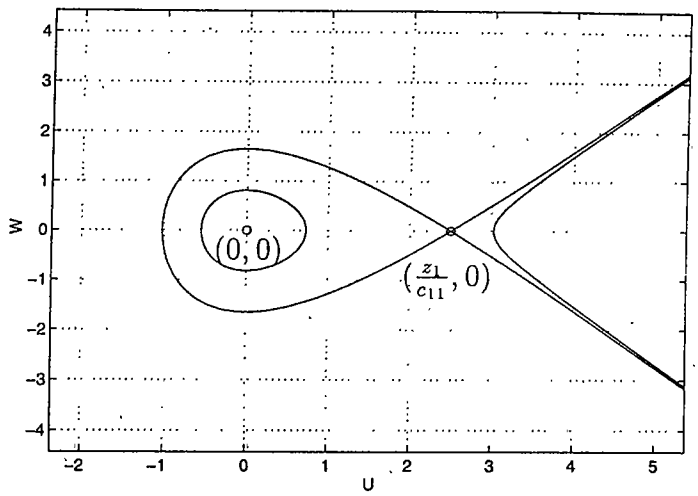

Figure 27: Phase plane portrait for the first order system with $Y_{1_0}^+$. Calculated for the Selgrade model with $c_{11} = 0.2$, $c_{22} = 1$.

using pplane [20] in Matlab, for this system is in Figure 27. From this figure we see that for increasing values of z there exists a unique monotone increasing function, call it U^+ that is a solution to (4.51) with the limit condition satisfying $\lim_{z\to\infty} U_0^+ = \frac{z_1}{c_{11}}$. This solution lies on the stable manifold of the saddle point $(\frac{z_1}{c_{11}}, 0)$ in the first quadrant. Notice that if we follow this solution for $z \to -\infty$ it would not satisfy $\lim_{z\to-\infty} U^+ = 0$. Thus we have only half of the outer $O(1)$ solution to (4.38).

We now have to find a solution to (4.46) with V_0 given by (4.44), the outer solution along the upper nullcline for the climax species. Thus we consider

$$U_0'' + \tilde{f}(Y_{1_0}^-) = 0. \tag{4.57}$$

where

$$Y_{1_0}^- = c_{11}U_0 + h_-(U_0) = \frac{det(C)}{c_{22}}U_0 + \frac{w_2}{c_{22}}, \tag{4.58}$$

and the first limit in (4.48) is satisfied. Writing (4.57) as a first-order system we get

$$\begin{aligned} U_0' &= W_0 \\ W_0' &= -\tilde{f}(Y_{1_0}^-). \end{aligned} \tag{4.59}$$

The equilibria for this system are given by

$$(U_0, W_0) = (0,0) \text{ and } (\frac{c_{22}z_1 - w_2}{det(C)}, 0). \tag{4.60}$$

The Jacobian for the system (4.59) is

$$J = \begin{bmatrix} 0 & 1 \\ -\tilde{f}_{U_0} & 0 \end{bmatrix} \tag{4.61}$$

with eigenvalues

$$\lambda = \pm\sqrt{-\tilde{f}_{U_0}}. \tag{4.62}$$

At $(0,0)$ we see from (4.58) that $Y_{1_0}^- = \frac{w_2}{c_{22}}$ so that $\tilde{f}_{U_0} = f(\frac{w_2}{c_{22}})$. From Figure 1 it is evident that for

$$\frac{w_2}{c_{22}} < z_1 \tag{4.63}$$

the pioneer fitness function $f(\frac{w_2}{c_{22}}) > 0$ whereas for

$$\frac{w_2}{c_{22}} > z_1 \tag{4.64}$$

this function is less than zero. Therefore with (4.63) the point $(0,0)$ is a center and (4.64) implies $(0,0)$ is a saddle with two real eigenvalues of opposite sign. However because we wish to find a solution such that $\lim_{z\to-\infty} U_0 = 0$ we can not have $(0,0)$ a center. Thus we assume (4.64) and that $(0,0)$ is a saddle.

Next we consider the equilibrium $(\frac{c_{22}z_1-w_2}{det(C)}, 0)$. The eigenvalues for this equilibrium are again of the form (4.62). By evaluating (4.58) at this equilibrium point we get that $Y_{1_0}^- = z_1$ and $\frac{dY_{1_0}^-}{dU_0} = \frac{det(C)}{c_{22}}$. Therefore from (4.54) we have

$$\begin{aligned} \tilde{f}_{U_0} &= \frac{c_{22}z_1 - w_2}{det(C)} \frac{df}{dY_{1_0}^-} \frac{det(C)}{c_{22}} \\ &= (z_1 - \frac{w_2}{c_{22}}) \frac{df}{dY_{1_0}^-}. \end{aligned} \tag{4.65}$$

The fact that f is a decreasing function of $Y_{1_0}^-$ and that (4.64) must hold for $(0,0)$ imply $\tilde{f}_{U_0} > 0$. Hence $(\frac{c_{22}z_1 - w_2}{det(C)}, 0)$ is a center.

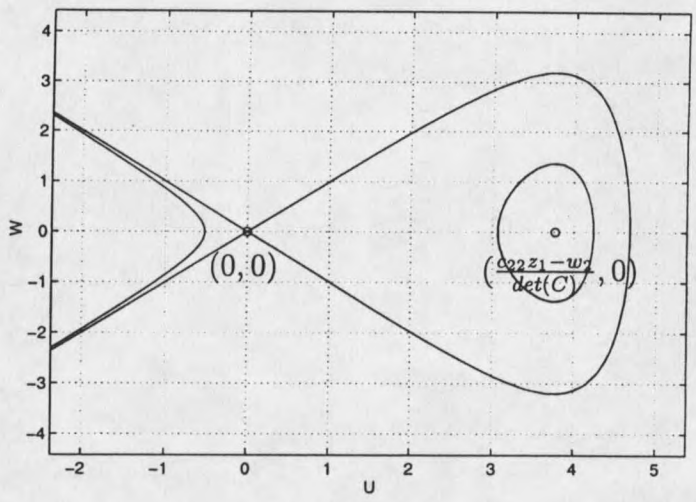

Figure 28: Phase plane portrait for the first order system with $Y_{1_0}^-$. Calculated for Selgrade model with $c_{11} = 0.2$, $c_{22} = 1$.

The phase plane diagram given in Figure 28, also calculated using pplane, demonstrates that for (4.64) satisfied there will exist a unique solution to (4.59) with $\lim_{z\to-\infty} U_0 = 0$. Let U^- represent this monotonically increasing solution to (4.59) with the limit condition as $z \to -\infty$ satisfied. This solution lies in the first quadrant on the unstable manifold of the point $(0,0)$. This gives us a solution to outer problem along the upper nullcline for the climax species.

We would like to combine these two solutions, U^+ and U^- in such a fashion that the combined solution will be a C^1 solution to (4.42) satisfying (4.48). By allowing $w_2 > \frac{z_1}{c_{11}}$ the equilibrium point, $(\frac{c_{22}z_1 - w_2}{det(C)}, 0)$, will lie to the right of $(\frac{z_1}{c_{11}}, 0)$ and we can produce the phase plane diagram given in Figure 29, with U^+ and U^- labeled. U^* in Figure 29 is the value of U such that U^+ and U^- intersect with matching first

derivatives. Referring to Figure 29 we see that if we define the combined solution such that it is U^- for $U < U^*$ and U^+ for $U \geq U^*$ then we would create the solution we are looking for. The question is "does such a U^* exist for our general system?".

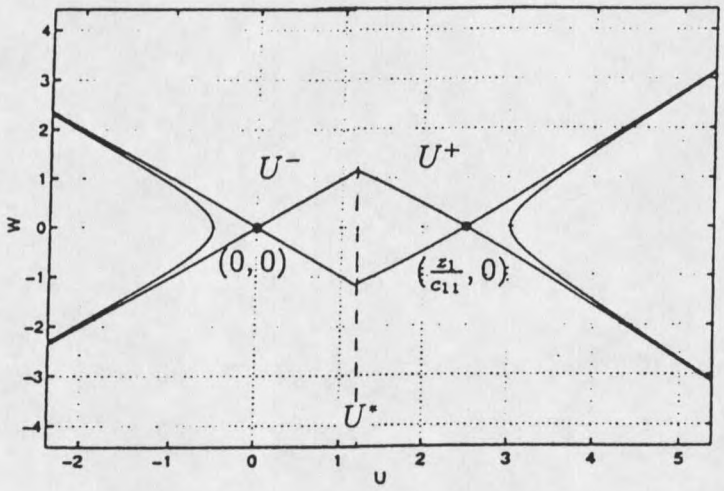

Figure 29: Combined Phase portrait of the two portions of the outer Pioneer solution. Calculated for the Selgrade model with $c_{11} = 0.2$, $c_{22} = 1$.

To search for U^* we let $U_0' = P(U_0)$. $P(U_0)$ is well defined for the trajectory we are considering because along this trajectory U_0 is a monotone increasing function. Using this definition we get $U_0'' = \frac{dP}{dU_0}\frac{dU_0}{dz} = P\frac{dP}{dU_0}$ so (4.46) can be written

$$P\frac{dP}{dU} = -\tilde{f}(Y_{1_0}^{\pm}) \tag{4.66}$$

Let P^+ and P^- denote solutions to (4.66) corresponding to $Y_{1_0}^+$ and $Y_{1_0}^-$ respectively. Looking at the equation for P^+ first, separation of variables and integrating in U_0 from U^* to $\frac{z_1}{c_{11}}$ gives

$$\int_{P^+(U^*)}^{P^+(\frac{z_1}{c_{11}})} GdG = -\int_{U^*}^{\frac{z_1}{c_{11}}} \tilde{f}(Y_{1_0}^+(s))ds. \tag{4.67}$$

This gives us

$$\frac{(P^+)^2}{2}(U^*) = \int_{U^*}^{\frac{z_1}{c_{11}}} \tilde{f}(Y_{1_0}^+(s))ds \tag{4.68}$$

where $P^+(\frac{z_1}{c_{11}}) = 0$.

Now we consider (4.66) for P^-. Again using separation of variables and in this case integrating in U_0 between 0 and U^*, noting that $P^-(0) = 0$ we have

$$\frac{(P^-)^2}{2}(U^*) = -\int_0^{U^*} \tilde{f}(Y_{1_0}^-(s))ds. \tag{4.69}$$

We are looking for a U^* value such that the trajectories U^+ and U^- intersect with matching derivatives at U^*, thus we require $P^+(U^*) = P^-(U^*)$ at $U^+ = U^- = U^*$. To satisfy these requirements we see from (4.68) and (4.69) that we need

$$\int_{U^*}^{\frac{z_1}{c_{11}}} \tilde{f}(Y_{1_0}^+(s))ds = -\int_0^{U^*} \tilde{f}(Y_{1_0}^-(s))ds. \tag{4.70}$$

By considering $\tilde{f}(Y_{1_0}^+(U))$ we find that the zeros of this function occur at $U_0 = 0$ and $U_0 = \frac{z_1}{c_{11}}$. From (4.55) we have $\tilde{f}_{U_0}(Y_{1_0}^+(0)) > 0$ and from (4.56), $\tilde{f}_{U_0}(Y_{1_0}^+(\frac{z_1}{c_{11}})) < 0$. Thus for $U_0 \in (0, \frac{z_1}{c_{11}})$, $\tilde{f}(Y_{1_0}^+(U_0)) > 0$ so that

$$\int_{U^*}^{\frac{z_1}{c_{11}}} \tilde{f}(Y_{1_0}^+(s))ds > 0, \tag{4.71}$$

and the integral is a decreasing function of U^*.

$\tilde{f}(Y_{1_0}^-(U_0))$ has two zeros, $U_0 = 0$ and $U_0 = \frac{c_{22}z_1 - w_2}{det(C)}$. For $(0,0)$ to be a saddle we assumed (4.64) to be true and thus we need $det(C) < 0$ for $U_0 > 0$. This implies $\tilde{f}_{U_0}(Y_{1_0}^-(0)) < 0$ and from (4.65) we have $\tilde{f}_{U_0}(Y_{1_0}^-(\frac{c_{22}z_1 - w_2}{det(C)})) > 0$. Therefore we have for $U_0 \in (0, \frac{c_{22}z_1 - w_2}{det(C)})$ that $\tilde{f}(Y_{1_0}^-(U_0)) < 0$, thus

$$-\int_0^{U^*} \tilde{f}(Y_{1_0}^-(s))ds > 0. \tag{4.72}$$

Furthermore the (4.72) is an increasing function of U^*. For $U^* = 0$ we have (4.71) greater than zero and (4.72) equal to zero, just the opposite is true for $U^* = \frac{z_1}{c_{11}}$.

Since the left hand side of (4.71) is a monotonically decreasing function of U^* and the left hand side of (4.72) is a monotonically increasing function of U^* we see that there will be a unique value of U^* such that (4.70) is satisfied.

If we define our $O(1)$ outer solution to (4.38) to be

$$U_{Outer} = \begin{cases} U^- & \text{if } 0 \le U_0 < U^* \\ U^+ & \text{if } U^* \le U_0 \le \frac{z_1}{c_{11}} \end{cases} \tag{4.73}$$

$$V_{Outer} = \begin{cases} h_-(U_0) = \frac{w_2}{c_{22}} - \frac{1}{c_{22}} U_0 & \text{if } 0 \le U_0 < U^* \\ h_+(U_0) = 0 & \text{if } U^* < U_0 \le \frac{z_1}{c_{11}} \end{cases} \tag{4.74}$$

then U_{Outer} is C^1 in the outer region but V_{Outer} is not even C^0 at $U_0 = U^*$. To smooth out V near U^* we will now consider the inner solution to (4.38). For this we rescale z near z^*, the value of z such that $U(z^*) = U^*$. Let

$$\xi = \frac{z - z^*}{\epsilon}. \tag{4.75}$$

with

$$U = \hat{U}(\xi) \tag{4.76}$$

$$V = \hat{V}(\xi) \tag{4.77}$$

Substituting this into (4.38) we obtain

$$\begin{aligned} \hat{U}'' + \epsilon^2(c\hat{U}' + \tilde{f}(\hat{Y}_1)) &= 0 \\ \hat{V}'' + c\hat{V}' + \tilde{g}(\hat{Y}_2) &= 0. \end{aligned} \tag{4.78}$$

Again we will only be looking for an $O(1)$ approximation to the inner solution corresponding to a solution to the system (4.78) with $\epsilon = 0$. Thus we consider

$$\begin{aligned} \hat{U}'' &= 0 \\ \hat{V}'' + c\hat{V}' + \tilde{g}(\hat{Y}_2) &= 0, \end{aligned} \tag{4.79}$$

In the inner layer, V jumps from the nullcline $h_-(U)$ to $h_+(U)$ and $\hat{U}'' = 0$ thus U is constant on this layer since it is the only solution of $\hat{U}'' = 0$ which remains bounded

in an intermediate overlapping (matching) domain. We define $\hat{U} = U_{Inner} = U^*$. Therefore (4.79) becomes

$$\hat{V}'' + c\hat{V}' + \tilde{g}(\hat{Y}_2^*) = 0 \tag{4.80}$$

with matching conditions

$$\lim_{\xi \to -\infty} \hat{V} = h_-(U^*) = \frac{w_2}{c_{22}} - \frac{1}{c_{22}} U^* \tag{4.81}$$

$$\lim_{\xi \to \infty} \hat{V} = h_+(U^*) = 0 \tag{4.82}$$

and

$$\hat{Y}_2^* = U^* + c_{22}\hat{V}. \tag{4.83}$$

The equivalent first order system is given by

$$\begin{aligned} \hat{V}' &= \hat{P} \\ \hat{P}' &= -c\hat{P} - \tilde{g}(\hat{Y}_2^*) \end{aligned} \tag{4.84}$$

with equilibria $(\hat{V}, \hat{P})$ equal to

$$(0,0), \quad (\frac{w_1}{c_{22}} - \frac{1}{c_{22}} U^*, 0) \quad \text{and} \quad (\frac{w_2}{c_{22}} - \frac{1}{c_{22}} U^*, 0). \tag{4.85}$$

We wish to find a solution to (4.84) connecting the first and last equilibria listed (4.85) so that the matching conditions (4.81) and (4.82) are satisfied. The Jacobian of (4.84) has eigenvalues given by

$$\lambda\pm = \frac{1}{2}\left(-c \pm \sqrt{c^2 - 4\tilde{g}_{\hat{V}}(\hat{Y}_2^*)}\right). \tag{4.86}$$

From (4.37) we see that

$$\tilde{g}_{\hat{V}} = \hat{V}\frac{d\tilde{g}}{d\hat{Y}_2^*}\frac{d\hat{Y}_2^*}{d\hat{V}} + g(\hat{Y}_2^*). \tag{4.87}$$

At $(0,0)$ using (4.83) we find $\hat{Y}_2^* = U^*$ and thus (4.87) gives us $\tilde{g}_{\hat{V}} = g(U^*)$. Previously for the outer solutions we assumed that $w_2 > \frac{z_1}{c_{11}}$ and that $U^* \in (0, \frac{z_1}{c_{11}})$, therefore we have $U^* < w_2$. If $0 < U^* < w_1$ then $g(U^*) < 0$ and if $w_1 < U^* < w_2$ then $g(U^*) > 0$,

see Figure 2. For the first case, with $0 < U^* < w_1$, $(0,0)$ would be a saddle. In the second case, with $w_1 < U^* < w_2$, if $|c| < 2\sqrt{g(U^*)}$ we would get a spiral and for $|c| > 2\sqrt{g(U^*)}$ we would get a node. A spiral at $(0,0)$ is not biologically feasible, thus we must have $|c| > 2\sqrt{g(U^*)}$. The stability of the resulting node is dependent on the sign of c: for $c < 0$ the node is unstable and for $c > 0$ it is stable.

Again we will consider the sign of c, using the same methods as the earlier sections. We will multiply (4.80) by $\hat{V}'$ and integrate over ξ assuming the limits in (4.81)-(4.82). Because the limits are equilibria of the system we have $\hat{V}' = 0$ for $\xi = \pm\infty$. Therefore we obtain

$$c = \frac{-\int_{-\infty}^{\infty} \tilde{g}(\hat{Y}_2^*)\hat{V}'d\xi}{\int_{-\infty}^{\infty}(\hat{V}')^2 d\xi}. \tag{4.88}$$

Letting $s = \hat{Y}_2^*(\hat{V}(\xi))$ so that $ds = \frac{d\hat{Y}_2^*}{d\hat{V}}\frac{d\hat{V}}{d\xi}d\xi$ with $\frac{d\hat{Y}_2^*}{d\hat{V}} = c_{22}$ and $\hat{Y}_2^*(\hat{V}(\infty)) = U^*$, $\hat{Y}_2^*(\hat{V}(-\infty)) = w_2$ equation (4.88) becomes

$$c = \frac{\frac{1}{c_{22}}\int_{U^*}^{w_2} \tilde{g}(s)ds}{\int_{-\infty}^{\infty}(\hat{V}')^2 d\xi} \tag{4.89}$$

Thus c is the same sign as $\int_{U^*}^{w_2} \tilde{g}(s)ds$. For these calculations we have assumed $w_1 < U^* < w_2$. In this region $\tilde{g}(s) > 0$, therefore $c > 0$ and thus for $c > 2\sqrt{g(U^*)}$, $(0,0)$ is a stable node.

Now we consider the eigenvalues of the equilibrium $(\frac{w_2}{c_{22}} - \frac{1}{c_{22}}U^*, 0)$. Noticing from (4.83) that at this equilibrium $Y_2^* = w_2$ and $\frac{dY_2^*}{d\hat{V}} = c_{22}$ we get $\tilde{g}_{\hat{V}} = (w_2 - U^*)\frac{d\tilde{g}}{d\hat{Y}_2^*}$. At this equilibrium we have $\frac{d\tilde{g}}{d\hat{Y}_2^*} < 0$ so the eigenvalues in (4.86) are real and of opposite sign, and thus $(\frac{w_2}{c_{22}} - \frac{1}{c_{22}}U^*, 0)$ is a saddle.

We consider the possibility of a trajectory connecting $(0,0)$ to $(\frac{w_2}{c_{22}} - \frac{1}{c_{22}}U^*, 0)$ with $\lim_{\xi\to\infty}\hat{V} = 0$ and $\lim_{\xi\to-\infty}\hat{V} = \frac{w_2}{c_{22}} - \frac{1}{c_{22}}U^*$. There are two cases to consider. In the first case, $0 < U^* < w_1$, $(0,0)$ and $(\frac{w_2}{c_{22}} - \frac{1}{c_{22}}U^*, 0)$ are both saddles. The phase plane diagram for this case is given in Figure 30. Here we want to show a saddle-saddle connection. The proof of the existence of such a connection was sketched

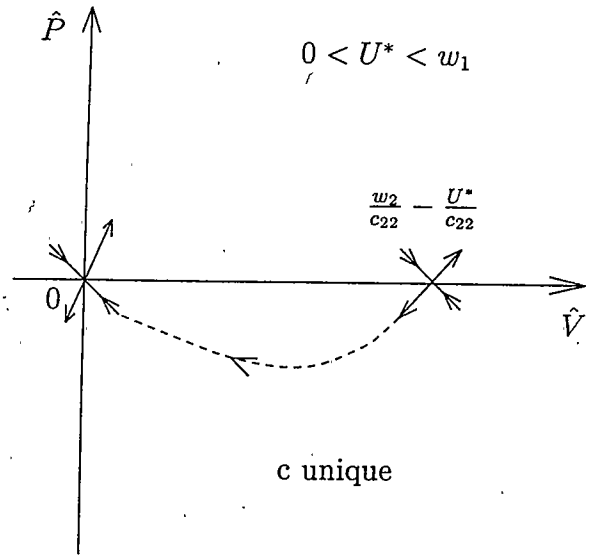

Figure 30: Saddle-saddle phase plane connections for inner problem with $0 < U^* < w_1$.

in the section dealing with traveling waves along the V-axis. There we found that such a connection would exist for a unique value of c. This system is analogous to the generalized (bistable) Nagumo equation for which from [1] we get the following theorem

Theorem 4.5 *[1] For the generalized Nagumo equation: $v_t = \tilde{g} + v_{xx}$, where $\tilde{g}$ satisfies, $\tilde{g}(0) = \tilde{g}(w_1) = \tilde{g}(w_2) = 0$, $\tilde{g} < 0$ in $(0, w_1)$, $\tilde{g} > 0$ in (w_1, w_2), $\tilde{g}'(0) < 0$, $\tilde{g}'(w_2) < 0$ and $G(w_2) = \int_0^{w_2} \tilde{g}(s)ds > 0$, there is a unique $c > 0$ such that there exists a wave front from w_2 to 0.*

In this first case, with $0 < U^* < w_1$, there exists a unique value of c, such that there will be a connection between $(0, 0)$ and $(\frac{w_2}{c_{22}} - \frac{1}{c_{22}}U^*, 0)$.

In the second case we are looking for a connection between $(0, 0)$ and $(\frac{w_2}{c_{22}} - \frac{1}{c_{22}}U^*, 0)$ when $w_1 < U^* < w_2$ with $c > 0$, $c > 2\sqrt{g(U^*)}$. Under these conditions $(0, 0)$ is a stable node and $(\frac{w_2}{c_{22}} - \frac{1}{c_{22}}U^*, 0)$ is a saddle. See Figure 31 for the phase

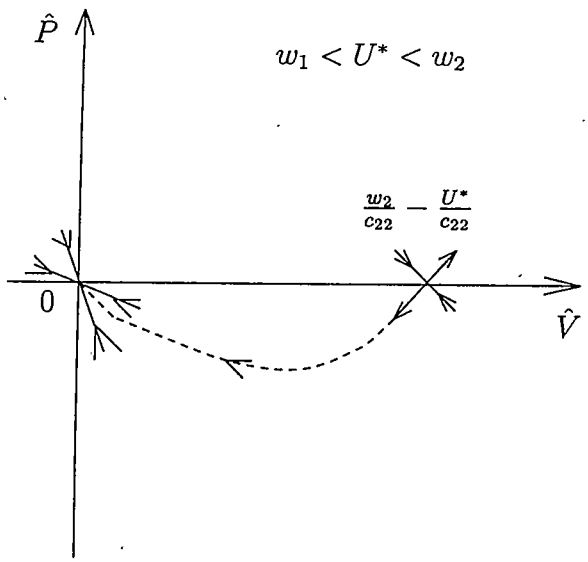

Figure 31: Node-saddle connection for inner problem with $w_1 < U^* < w_2$.

diagram of this case. Notice that in this case with $w_1 < U^* < w_2$ that the middle equilibrium in (4.85) has a value of $\hat{V} < 0$. In this second case the system is analogous to the generalized Fisher equation [1]. Using the following theorem we can show the existence of a connection between $(0,0)$ and $(\frac{w_2}{c_{22}} - \frac{1}{c_{22}}U^*, 0)$.

Theorem 4.6 *[1] For the equation $v_t = h(v) + v_{xx}$, where $h(v)$ satisfies $h(0) = h(w_2) = 0$, $h > 0$ in $(0, w_2)$, $h'(0) > 0$, $h'(w_2) < 0$, has a traveling wave solution $v(x,t) = V(x - ct) = V(\xi)$ satisfying $V(\xi) \to 0$ as $\xi \to \infty$ and $V(\xi) \to w_2$ as $\xi \to -\infty$ for every c satisfying $c \geq 2\sqrt{k}$, where $k = \sup_{V \in (0,w_2)} \frac{h(V)}{V}$.*

Proof of this theorem was sketched in the section dealing with traveling waves along the u-axis and presented in [1], [7].

In both cases we can thus show the existence of a heteroclinic connection between $(0,0)$ and $(\frac{w_2}{c_{22}} - \frac{1}{c_{22}}U^*, 0)$. Therefore we can find a $\hat{V}$ satisfying (4.79) and (4.81)-(4.82). Call this solution V_{Inner} with $U_{Inner} = U^*$.

We wish to now define the composite $O(1)$ solution to the original system

(4.38). This will consist of combining both the outer and inner $O(1)$ solutions so that they match at the layer edges. Let U_c and V_c be these composite solutions given by

$$U_c = U_{Outer}(z) \tag{4.90}$$

$$V_c = \begin{cases} h_-(U_c(z)) + V_{Inner}(\frac{z-z^*}{\epsilon}) - h_-(U^*) & \text{for } z < z^* \\ h_+(U_c(z)) + V_{Inner}(\frac{z-z^*}{\epsilon}) - h_+(U^*) & \text{for } z > z^*. \end{cases} \tag{4.91}$$

Substituting in (4.44) and (4.45) into (4.91) simplifies V_c to the following

$$V_c = \begin{cases} \frac{1}{c_{22}}(U^* - U_c(z)) + V_{Inner}(\frac{z-z^*}{\epsilon}) & \text{for } z < z^* \\ V_{Inner}(\frac{z-z^*}{\epsilon}) & \text{for } z > z^*. \end{cases} \tag{4.92}$$

Now to check matching we merely need to see that the solutions are continuous for all z. By construction we have that $U_{Outer}(z)$ is a C^1 approximate solution to the wave equation so U_c is also C^1. Examining V_c at $z = z^*$ we observe this is the only value at which v_c or its derivative could be discontinuous. Looking at the limit of (4.92) we see that

$$\lim_{z \to z^{*-}} V_c(z) = V_{Inner}(0) \tag{4.93}$$

$$\lim_{z \to z^{*+}} V_c(z) = V_{Inner}(0), \tag{4.94}$$

and thus $V_c(z)$ is at least C^0. Next we consider the first derivative.

$$V_c'(z) = \begin{cases} \frac{1}{c_{22}}(-U_c'(z)) + \frac{1}{\epsilon}V_{Inner}'(\frac{z-z^*}{\epsilon}) & \text{for } z < z^* \\ \frac{1}{\epsilon}V_{Inner}'(\frac{z-z^*}{\epsilon}) & \text{for } z > z^*. \end{cases} \tag{4.95}$$

Thus we get continuity of V_c' at $z = z^*$ if $U_c'(z^*) = 0$. But in general for U^* not an equilibrium of the system we get $U_c'(z) > 0$. Therefore V_c' is not continuous and thus V_c is merely C^0.

In conclusion for the system (4.38) we can find an $O(1)$ approximate solution given by (4.90) and (4.92) that is C^1 in U and C^0 in V with (4.48) and (4.81)-(4.82) satisfied. The existence of such an approximate solution does not guarantee the existence of a true solution. In the next section we will consider the system using geometric perturbation techniques discussed in [13], [30], [29] and [6] to prove the existence of a true solution that is near the asymptotic solution.

Geometric Singular Perturbation

In this section what we want to consider is a traveling wave solution for the system (4.35) were ϵ is a small positive parameter. $\tilde{f}(y_1)$ and $\tilde{g}(y_2)$ are given by (4.36) and (4.37), y_1 and y_2 from (2.1) and (2.2), zeros of $\tilde{f}(y_1)$ and $\tilde{g}(y_2)$ are given by (2.6) and (2.7) respectively and we assume the conditions $f'(z_1) < 0$, $g'(w_1) > 0$ and $g'(w_2) < 0$ with $z_1 > 0$, $0 < w_1 < w_2$. We wish to consider a traveling wave between the equilibria $(\frac{z_1}{c_{11}}, 0)$ and $(0, \frac{w_2}{c_{22}})$. The particular traveling wave we are looking for would have wave speed of order ϵ. Thus we will let the traveling wave variable $z = x - \epsilon ct$. The equations in traveling wave coordinates then become

$$\begin{aligned} u'' + \epsilon c u' + \tilde{f}(y_1) &= 0 \\ \epsilon^2 v'' + \epsilon c v' + \tilde{g}(y_2) &= 0 \end{aligned} \tag{4.96}$$

where $' = \frac{d}{dz}$.

To enable an analysis of (4.96) using geometric singular perturbation we need to introduce some terminology and results from [6], [30], [29] and [13]. We will then apply these results to our system.

Introduction to Geometric Singular Perturbation Theory In this section we briefly summarize the necessary results of [6], [29] and [30]. We will consider the singularly perturbed system of differential equations,

$$\begin{aligned} x' &= f(x, y, \epsilon) \\ \epsilon y' &= g(x, y, \epsilon) \end{aligned} \tag{4.97}$$

with $\epsilon \in (-\epsilon_0, \epsilon_0)$, with $\epsilon_0 > 0$ small, and $(x, y) \in \Omega$, an open subset $\Omega \in \mathbb{R}^{n+k}$. In the above equations (4.97) " $'$ " denotes differentiation with respect to z, the slow variable. The system (4.97) is referred to as the slow system and will be denoted

S_ϵ. We assume that f and g are $C^r(\Omega \times (-\epsilon_0, \epsilon_0))$, with r sufficiently large. For $\epsilon \neq 0$ (4.97) defines a smooth dynamical system on Ω. The fast scale is defined by $\xi := \frac{z-z^*}{\epsilon}$, which transforms the system (4.97) to

$$\begin{aligned} \dot{x} &= \epsilon f(x, y, \epsilon) \\ \dot{y} &= g(x, y, \epsilon) \end{aligned} \tag{4.98}$$

where " $\dot{}$ " denotes differentiation with respect to ξ. This system, called the fast system, will be denoted F_ϵ. By setting the perturbation parameter $\epsilon = 0$ in (4.97) and (4.98) we will obtain simpler or lower-dimensional problems which are often easier to analyze. In (4.97) we get the reduced problem, S_0, by setting $\epsilon = 0$;

$$\begin{aligned} x' &= f(x, y, 0) \\ 0 &= g(x, y, 0), \end{aligned} \tag{4.99}$$

and doing the same in (4.98), gives us the layer problem F_0,

$$\begin{aligned} \dot{x} &= 0 \\ \dot{y} &= g(x, y, 0). \end{aligned} \tag{4.100}$$

The idea is to obtain solutions of (4.97) as smooth perturbations of the composite orbits of the simpler or lower dimensional equations (4.99) and (4.100). We will be concerned with the persistence of transversal intersections of invariant manifolds under small regular perturbations. In particular the transversal intersection of stable and unstable manifolds of hyperbolic equilibria in a heteroclinic orbit that persists under small regular perturbations. We make the following assumptions.

(*i*) The equation $g(x, y, 0) = 0$ has a smooth n-dimensional manifold, $\mathcal{M}$, of solutions. Let $\mathcal{M}_0$ be a compact submanifold of this manifold which is given as a graph of a C^r function $h : U \subset \mathbb{R}^n \to \mathbb{R}^k$.

(*ii*) There exist integers k_s and k_u with $k = k_s + k_u$ such that the linearization of (4.98) at $\epsilon = 0$ for each point in $\mathcal{M}$ has k_s eigenvalues with negative real part, k_u eigenvalues with positive real part and n eigenvalues with zero real part, i.e. $\mathcal{M}$ is normally hyperbolic.

Under the above assumptions the reduced problem, S_0, (4.99) defines a flow on $\mathcal{M}_0$. Additionally $\mathcal{M}$ is an invariant manifold of equilibria for the flow defined by F_0, (4.100). We denote the k_s-dimensional local stable manifold of $q \in \mathcal{M}_0$ by $\mathcal{F}^s(q)$ and, similarly, the k_u-dimensional unstable manifold by $\mathcal{F}^u(q)$. Fenichel in [6] showed that for sufficiently small ϵ the manifold $\mathcal{M}_0$ perturbs to a locally invariant center-like manifold $\mathcal{M}_\epsilon$ with $n + k_s$-dimensional center-stable manifold $\mathcal{M}_\epsilon^s$ and a $n + k_u$-dimensional center-unstable manifold $\mathcal{M}_\epsilon^u$. The flow on $\mathcal{M}_\epsilon$ is a regular perturbation of the reduced problem on $\mathcal{M}_0$. Furthermore, there exist invariant foliations of $\mathcal{M}_\epsilon^s$ and $\mathcal{M}_\epsilon^u$ by k_s-dimensional manifolds $\mathcal{F}_\epsilon^s(q)$ and k_u-dimensional manifolds $\mathcal{F}_\epsilon^u(q)$, $q \in \mathcal{M}_\epsilon$, respectively. The dependence of these manifolds on ϵ is C^{r-1}, even at $\epsilon = 0$.

Let $m \in \mathcal{M}_0$ be a hyperbolic equilibrium point of (4.99). Let $\Gamma^s(m)$ and $\Gamma^u(m)$ denote the local stable and unstable manifold of m for the reduced problem. We define the singular stable and unstable manifold, respectively by

$$W_0^s(m) = \bigcup_{q \in \Gamma^s(m)} \mathcal{F}^s(q), \qquad W_0^u(m) = \bigcup_{q \in \Gamma^u(m)} \mathcal{F}^u(q). \tag{4.101}$$

From [6] is follows that $W_0^s(m)$ perturbs smoothly to the stable manifold $W_\epsilon^s(m)$ of the hyperbolic equilibrium point of (4.97) for small ϵ. Similarly, $W_0^u(m)$ perturbs smoothly to the unstable manifold $W_\epsilon^u(m)$.

In our case the manifold of solutions of $g(x, y, 0)$ has two branches under consideration. Let $\mathcal{M}_0^+$ and $\mathcal{M}_0^-$ be two manifolds which satisfy conditions (*i*) and (*ii*). Let $m^- \in \mathcal{M}_0^-$ be a hyperbolic equilibrium point of (4.99) with unstable manifold $\Gamma_0^u(m^-)$, and $m^+ \in \mathcal{M}_0^+$ be a hyperbolic equilibrium point of (4.99) with stable manifold $\Gamma_0^s(m^+)$. Assume that $q^- \in \Gamma_0^u(m^-)$ and $q^+ \in \Gamma_0^s(m^+)$ are connected by

a heteroclinic orbit of (4.100). We will let ω be the full orbit from m^- to m^+ that contains this heteroclinic connection.

Theorem 4.7 *[29] Under the assumptions of this section and assuming in addition that $W_0^u(m^-)$ and $W_0^s(m^+)$ intersect transversally along the heteroclinic orbit ω. Then there exists $\epsilon_1 > 0$ and a C^{r-1} family $\{\omega_\epsilon : \epsilon \in (0, \epsilon_1)\}$ such that:*

(i) ω_ϵ is a transversal heteroclinic orbit connecting the hyperbolic fixed points m_ϵ^- and m_ϵ^+ of the singularly perturbed problem F_ϵ.

(ii) The orbits ω_ϵ are uniformly close to the singular orbit ω_0.

The proof of this theorem along with examples are given in Szmolyan [30]. By Theorem 4.7 if the singular stable and unstable manifolds intersect transversally along the singular heteroclinic orbit, we obtain the existence of a heteroclinic orbit for (4.97) for sufficiently small ϵ. The persistence of these heteroclinic orbits for small ϵ will enable us to show the existence of a traveling wave solution for (4.35) with $O(\epsilon)$ wave speed.

Geometric Singular Perturbation for Pioneer/Climax Model We now consider (4.96). Writing (4.96) as a first order system of differential equations we get

$$\begin{aligned} u' &= p \\ p' &= -\epsilon c p - \tilde{f}(y_1) \\ \epsilon v' &= q \\ \epsilon q' &= -cq - \tilde{g}(y_2). \end{aligned} \tag{4.102}$$

This is our slow system, S_ϵ. Here $(u, p, v, q) \in \Omega$, where Ω is an open subset of $\mathbb{R}^4$ and the right hand terms of (4.102) are C^∞. We seek a solution to this system which is a heteroclinic connection of the equilibria $(\frac{z_1}{c_{11}}, 0, 0, 0)$ and $(0, 0, 0, \frac{w_2}{c_{22}})$. Considering

(4.102) and letting $\xi = \frac{z-z^*}{\epsilon}$ we get the following equivalent system for $\epsilon \neq 0$ with $\cdot = \frac{d}{d\xi}$:

$$\begin{aligned} \dot{u} &= \epsilon p \\ \dot{p} &= -\epsilon^2 cp - \epsilon \tilde{f}(y_1) \\ \dot{v} &= q \\ \dot{q} &= -cq - \tilde{g}(y_2). \end{aligned} \tag{4.103}$$

This is the fast system, denoted F_ϵ. We have two limits for these equations associated with each scaling as $\epsilon \to 0$. In (4.103) letting $\epsilon \to 0$ we obtain the layer system

$$\begin{aligned} \dot{u} &= 0 \\ \dot{p} &= 0 \\ \dot{v} &= q \\ \dot{q} &= -cq - \tilde{g}(y_2). \end{aligned} \tag{4.104}$$

This implies v and q will vary while u and p remain constant. Therefore v and q are the fast variables and u and p the slow variables. The last two equations of (4.104) are the layer problem, F_0, with u and p assumed constant,

$$\begin{aligned} \dot{v} &= q \\ \dot{q} &= -cq - \tilde{g}(y_2). \end{aligned} \tag{4.105}$$

If we let $\epsilon \to 0$ in (4.102) we obtain

$$\begin{aligned} u' &= p \\ p' &= -\tilde{f}(y_1) \\ 0 &= q \\ 0 &= -cq - \tilde{g}(y_2). \end{aligned} \tag{4.106}$$

The conditions, $\tilde{g}(y_2) = 0$ and $q = 0$, determine a manifold on which the flow is given by

$$\begin{aligned} u' &= p \\ p' &= -\tilde{f}(y_1). \end{aligned} \tag{4.107}$$

As in the previous section we can solve $\tilde{g}(y_2) = 0$ for v in terms of u. The solutions we are concern with are $v = h_\pm(u)$ where $h_\pm(u)$ are given in (4.44) and (4.45). With these functions we can write (4.107) as the reduced system, $S_0^\pm$, given by

$$\begin{aligned} u' &= p \\ p' &= -\tilde{f}(y_1^\pm) \end{aligned} \tag{4.108}$$

where

$$y_1^\pm = \begin{cases} c_{11}u + h_-(u) & \text{for } 0 < u < u^* \\ c_{11}u + h_+(u) & \text{for } u^* < u < \frac{z_1}{c_{11}}. \end{cases} \tag{4.109}$$

The set $\{\tilde{g}(y_2) = 0, q = 0\}$ defines two C^r slow manifolds, $\mathcal{M}^\pm$, on which (4.108) defines a dynamical system. $\mathcal{M}^\pm$ is given as

$$\mathcal{M}^\pm = \{(u, p, v, q) | u \in \mathbb{R}, p \in \mathbb{R}, v = h_\pm(u), q \equiv 0\}. \tag{4.110}$$

These are also manifolds of equilibria for F_0, (4.104). We will define the compact slow manifold $\mathcal{M}_0^\pm$, a subset of $\mathcal{M}^\pm$ shortly.

The singular heteroclinic orbit we wish to construct will be the union of three trajectories, two for the slow equations, $S_0^\pm$, and one transition layer coming from the fast equations, F_0. On the slow manifold $\mathcal{M}_0^-$ the solution remains on the unstable manifold of the equilibrium $m^- = (0, 0)$ for S_0^- until (u, p) attains the value (u^*, p^*), where p^* is the value of p on the unstable manifold of the equilibrium when $u = u^*$. This piece of the singular solution is embedded in $\mathbb{R}^4$ by taking $v = h_-(u)$, $q \equiv 0$.

At (u^*, p^*) the solution is required to jump to the slow manifold $\mathcal{M}_0^+$ via a transition layer coming from the solution of the layer problem with $u = u^*$ and

satisfying $v(\pm\infty) = h_{\pm}(u^*)$. Along this piece of the solution u and p remain at the constant values u^* and p^* respectively. The value of (u^*, p^*) where the solution jumps form $\mathcal{M}_0^-$ to $\mathcal{M}_0^+$ is determined in the same fashion as the previous section. Once on the slow manifold $\mathcal{M}_0^+$ the singular orbit evolves according to S_0^+ with initial data (u^*, p^*) on the stable manifold of the equilibrium $m^+ = (\frac{z_1}{c_{11}}, 0)$ of S_0^+. Again this piece of the orbit is embedded in $\mathbb{R}^4$ by taking $v = h_+(u)$, $q \equiv 0$. An illustration of this orbit is depicted in Figure 32.

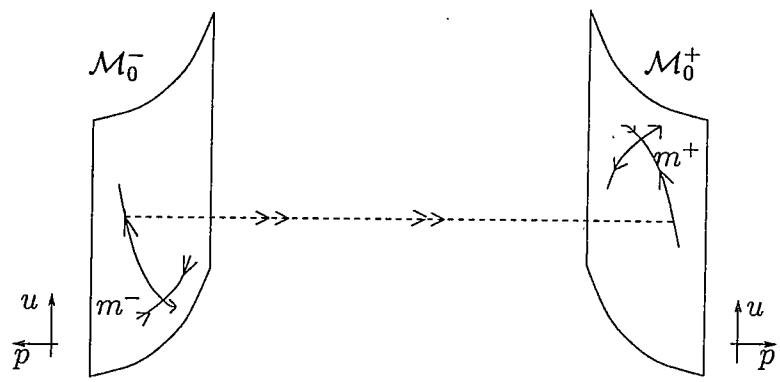

Figure 32: Heteroclinic orbit connecting equilibria $(\frac{z_1}{c_{11}}, 0, 0, 0)$ and $(0, 0, \frac{w_2}{c_{22}})$,0.

First we consider the stability of $m^{\pm}$ on $S_0^{\pm}$ respectively. The eigenvalues of the Jacobian of $S_0^{\pm}$ are $\lambda = \pm\sqrt{-\tilde{f}_u}$. Looking first at $m^- = (0, 0)$ on S_0^- we have that $y_1^- = \frac{w_2}{c_{22}}$. As in the previous section we will assume $\frac{w_2}{c_{22}} > z_1$, (4.64), so that m^- is a saddle with one stable and one unstable manifold for S_0^-. We define $j_s^- = 1$ equal the number of eigenvalues in the left half plane, $j_u^- = 1$ the number in the right half plane for m^- on $\mathcal{M}^-$. For $m^+ = (\frac{z_1}{c_{11}}, 0)$ on S_0^+ we see that $y_1 = z_1$ and by equation (4.56) that $-\tilde{f}_u > 0$. This gives us that m^+ is also a saddle with one stable and one unstable manifold for S_0^+. So that for m^+, $j_s^+ = 1$ and $j_u^+ = 1$ on $\mathcal{M}^+$. Both m^- and m^+ are hyperbolic equilibria for the reduced system (4.108).

Along the slow manifolds, $\mathcal{M}^{\pm}$, for the trajectories we are concerned with we

can define $p^{\pm} = P^{\pm}(u)$, where $P^{-}(u)$ corresponds to the one dimensional unstable manifold of m^{-} on $\mathcal{M}^{-}$ and $P^{+}(u)$ corresponds to the one dimensional stable manifold of m^{+} on $\mathcal{M}^{+}$ as in the previous section (see Figure 33).

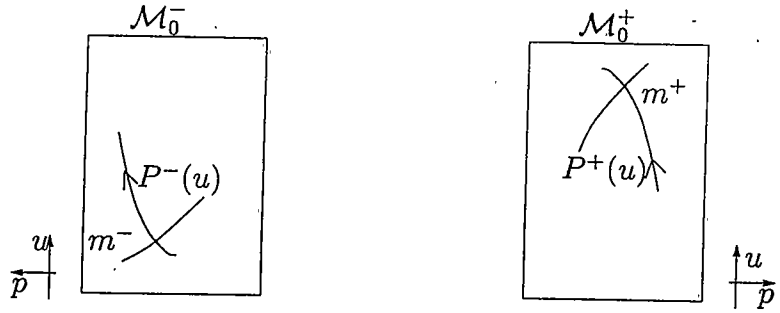

Figure 33: Slow Manifolds $\mathcal{M}^{-}$ and $\mathcal{M}^{+}$ with $P^{-}(u)$ and $P^{+}(u)$.

We can define the compact submanifold $\mathcal{M}_0^{\pm}$ as follows:

$$\mathcal{M}_0^- = \left\{(u,p,v,q) | 0 \leq u < u^* + \delta, p = P^-(u), v = h_-(u), q = 0\right\}, \quad (4.111)$$

$$\mathcal{M}_0^+ = \left\{(u,p,v,q) | u^* - \delta < u \leq \frac{z_1}{c_{11}}, p = P^+(u), \right.$$
$$\left. v = h_+(u), q = 0\right\}, \quad (4.112)$$

where $\delta > 0$ small.

The fundamental hypotheses on $\mathcal{M}^{\pm}$ defined in (4.110) is that they be normally hyperbolic. To show that both $\mathcal{M}^{\pm}$ are normally hyperbolic we consider the Jacobian of (4.103) at $\epsilon = 0$. The Jacobian is given by:

$$J = \left[\begin{array}{cccc} 0 & \epsilon & 0 & 0 \\ -\epsilon\tilde{f}_u & \epsilon^2 c & -\epsilon\tilde{f}_v & 0 \\ 0 & 0 & 0 & 1 \\ -\tilde{g}_u & 0 & -\tilde{g}_v & -c \end{array}\right]_{|(u,p,h_{\pm}(u),q=0)} \quad (4.113)$$

Evaluating (4.113) on $\mathcal{M}^{\pm}$ with $\epsilon = 0$ we find that the characteristic equation is

$$\lambda^2[\lambda^2 + \lambda + \tilde{g}_v] = 0. \quad (4.114)$$

The eigenvalue $\lambda = 0$ has multiplicity two. We consider the nontrivial eigenvalues $\lambda = \frac{1}{2}(-c \pm \sqrt{c^2 - \tilde{g}_v})$.

If we consider the eigenvalues for points on $\mathcal{M}^-$, i.e. $(u, p, h_-(u), 0)$ we have from the previous section that for $u^* < w_2$ that $\tilde{g}_v < 0$ on this manifold, (u^* being the value of u in the layer problem when $\epsilon = 0$). Therefore $\lambda = \frac{1}{2}(-c \pm \sqrt{c^2 - \tilde{g}_v})$ will give us two real eigenvalues of opposite sign. Thus $\mathcal{M}^-$ is normally hyperbolic and $k_s^- = k_u^- = 1$. Looking at the eigenvalues for points on $\mathcal{M}^+$, i.e. $(u, p, h_+(u), 0) = (u, p, 0, 0)$ we see from analysis of the previous section that if $0 < u^* < w_1$ then $\tilde{g}_v < 0$ and if $w_1 < u^* < w_2$ then $\tilde{g}_v > 0$. Thus for $u^* \neq w_1, w_2$ we get two nonzero eigenvalues and in both cases the manifold, $\mathcal{M}^+$ is normally hyperbolic. Because $\mathcal{M}_0^\pm$ (4.110) are compact subsets of $\mathcal{M}^\pm$, respectively, we have that they are normally hyperbolic invariant manifolds of the layer problem (4.103). However there are now two cases to consider. If $0 < u^* < w_1$ we have that $k_s^+ = 1$, and $k_u^+ = 1$ and if $w_1 < u^* < w_2$ then $k_s^+ = 2$, and $k_u^+ = 0$. We will deal with each case separately.

Saddle-Node Connection in the Layer System The first case we will examine is for $w_1 < u^* < w_2$, where in the layer problem at $\epsilon = 0$ we have a saddle-node connection. We wish to be able to characterize the stable and unstable manifolds of our equilibria for the full system in this case. In particular because the solution we are looking for is an intersection of the unstable manifold of m^- and the stable manifold of m^+ we want to give a representation of these particular manifolds. These manifolds will be made up of parts from the reduced system and the layer system. First we will describe the local stable manifold of m^+, $\Gamma_0^s(m^+)$, and the unstable manifold of m^-, $\Gamma_0^u(m^-)$, for the reduced problem $S_0^\pm$.

$$\Gamma_0^s(m^+) = \left\{(u, P^+(u)) | u^* - \delta < u \leq \frac{z_1}{c_{11}}\right\}, \tag{4.115}$$

$$\Gamma_0^u(m^-) = \left\{(u, P^-(u)) | 0 \leq u < u^* + \delta\right\}. \tag{4.116}$$

Both are one dimensional manifolds parameterized by u. Now off of each of these unstable and stable manifolds of m^- and m^+ respectively there are unstable and stable fibers of the layer system, (4.104), with $\epsilon = 0$. Notice that the layer problem, F_0, is the same as (4.84) with $\hat{V} = v$, $\hat{P} = q$ and $Y_2^* = y_2$. As in that problem, we are assuming u and p are constants such that $u = u^*$ and $p = P^+(u^*) = P^-(u^*)$ and $v(\pm\infty) = h_\pm(u^*)$. We found that for $w_1 < u^* < w_2$ there was a saddle-node connection between $(0,0)$ and $(\frac{w_2}{c_{22}} - \frac{1}{c_{22}}u^*, 0)$ (see Figure 31). In a saddle-node connection there is a family of trajectories that may occur. For these trajectories a range of q values exist. Let q_{min} denote the minimum of q along the orbit for the layer problem if $w_1 < u^* < w_2$, then choose q_0 so that $q_0 < q_{min}$.

The unstable and stable manifold of m^- and m^+ can be given as follows:

$$\begin{aligned} W_0^u(m^-) &= \left\{(u,p,v,q) | 0 \le u < u^* + \delta, p = P^-(u), \right. \\ &\qquad \left. 0 \le v \le h_-(u), q = q^-(v)\right\}, \qquad (4.117) \\ W_0^s(m^+) &= \left\{(u,p,v,q) | u^* - \delta < u \le \frac{z_1}{c_{11}}, p = P^+(u), \right. \\ &\qquad \left. 0 \le v \le h_-(u), q_0 \le q < 0\right\}. \qquad (4.118) \end{aligned}$$

Now from the previous section we know that the unstable manifold $W_0^u(m^-)$ intersects the stable manifold $W_0^s(m^+)$ along the heteroclinic connection in the layer problem. Let ω denote the full orbit from m^- to m^+ that contains this heteroclinic connection. Using Theorem 4.7 we will be able to show the persistence of this orbit in the perturbed system with ϵ small.

To Theorem 4.7 we need to show that the stable and unstable manifolds intersect transversally along the layer. To show transversality of the manifolds at the intersection point we need the tangent space at that intersection to span all of $\mathbb{R}^4$ [30], i.e. $T_r W_0^u(m^-) + T_r W_0^s(m^+) = \mathbb{R}^4$. The intersection takes place in the layer region where $u = u^*$ and $p = p^*$ on a plane such that v and q are constant. Let the point of

intersection be $r = (u^*, p^*, a, b)$ where $0 \leq a \leq h^-(u^*)$ and $q_0 < b \leq 0$. Considering the Jacobian of $W_0^u(m^-)$ and $W_0^s(m^+)$, at the intersection we need to show that there are four linearly independent vectors between the stable and unstable manifolds.

The Jacobian for $W_0^u(m^-)$ is given by:

$$J_{(m^-)} = \left[\begin{array}{cccc} 1 & 0 & 0 & 0 \\ \frac{dP^-}{du} & 0 & 0 & 0 \\ 0 & 0 & 1 & 0 \\ 0 & 0 & \frac{dq^-}{dv} & 0 \end{array} \right]_{|_{r=(u^*,p^*,a,b)}} \tag{4.119}$$

The Jacobian for $W_0^s(m^+)$ is as follows:

$$J_{(m^+)} = \left[\begin{array}{cccc} 1 & 0 & 0 & 0 \\ \frac{dP^+}{du} & 0 & 0 & 0 \\ 0 & 0 & 1 & 0 \\ 0 & 0 & 0 & 1 \end{array} \right]_{|_{r=(u^*,p^*,a,b)}} \tag{4.120}$$

We will obtain four linearly independent vectors as long as $\frac{dP^-}{du}(u^*) \neq \frac{dP^+}{du}(u^*)$.

By equation (4.66) we see

$$\frac{dP^+}{du}(u^*) = -\frac{\tilde{f}(y_1^+(u^*))}{P^+(u^*)} \tag{4.121}$$

and

$$\frac{dP^-}{du}(u^*) = -\frac{\tilde{f}(y_1^-(u^*))}{P^-(u^*)}. \tag{4.122}$$

We have already assumed that $P^+(u^*) = P^-(u^*)$, so for an inequality to occur it must be that $\tilde{f}(y_1^+(u^*)) \neq \tilde{f}(y_1^-(u^*))$. Recall from (4.36) that

$$\tilde{f}(y_1) = uf(y_1)$$

where $f(y_1)$ is a monotonically decreasing function of y_1. Therefore if $y_1^+(u^*) \neq y_1^-(u^*)$, then $\tilde{f}(y_1^+(u^*)) \neq \tilde{f}(y_1^-(u^*))$. From (4.50) we have that $y_1^+(u^*) = c_{11}u^*$ and from (4.58) that $y_1^-(u^*) = \frac{det(C)}{c_{22}}u^* + \frac{w_2}{c_{22}}$. Setting these two equal gives us that if $u^* \neq \frac{w_2}{c_{22}}$ then $y_1^+ \neq y_1^-$ at $u = u^*$, so that $\frac{dP^+}{du}(u^*) \neq \frac{dP^-}{du}(u^*)$. Therefore for $u^* \neq \frac{w_2}{c_{22}}$ and $w_1 < u^* < w_2$ we have that $T_r W_0^u(m^-) + T_r W_0^s(m^+) = \mathbb{R}^4$, and there is a

transversal intersection for the heteroclinic connection. Theorem 4.7 gives us that this connection will persist for small ϵ. The persistence of this connection implies that there exists traveling wave solutions to (4.35) with $O(\epsilon)$ wave speeds.

Saddle-Saddle Connection in the Layer System The next case we will consider is when $0 < u^* < w_1$. In this case the layer problem has a saddle-saddle connection. We will be using Theorem 4.7 again to show the persistence of the heteroclinic connection for (4.35) with $O(\epsilon)$ wave speeds. Therefore, we must again characterize the stable and unstable manifold of m^+ and m^- respectively.

We found from problem (4.84) that if $0 < u^* < w_1$ then the layer problem F_0 will have a saddle-saddle connection with a unique wave speed, $c = c^*$. Because of the dependency of this trajectory on the wave speed we need to introduce a fifth equation to our system in order to show transversality of the intersection. Thus we will supplement (4.102) and (4.103) with

$$c' = 0 \tag{4.123}$$

and

$$\dot{c} = 0 \tag{4.124}$$

respectively. Now the slow variables are u, p and c while the fast variables are unchanged. The introduction of this supplementary equation will not change the normal hyperbolicity of the slow manifolds. It will allow us to show the transversality of the intersection of the stable and unstable manifolds of $m^- = (0, 0, c)$ and $\hat{m}^+ = (\frac{z_1}{c_{11}}, 0, c)$.

The dependence of the heteroclinic connection in the layer problem on the wave speed is depicted in the dependence of q on both v and c. The unstable and stable manifolds of m^- and m^+ respectively are given by:

$$W_0^u(m^-) = \Big\{(u, p, v, q, c) | 0 \leq u < u^* + \delta, p = P^-(u), 0 \leq v \leq h_-(u),$$

$$q = q^-(v,c), c^* - \delta < c < c^* + \delta \Big\}, \tag{4.125}$$

$$W_0^s(m^+) = \Big\{(u,p,v,q,c) | u^* - \delta < u \leq \frac{z_1}{c_{11}}, p = P^+(u), 0 \leq v \leq h_-(u),$$

$$q = q^+(v,c), c^* - \delta < c < c^* + \delta \Big\}. \tag{4.126}$$

Again we will let ω denote the full orbit from m^- to m^+ that contains the heteroclinic connection. We now need to show that the intersection of $W_0^u(m^-)$ and $W_0^s(m^+)$ spans all of $\mathbb{R}^5$. The intersection will take place in the layer region with $u = u^*$ and $p = p^*$ along the unique trajectory defined by $c = c^*$. We define the point of intersection to be $r = (u^*, p^*, a, b, c^*)$ where $0 \leq a \leq h^-(u^*)$ and $b = q(a, c^*)$. We will once again consider the Jacobian of $W_0^u(m^-)$ and $W_0^s(m^+)$ at the intersection to show there are five linearly independent vectors between the stable and unstable manifolds.

The Jacobian of $W_0^u(m^-)$ is

$$J_{(m^-)} = \begin{bmatrix} 1 & 0 & 0 & 0 & 0 \\ \frac{dP^-}{du} & 0 & 0 & 0 & 0 \\ 0 & 0 & 1 & 0 & 0 \\ 0 & 0 & \frac{dq-}{dv} & 0 & \frac{dq-}{dc} \\ 0 & 0 & 0 & 0 & 1 \end{bmatrix}_{|_{r=(u^*,p^*,a,b,c^*)}} \tag{4.127}$$

and the Jacobian for $W_0^s(m^+)$ is given by

$$J_{(m^+)} = \begin{bmatrix} 1 & 0 & 0 & 0 & 0 \\ \frac{dP^-}{du} & 0 & 0 & 0 & 0 \\ 0 & 0 & 1 & 0 & 0 \\ 0 & 0 & \frac{dq+}{dv} & 0 & \frac{dq+}{dc} \\ 0 & 0 & 0 & 0 & 1 \end{bmatrix}_{|_{r=(u^*,p^*,a,b,c^*)}} \tag{4.128}$$

In the previous Jacobian calculation for the case where $w_1 < u^* < w_2$ we found for $u^* \neq \frac{w_2}{c_{22}}$ that $\frac{dP^+}{du}(u^*) \neq \frac{dP^-}{du}(u^*)$. However, we know $\frac{dq-}{dv}(a, c^*) = \frac{dq+}{dv}(a, c^*)$. Thus to show there are 5 linearly independent vectors we need $\frac{dq-}{dc}(a, c^*) \neq \frac{dq+}{dc}(a, c^*)$. This inequality is proven in [13] in section 4.5. With this result we have $T_r W_0^u(m^-) + T_r W_{0,2}^s(m^+) = \mathbb{R}^5$, and thus the manifolds intersect transversally. By Theorem 4.7 the heteroclinic connection will persist for small ϵ and thus there exists a traveling wave solution to (4.35) with $O(\epsilon)$ wave speed.

Biologically the existence of the slow traveling wave in both cases describes an invasion of the climax species into the pioneer domain but at an extremely slow speed so that for long periods of time both species will coexisted in a shared domain. The dynamics still suggested that the climax species will eventually drive the pioneer to extinction but the speed at which this will occur is very gradual. This would seem reasonable under the original assumption that the diffusion coefficient for the climax species is of $O(\epsilon^2)$.

CHAPTER 5

Conclusion

In this thesis we have analyzed a system of reaction-diffusion equations modeling the interaction of a pioneer and climax species. In Chapter 2 we dealt solely with the kinetic equations showing the existence of a Hopf bifurcation of an interior equilibrium point. In Figure 5 we see for the specific Selgrade model that the bifurcating periodic solutions will be stable. This result suggests that there is a parameter space for which the pioneer and climax species will coexist with fluctuating population sizes.

In Chapter 3 we introduced a spatial variable through diffusion, thus modeling the spatial movement of species. We showed that for the same interior equilibrium that exhibited a Hopf bifurcation in the kinetic system a Turing bifurcation can occur for the full reaction-diffusion system. The stability of the bifurcating solutions are dependent on the form of the fitness functions of both the pioneer and climax species. Both the sign of the eigenvalue of the linearized system about the equilibrium point and the direction of the bifurcation diagram about the bifurcation point will be needed to determine the stability of the the bifurcating solutions. In the Selgrade model we found parameter values that produced a bifurcation diagram of both subcritical and supercritical type for the mode one solutions. We have also shown for this model that the mode one solution is not necessarily the first modal solution to go unstable in the bifurcation. Figures 11 and 12 demonstrate parameter values for which the model has a mode two solution becoming unstable for smaller values of d than the mode one solution. The existence of a Turing bifurcation for the system introduces the possibility of a stable spatially heterogeneous steady state where both the pioneer

and climax species would exist. Further analysis is necessary to determine if such a stable heterogeneous state exists for this system.

In Chapter 4 we looked again at the full reaction-diffusion system but with an eye toward traveling wave solutions to the system. Initially we looked for traveling wave solutions along the axis, corresponding to traveling waves in the absence of one of the species. We find the existence of such solutions for both the pioneer and climax species. These traveling wave solutions corresponded to heteroclinic connections in the corresponding traveling wave system of ordinary differential equations. Biologically they represent the movement over space from one population size to a different populations size. Next in Chapter 4 we examined the existence of a slow moving traveling wave for the full system. The wave was shown to exist using geometric singular perturbation theory. The existence of this wave suggests that although the climax species will eventually crowed out the pioneer species the process is extremely slow and for long periods of time both species will coexist. It would seem possible that with proper management the coexistence of both species could continue for as long as it is desirable. Future research could involve the study of the affects of such management decisions.

On a final note it is interesting to mention that while numerically examining the pioneer-climax system with diffusion, it was found that some interesting numerical solutions exist that look remarkably complex. These solutions are evident for small c_{11} values where there are two spatially homogeneous solutions in the positive cone of $\mathbb{R}^2$. The complicated behavior occurs for initial conditions near q_2 with both diffusion coefficients small, and the pioneer diffusion coefficient one order of magnitude smaller than the climax diffusion coefficient. See Figure 34 for an example of the pioneer and climax species curves in this case. Figure 35 shows the solution of Figure 34 for a later time. This particular choice of c_{11}, D_1 and D_2 values give solutions that

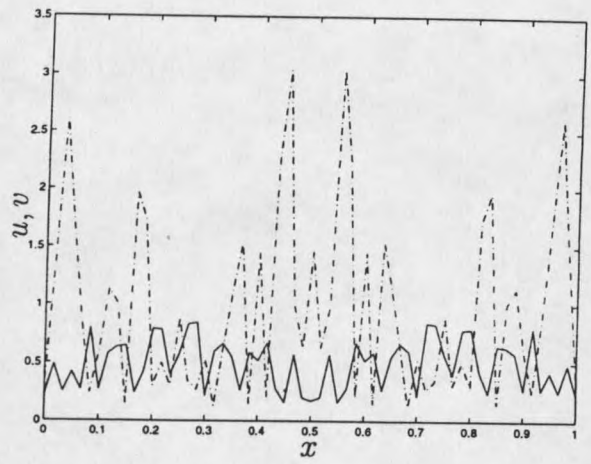

Figure 34: Pioneer and Climax solutions showing complex behavior with $c_{11} = 0.112$, $D_1 = .001$, $D_2 = .01$ and initial conditions started near q_2. Numerics done for Selgrade model, $c_{22} = 1$. Dashed line represents the Pioneer species, solid line represents the Climax species.

appear chaotic for a period of time but eventual become spatially homogeneous via a traveling wave. The next figure, Figure 36, shows a solution for a slightly larger

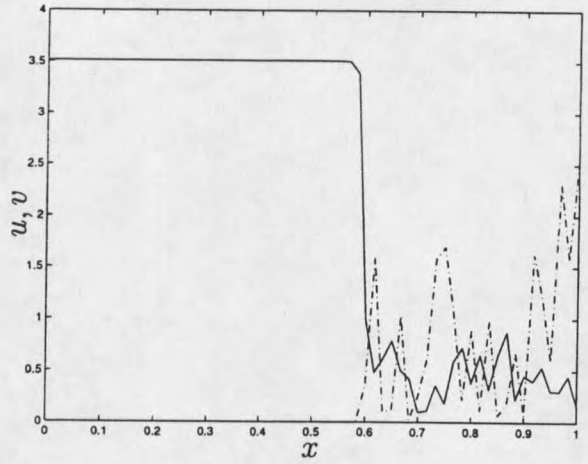

Figure 35: Pioneer and Climax solutions showing complex behavior with $c_{11} = 0.112$, $D_1 = .001$, $D_2 = .01$ and initial conditions started near q_2. Complex behavior taken over by traveling wave front moving to $(0, \frac{w_2}{c_{22}})$ steady state. Numerics done for Selgrade model, $c_{22} = 1$. Dashed lines represent Pioneer species, solid line represents the Climax species. The wave front is moving from the left to the right.

value of c_{11}. For this parameter value the solutions appear to stay chaotic. Further study would involve a closer look at this behavior and the parameter range where such dynamics is occurring.

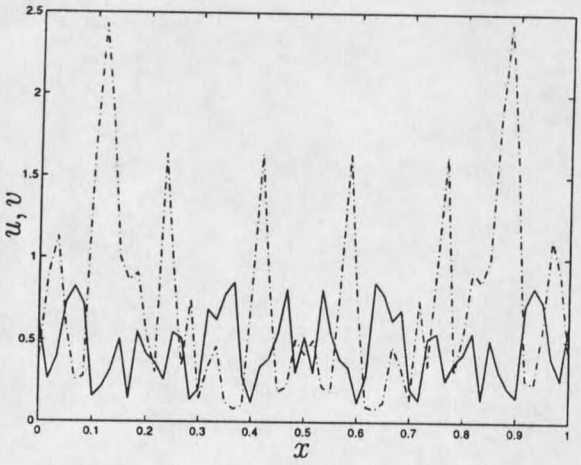

Figure 36: Pioneer and Climax solutions showing complex behavior with $c_{11} = 0.118$, $D_1 = .001$, $D_2 = .01$ and initial conditions started near q_2. This behavior appears to persist. Numerics done for Selgrade model, $c_{22} = 1$. Dashed lines represent Pioneer species, solid lines represent Climax species.

Sherratt in ([25],[26]) and Sherratt, Lewis and Fowler in [11] look at invading wave fronts with oscillatory and chaotic wakes behind the wave. The oscillations and chaotic behavior appear to be due to a change in the domain size. It is believed that an increase in the domain size, produced by a moving boundary condition, causes a once stable periodic point to become unstable in the full reaction-diffusion system. This results in causing the wake behind the wave front to go from an oscillatory pattern to chaotic pattern. In their work they however look at solutions near a Hopf bifurcation point in the kinetic system and have equal diffusion coefficients. In our system we have not observed this chaotic type of behavior when the species have equal diffusion coefficients, or when the initial condition is near q_1, the Hopf bifurcation point of the kinetic system.

Further work on this model could involve a deeper study of the Turing bifurcation that occurs in the system and analyses of the stability and bifurcation diagram of the bifurcating solutions. For the Selgrade model creating a bifurcation curve in the parameter space and categorizing the stability regions of the model solutions would be of value.

Further study of the complicated behavior of the system is of interest. We would need to look at the system and determine if the behavior is qualitatively the same as that presented in [25], [26] and [11] or if something of a different matter is occurring. Mapping the parameter regions that produce the complex behavior and the conditions that form the boundary of that region would be a possible first step in increasing our understanding of the dynamics behind this behavior.

In terms of advancing the model, it would seem that including some form of management into the model such as harvesting or stocking and then examining what effects this will have on the two species survival is a possible extension of the model. It seems reasonable to assume that to use the model for specific species we would need to form more accurate fitness functions than those used throughout this work. The model presented here was used to study a wide range of species that would generally fit into the category of pioneer or climax species but it was not assumed to apply to any specific species.

REFERENCES CITED

[1] N.F. Britton. *Reaction-Diffusion Equations and Their Applications to Biology.* Academic Press, San Diego, CA, 1986.

[2] J.M. Cushing. Nonlinear matrix models and population dynamics. *Natur. Resouce Modeling*, no. 2:539–580, 1988.

[3] Leah Edelstein-Keshet. *Mathematical Models in Biology.* McGraw-Hill, Inc, San Francisco, CA, 1988.

[4] Bard Ermentrout. Xtc-a tool for modeling spatial evolution equations. 1994.

[5] Bard Ermentrout. Xppaut1.0- the differential equations tool. 1997.

[6] Neil Fenichel. Geometric singular perturbation theory for ordinary differential equations. *Journal of Differential Equations*, Vol. 31:53–98, 1979.

[7] Paul C. Fife. *Lecture Notes in Boimathematics: Mathematical Aspects of Reacting and Diffusing Systems.* Springer-Verlag, New York,NY, 1979.

[8] Peter Grindrod. *The Theory and Applications of Reaction-Diffusion Equations, Patterns and Waves.* Clarendon Press, Oxford, UK, second edition edition, 1996.

[9] J. Guckenheimer and P. Holmes. *Nonlinear Oscillations, Dynamical Systems, and Bifrucations of Vector Fields.* Springer-Verlag, New York,NY, 1983.

[10] M.P. Hassell and H.N. Comins. Discrete time models for two-species competition. *Theoret. Population Biol.*, No. 9:202–221, 1976.

[11] A. Fowler J. Sherroatt, M. Lewis. Ecological chaos in the wake of invasion. *Proceedings of the National Academy of Science of the USA*, 92:2524–2528, 1995.

[12] J.Kevorkian and J.D. Cole. *Perturbation Methods in Applied Mathematics*, volume Vol. 34 of *Applied Mathematical Sciences.* Springer-Verlag, New York, NY, 1981.

[13] C.K.R.T. Jones. Geometric singular perturbation theory. *C.I.M.E. Lectures, Session on Dynamical Systems*, pages 1–82, 1994.

[14] James P. Keener. *Principles of Aplied Mathematics; Transformation and Approximation.* Addison-Wesley, New York, NY, 1988.

[15] D.J. Thompson M. Begon, M. Mortimer. *Population Ecology; A Unified Study of Animals and Plants.* Blackwell Science, Cambridge, MA, third edition edition, 1996.

[16] J.D. Murray. *Mathematical Biology.* Springer-Verlag, New York, NY, second edition, 1989.

[17] Akira Okubo. *Diffusion and Ecological Problems-Mathematical Models.* Springer-Verlag, New York, NY, 1980.

[18] Michael Olinick. *An Introduction to Mathematical Models in the Social and Life Sciences.* Addison-Welsey, Reading, MA, 1978.

[19] T.F. Fairgrieve P. Doedel, X. Wang. Auto94: Software for continuation and bifurcation problems in ordinary differential equations. 1995.

[20] John C. Polking. Matlab: pplane. Last modified: March 13, 1997.

[21] W.E. Ricker. Stock and recruitment. *J. Fish. Res. Bd. Can.*, 11:559–623, 1954.

[22] J.F. Selgrade. Planting and harvesting for pioneer-climax models. *Rocky Mountain Journal of Mathematics*, 24:293–309, 1994.

[23] J.F. Selgrade and G. Namkoong. Stable periodic behavior in a pioneer-climax model. *Natural Resource Modeling*, 4:215–227, 1990.

[24] J.F. Selgrade and G. Namkoong. Population interactions with growth rates dependent on weighted densities. *Differential equations models in biology, epidemiology and ecology (S. Busenberg, M. Martelli, eds.), Lecture Notes in Biomath*, 92:247–256, 1991.

[25] J. Sherroatt. Oscillatory and chaotic wakes behind moving boundaries in reaction- diffusion systems. *Dynamics and Stability of Systems*, 11(4):303–324, 1996.

[26] J. Sherroatt. Invading wave fronts and their oscillatory wakes are linked by a modulated travelling phase resetting wave. *Physica D*, in press.

[27] J.G. Skellam. Rondom dispersal in theoretical populations. *Biometrika*, 38:196–218, 1951.

[28] Joel Smoller. *Shock Waves and Reaction-Diffusion Equations.* Springer-Verlag, New York,NY, second edition, 1994.

[29] P. Szmolyan. Heteroclinic orbits in singularly perturbed differential equations. *IMA Preprint Series*, 576:1–24, 1989.

[30] P. Szmolyan. Transversal heteroclinic and homoclinic orbits in singular perturbation problems. *Journal of Differential Equations*, 92:252–281, 1991.

[31] S. Wiggins. *Introduction to Applied Nonlinear Dynamical Systems and Chaos.* Springer-Verlag, New York,NY, 1990.